APPLICATION OF ARTIFICIAL NEURAL NETWORKS FOR VOLTAGE STABILITY EVALUATION OF POWER SYSTEMS

SATISH C. VALLABHAN

Application of Artificial Neural Networks for Voltage Stability Evaluation of Power Systems

By

© Satish. C. Vallabhan, B.Tech.

A thesis submitted to the School of Graduate Studies in partial fulfillment of the requirements

for the degree of

Master of Engineering.

Faculty of Engineering and Applied Science

Memorial University of Newfoundland

August, 1995.

St.John's Newfoundland Canada

ISBN 0-612-13957-3

Abstract

Voltage instability has emerged as one of the most important areas of concern to modern power utilities. Once associated with weak power systems and long transmission lines, voltage instability problems are now acutely felt in highly developed networks. This is because many utilities are loading their bulk transmission networks to their maximum capacity to avoid the enormous capital costs of building new lines. In recent years, voltage instability has been responsible for several system collapses in Europe, Asia and North America.

Voltage instability is concerned with the ability of a power system to maintain acceptable voltage at all buses in the system under normal loading conditions and after being subjected to a disturbance. A system enters a state of voltage instability when a disturbance, increase in load demand, or change in system condition causes a progressive and uncontrollable decline in voltage. The main reason causing voltage instability is the inability of the power system to meet the demand for reactive power. The other factors contributing to voltage instability are generator reactive power/voltage control limits, load characteristics, characteristics of static var compensators, and action of on load transformer tap changers .

The study of voltage instability has become an important area of research in the field of power system engineering. The main thrust of research has been to arrive at an accurate and reliable indicator of the proximity of a system to voltage collapse. Such an indicator would be useful to utilities in operating their systems with maximum economy and security. However, for such voltage stability indices to be truly useful to utilities from an operations point of view, they should be implemented on-line in the Energy Management System (EMS). The Energy Management System has become a very important tool in modern power system control and operation and has versatile capabilities for power system control, analysis and monitoring. The major hurdle in the on-line implementation of voltage stability indices in an EMS would be the heavy computational costs involved in terms of time, memory and hardware costs. This is because most methods for voltage stability analysis need repeated solutions of power flows and associated calculations. Thus, for on-line applications, there is a need for tools which can quickly identify potentially dangerous conditions and provide the operator with guidance to steer the system from voltage collapse. Also,

in view of the large size of modern power networks, it is important that the memory requirements of the computational tools be as low as possible.

In recent years, there has been considerable interest in the application of Artificial Neural Networks (ANN) to power system problems. Artificial Neural Networks have the ability to identify and classify complex relationships, which are nonlinear and result from large mathematical models. The main feature of an ANN is the ability to achieve complicated input-output mappings through a learning process, without explicit programming. Once an ANN has been trained, it can classify new data much faster than would be possible by solving the model analytically. ANNs have the potential to play an important role in Energy Management Systems by providing system operators with a fast and reliable indication of the voltage stability of a power system.

This thesis presents the application of ANNs for evaluation of power system voltage instability. Two popular voltage stability indices are studied and simulations are carried out on the IEEE 24 Bus system and the 39 Bus New England system. The effect of contingencies on the voltage stability of the above two systems was investigated. ANN models were designed to evaluate the voltage stability indices using the system parameters available from the EMS as inputs. For the energy margin based voltage stability index, separate ANN models were used for each contingency. However, for the load margin index, a single ANN model which takes into account the network topology, was used to evaluate the voltage stability. This single ANN model is able to evaluate the voltage stability of a system under normal operating condition (i.e., all lines in service) and also in the event of a line outage. Simulation results are presented on the application of the above indices to both power systems. The performance of the ANN models are presented, which compares the predicted accuracy to the expected value. The thesis also proposes a scheme for integrating the ANN based system into the EMS environment.

Acknowledgments

I would like to express my sincere gratitude and appreciation for the invaluable help and guidance given to me by Dr. Benjamin Jeyasurya during all stages of this work. My thanks are also due to Dr. Jeyasurya, the Faculty of Engineering and Applied Science and the School of Graduate Studies for the financial support provided to me during the course of my M.Eng. program.

I acknowledge the assistance received from faculty members, fellow graduate students and other staff of the Faculty of Engineering and Applied Science.

Finally, I express my sincere gratitude to my family for their encouragement, support and understanding, without which this work would not have been possible.

Contents

List of Figures

List of Tables

Nomenclature :

E : Internal Voltage behind the synchronous reactance

V : Voltage at a bus

δ : Machine angle or Power angle

φ : Power factor angle

M : Inertia Constant

ω : Speed of the generator

P_L : Active power at load bus

Q_L : Reactive power at load bus

P_G : Active power generation at generation bus

Q_G : Reactive power generation at generation bus

V_{PV} : Voltage at PV (Voltage Controlled) bus

B_{ij} : Elements of the Bus Admittance Matrix
G_{ij}

V^s : Voltage at the stable operating point

V^u : Voltage at the unstable equilibrium point or low voltage solution

PV : Voltage Controlled bus

x : System state vector

ρ : Parameter vector

I : Line Current

S : Apparent power

X : System Reactance

Z : System Impedance

e_i : Real part of voltage at bus I

f_i : Imaginary part of voltage at bus I

f^o : Neural Network output function

w_{ji} : Weight of connection between hidden layer and input layer

w_{kj} : Weight of connection between output layer and hidden layer

η : Learning rate of the neural network

δ_{pk} : Error at a single output unit

Chapter 1

Introduction and Literature Survey on Voltage Collapse Phenomenon

1.0 Introduction

Traditionally, the primary concern of power system designers and planners has been ensuring rotor angle (synchronous) stability and thermal loading capabilities. Till the early eighties, when environmental issues came to the forefront, the expansion of the transmission and distribution network was dictated largely by the load demand. Generation, transmission and distribution facilities were planned and installed depending on the load growth. The only constraint system planners faced was to maintain angle stability. The few blackouts that took place were attributed to transient stability problems. The arrival of fast protective relays and circuit breakers have helped in part to alleviate this problem. The transmission and distribution network continued to expand to meet the load growth limited only by the utilities' financial constraints. The "normal" operation of a power system was defined by its ability to maintain angle stability.

However, this scenario started to change by the early eighties. A host of new issues came up which have combined to completely alter the way power systems have been planned and designed. The foremost among these was the general economic depression which characterised all major economies of the world. Utilities no longer had the resources to build new facilities either for generation, transmission or distribution. Another major development was the heightened awareness of environmental issues. Environmental issues became the centre stage of any developmental activity. All new developments, be it construction of a new generation plant or construction of a new transmission line, were examined for their environmental impact. Naturally, this resulted in a severe curtailment of any new construction of facility, which in normal course would have been approved. The problem was twofold. On the one hand, utilities were strapped for funds and even if they

could find funds for essential projects, long delays became the order of the day due to complicated approval procedures. However, all through this period, there was no appreciable decline in the load growth. Thus, the scenario in the eighties was that of increasing load and very little expansion of the facilities that existed. Utilities were faced with the task of squeezing the maximum possible power through the existing networks. These new developments brought in their wake, a new set of power system problems which had not been seriously thought of or studied before.

1.1 The Phenomenon of Voltage Stability

As a result of the above mentioned situation, system planners and designers were now being increasingly faced with a new problem: How to maintain the voltage profile at the transmission and distribution levels to acceptable values?

1.1.1 The MegaWatt - rotor angle and MegaVar - Voltage interaction

It has been long recognized that there is a strong coupling between MegaWatt (MW) and rotor angle and MegaVar (MVAR) and the voltage [1]. In other words, the availability of MW is dictated by the machine angle which in turn is decided by the input to the prime movers. On the other hand, voltage is related to the MVAR availability at that point. In figure 1.1, E_s is the sending end voltage, X is the reactance of the transmission line , E_r is the voltage at the receiving end and δ is the power angle or machine angle. I is the current through the line and S_r is the power in MVA. The relationship between active power, reactive power, sending end voltage, receiving end voltage, system angle and system reactance is as given by the equations below.

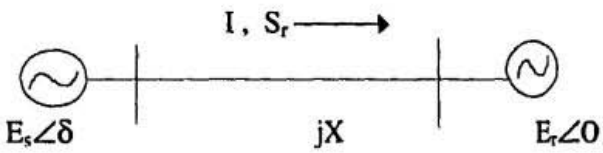

Fig. 1.1 Simple model for calculation of real and reactive power transmission

The relationship can be derived as follows :

$$S_r = P_r + j\,Q_r = E_r\,I^* \tag{1.1}$$

$$= E_r\,[\frac{E_s\cos\delta + jE_s\sin\delta - E_r}{jX}]^* \tag{1.2}$$

$$P_r + j\,Q_r = \frac{E_sE_r}{X}\sin\delta + j\frac{E_sE_r\cos\delta - E_r^2}{X} \tag{1.3}$$

$$P_r = \frac{E_sE_r}{X}\sin\delta = P_{max}\sin\delta \tag{1.4}$$

$$Q_r = \frac{E_sE_r\cos\delta - E_r^2}{X} \tag{1.5}$$

Voltage instability can be ascribed to the lack of VAR support needed to maintain the voltage profile at the specified value. Since voltage collapse occurs under heavy loading conditions, it may be worthwhile to explore the effect of large load angle on reactive power transmission. From the above equation for reactive power (eqn 1.5), it may be seen that as the load angle increases the reactive power becomes negative and the transmission line becomes a drain on the receiving end system. Thus, as the real power transfer increases the reactive power required from both sending and receiving end system will increase, and at very heavy loadings, more than one unit MVAR will be required for each additional MW transmitted. An important reason why reactive power transfer should be minimised is the heavy reactive losses incurred. Since reactive loss is proportional to I^2X, the reactive losses increase in a non-linear current squared relation. If in an already heavily loaded system, there is a loss of a line, the losses in the remaining lines may become very high and the voltage problem may worsen. Thus, it may be seen that the reactive power availability is one of the key aspects of voltage stability.

Reference [1] defines voltage stability and voltage collapse as follows:

A power system at a given operating state and subject to a given disturbance is voltage stable if voltages near loads approach pre disturbance equilibrium values.

A power system at a given operating state and subject to a given disturbance undergoes voltage collapse if post disturbance equilibrium values are below acceptable levels.

Thus, voltage collapse is an extreme form of voltage instability. As opposed to angle instability, the main dynamics involved in voltage collapse is the load dynamics. Hence voltage stability has also been called load stability [2]. During the period of voltage decay, other dynamics no less important come into play. These are generator excitation control, on load tap changers (OLTCs), static var compensator (SVC) controls, thermostat controlled loads etc. Since all the above controls have a longer response time (of the order of seconds), the dynamics are termed as slow dynamics. Typically, the response time may range from 10-20 seconds to the order of several minutes. We will now examine how voltage stability can develop in a simple radial system and show how the various controls listed above contribute to voltage instability.

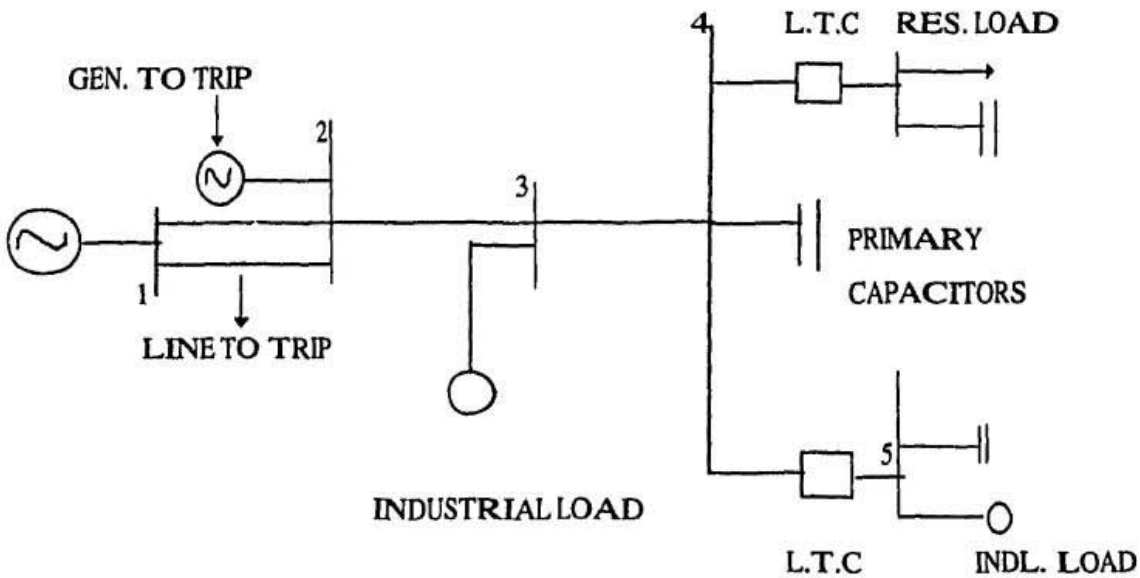

Fig. 1.2 Simple radial system.

Consider the radial system shown in Figure 1.2, which consists of a generator feeding three different types of distribution systems through a heavily loaded transmission line.

The three different types of loads are

1) Type 1 is domestic load which is mostly heating and lighting load and is relatively high power factor load. This type of load tends to drop with drop in voltage.

2) Type 2 is an industrial load on a load tap changer (LTC). Most of the industrial load comprises of induction motors and hence is low power factor and does not vary much with voltage.

3) Type 3 is an industrial load not on LTC.

In this heavily loaded system operating near its voltage stability limit, a small increase in load (active or reactive), a loss of generation or shunt compensation, a drop in sending end voltage etc. can bring in voltage instability. Assuming that one of the above mentioned changes happen, and the receiving end voltage falls, several mechanisms come into play. Since residential loads are voltage dependent, the active and reactive loads drops with drop in voltage. The industrial active and reactive loads dominated by induction motors change only by a small amount. Thus, the overall effect may be the stabilisation of voltage at a value slightly less than the rated value. The next action is operation of distribution transformer tap changers to restore distribution voltages. The residential active load will increase while the industrial reactive load will decrease. The increasing residential load will outweigh the decrease in reactive load causing the transformer primary voltage to fall further. The increased primary reactive losses will further drop the transformer primary voltage. In this scenario, the OLTCs (on load tap changer) may be close to their limits, primary voltage at around 90% and distribution voltages below normal. As voltage sensitive controlled loads (residential) creep back toward full power, primary and secondary voltages will drop further. The Type 3 industrial loads, i.e., without OLTCs will be exposed to the reduced voltage levels. This greatly increases the stalling of induction motors (stalling occurs when load torque is greater than developed torque). When a motor stalls, it will draw increasing reactive current , bringing down the voltage on the bus. This results in a "cascade" stalling of other induction motors resulting in a localised voltage collapse. Since

most large induction motors are controlled by magnetically held contactors, the voltage collapse would cause most motors to drop off from the system. This loss of load will cause the voltage to recover. However, the recovered voltage will again result in the contactor closing and motor stalling and another collapse. Thus, this loss and recovery of the load can cause alternate collapse and recovery of voltage. The effect of automatic voltage regulation (AVR) may be explained as follows: As the voltage drops the AVR steps in and increases the reactive generation. This increases the field current and when the current limit is reached, the excitation limiters come into play and the voltages are allowed to drop. Nearby generators may pick up the reactive load, but this may last only for a few minutes if they too reach their excitation limits.

Thus, from the above discussion it is clear that voltage stability is essentially "slow" dynamics and is affected by the nature and type of load, transformer tap changer action, generator AVR control etc.

To summarise, the various important factors contributing to long term voltage instability are:

1) Stressed power system, i.e., high active and reactive loading due to excessive load or line / transformer outages.
2) inadequate fast reactive power resources available locally, aggravated by action of field current limiters of generators.
3) load response at low voltages.
4) tap changer's response to distribution voltage magnitude and prop up loads as primary voltages continue to fall.

1.2. Voltage Stability- Static or Dynamic?

The above scenario which describes how a voltage collapse can evolve in a system shows that the time frame for a collapse to occur can be of the order of minutes depending on the response of the various controls involved. Traditionally, dynamic analysis as applied to angle stability has limited itself to the generator dynamics during the transient phase of the order of milliseconds. However, the time frame for voltage stability is much larger and

the computation requirements, if the generator dynamics are to be taken into account for such a long period of time, would be prohibitive. In view of the longer time frame involved, voltage stability has often been viewed as a steady state problem suitable for static analysis. Also, since a major factor in voltage instability is the availability of reactive power, the problem is ideal for power flow analysis. The static approach can offer an insight into the phenomena and can indeed give an approximate, yet acceptable solution which is computationally much simpler compared to the dynamic approach. However, since the effect of load dependency on voltage is of prime importance in voltage stability; it is desirable that the static load flow approach be modified suitably to incorporate the voltage dependency on load. This "quasi static" model can give a reasonable accuracy without a corresponding increase in computation requirement. Thus, it may be seen that there is a trade off involved in both approaches, and since engineering solutions should be practical and economical and not necessarily ideal, the static approach is widely used by most utilities today. The traditional methods of voltage stability analysis are discussed below.

1.3 Traditional Methods of Voltage Stability Analysis

As mentioned earlier, the 'static' or power flow approach has been the mainstay of voltage stability analysis. The two popular methods which make use of the load flow approach for voltage stability analysis are (1) P V curves (2) Q V curves

1.3.1 P V Curves

It has been shown in References [3-4] that if the receiving end voltage V is plotted against the active power P, the resulting curve is a parabola. Curves are obtained for different values of power factor. P V curves can be easily generated from the load flow by slowly increasing the load in discrete steps and noting the corresponding changes in voltage. It is observed that as the load increases the parabolic curve drops down, reaches a 'nose' point and then turns back toward the origin. This method can give the steady state loading limits which are related to voltage stability. A sample PV curve is shown in figure 1.3 and can be interpreted as below:

1) In the top half of the curve, the voltage V decreases as the receiving end power S increases. The slope of the curve is negative in this region.

2) The apex or nose point is the point at which the slope reverses direction. The X co-ordinate of this power represents the maximum power that can theoretically be delivered to the load.

3) The maximum power that can be delivered to the load is a function of the receiving end voltage and series external impedance between the sending end and the load point. It is equal to $V_s^2/4Z^*$, where V_s is the voltage of the sending end, and Z is the line impedance.

4) If the load demand were to increase beyond the maximum transfer limit, the amount of actual load which can be supplied as well as the receiving end voltage will both decrease. In other words, beyond the nose point, the ability to supply additional load is non existent.

Thus, the top half of the curve can be referred to as the stable region and the bottom part as the unstable region. Thus, it is reasonable to say that for every load, the top half of the curve represents the high voltage or feasible solution, and the bottom half the low voltage or fictitious solution. One of the major problems in generating the PV curve is that the load flow simulation will diverge near the nose point. This is due to the fact that under heavy loading conditions the Jacobian tends toward singularity and the load flow solutions are no longer reliable. Therefore, special programs are required to overcome this problem.

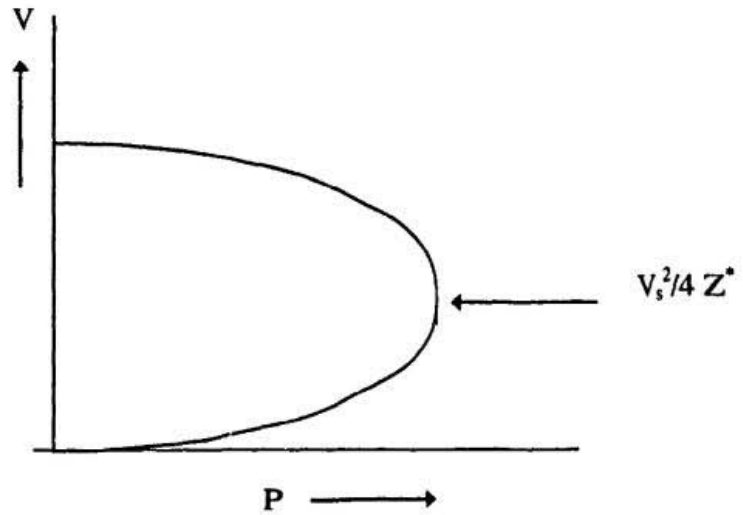

Fig. 1.3 Sample P V Curve

1.3.2 Q V Curves

The procedure for obtaining the Q V curves is similar to that for P V curves outlined above. The curves are obtained by a series of power flow simulations. Q V curves plot voltage at a bus against the reactive power at the same bus. In the Q V curve, voltage is on the X axis and the reactive power Q on the Y axis (Fig. 1.4). The main advantages of Q V curves are as follows:

* Since voltage security is closely related to the availability of reactive power, the Q V curve gives the reactive power margin at the test bus. The reactive power margin is the MVAR distance from the operating point to the bottom of the curve.

* The characteristics of bus shunt reactive compensation can be plotted directly on the Q V curve. The operating point is the intersection of the Q V characteristic and the reactive compensation characteristic.

Thus, Q V curves which also provide several means of determining the proximity of an operating point to voltage collapse have become quite popular with utilities in analysing voltage stability [5].

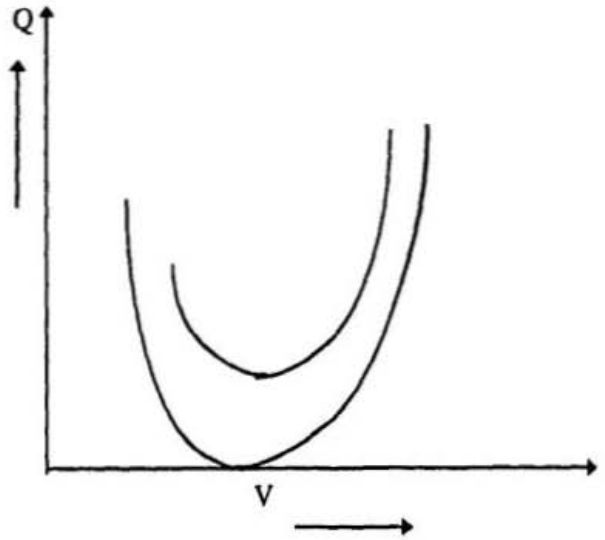

Fig. 1.4 Sample Q V curves

1.4 Recent Incidents of Voltage Collapse [1]

The recent interest in the phenomenon of voltage collapse has been triggered by several incidents of massive power failures in several power systems throughout the world. These incidents proved that the threat of voltage collapse was indeed very real and could not be ignored. The fact worth noting is that all these incidents took place not in weak and isolated systems, but in well developed and mature systems. A number of trends in system design and planning have contributed to this situation. Power systems have become more complex and are being operated closer to their capability limits due to economic and environmental reasons, as discussed earlier. The situation is complicated further by delays in building new transmission facilities. While these trends have contributed to angle instability also, it is clear from a study of recent incidents of system failure that it is voltage instability that is the major factor in these failures.

1.4.1 Voltage Collapse on French System

December 19,1978

The French system is a closely meshed and interconnected national grid comprising of both 400 KV and 220 KV transmission circuits. On the morning of December 19, a cold snap resulted in a rapid load rise of 4600 MW between 7 AM and 8 AM. The resulting increase in power transfer from eastern parts to the Paris metro area led to continuous voltage deterioration over the next 26 minutes. At approximately 8.20 AM, the voltage on the 400 KV system stabilised at about 350 KV. Within 6 minutes, the heavily loaded 400 KV feeder was tripped by the action of overload relays. This in turn led to overload tripping of other 400 KV and 220 KV lines. Widespread voltage oscillations spread over the entire French system and widespread islanding of the system took place.

January 12, 1987

This failure affected the whole western part of the French system. In this incident, three out of four thermal units of a major generating station tripped and operators called for gas turbines to start up. However, before the gas turbines could come on line, the fourth unit tripped on field overcurrent. Subsequently, nine generating units in another major generating station also tripped. The voltage on the 400 KV system stabilized at less than 300 KV.

The first incident, i.e., on December 19, 1978, was associated with rapid load increase, which in turn caused extremely high active and reactive power losses. It is characterized as a slow phenomena, the duration of the incident being nearly half an hour.

The second incident is characterized as relatively fast. It was initiated by sudden unforeseen loss of generating units. The response of load and OLTCs to the resulting low voltage contributed to further voltage deterioration and collapse.

Corrective Action taken

EDF (Electricite' de France) plans to use on line computation of voltage collapse proximity index , in view of the progressive and slow voltage deterioration, which will allow operators to take corrective measures. Also, studies have been initiated to improve co-ordination between automatic voltage regulation, field current limitations and protections. Automatic OLTC blocking based on a regional low voltage criterion is being implemented on the French system. Automatic load shedding is also being looked into.

1.4.2 Voltage Collapse on Swedish System

December 27, 1983

In the Swedish system, most of the generating plants are located in the north and the major load centres in the south. The hydroplants in the north are connected to the load areas in the south by seven 400 KV transmission lines. All lines are series and shunt compensated. Before the collapse, the total load including losses was 18,000 MW, i.e., less than the peak load. The voltages, on the network were stable between 400 and 405 KV and system frequency was close to 50 Hz. The voltage collapse was initiated by the failure of an isolator on a 400 KV switchgear at a substation west of Stockholm. This substation feeds the 220 KV network in the Stockholm area. As a result, two out of seven 400 KV transmission lines which bring power from north to south tripped. This resulted in high loading of the remaining five north-south transmission lines as well as a 220 KV line through Stockholm. Approximately 8 seconds after the initial ground fault, two 220 KV lines tripped due to overloading. After this tripping load started to restore due to transformer load tap changer action. Approximately 50 seconds after the initial fault, another 400 KV line tripped on overload. The remaining 400 KV lines became heavily loaded and a cascade tripping of all these lines between northern and southern Sweden took place. The loss of the EHV tie lines isolated southern Sweden from the hydroplants in the north. Because of the massive power deficit in the south, all generators in South were tripped on overload or underfrequency.

Corrective Measures taken

A number of research projects have been initiated by the Swedish Power Board after the above incidents. A co-ordinated control strategy for transformer load tap changers, shunt reactors, shunt capacitors and other equipment generating reactive power in the system has been designed. Also, since overload tripping of transmission triggered the collapse, the overload characteristics of the relays were also investigated. It was concluded that the offset mho characteristic of distance relays protecting long lines would have to be modified. Automatic blocking of OLTC's was also investigated.

1.4.3 Voltage Collapse at Tokyo on July 23, 1987

On July 23, 1987, Tokyo experienced unusually hot weather with record high temperatures of 36° C to 39° C. The demand increased at a rate of 400 MW/ minute far higher that the estimated level. The voltage on the 500 KV system gradually dropped to 460 KV. About 13:19, the voltage continued to drop and reached 370 KV (0.74 p.u.). These substations were tripped by operation of protective relays. It was found that the action of OLTCs contributed in a major way in accelerating the collapse. Thus a combination of heavy, unexpected load and the response of tap changers and loads contributed in a major way towards this collapse. One of the heartening aspects of the Tokyo collapse was that utilities and academics in Japan started serious research into the various contributing factors towards voltage collapse.

Corrective measures taken

In view of the Tokyo collapse, a number of measures were proposed. These include construction of a new 1000 MW generation facility, new shunt compensation equipment, upgrading of demand forecasts, sophisticated controls for OLTC's. Also, power purchases from neighbouring utilities would be encouraged.

1.5 Brief History of Research in the field of Voltage Instability

As discussed earlier, the static or power flow approach is a widely used and established method for voltage stability analysis. Though the past ten years has seen a lot of work in this field, some earlier researchers also had contributed a great deal on establishing a solid foundation. It was Venikov et al., who in 1975 showed that there is indeed a close connection between a load flow and steady state stability [6]. They proved that the change of sign of the Jacobian of the load low equation is an indicator of the onset of instability. This work would be made use of by future researchers. In 1978, one of the first papers on voltage collapse was published by Lachs[7] . He analysed in great detail the effect of heavy system loading and corresponding reactive losses, transformer tap changing, generator reactive capability etc. This was probably the first paper which made use of the PV curve to show the relation between system loading and voltage collapse. This paper is valuable in that for the first time an overall view of the various mechanisms contributing to voltage collapse was taken. In 1981, Tamura and Iwamoto followed upon Venikov et al.'s work and proposed a method to determine multiple load flow solutions [8]. They proposed the use of optimum multipliers or accelerators to the Newton-Raphson method. This method also would be made use of by future researchers. In 1982, Abe et. al. showed that load flow can indeed be used for the analysis of voltage instability [9]. They also proposed a model for tap changer and also the effect of tap changer operation on load models. In 1983, Tamura et. al. showed the relationship between voltage instability and multiple load flow solutions [10]. The authors showed that as the system gets more heavily loaded, the number of solutions decrease and at very high loadings, a pair of very close solutions are obtained. They also proposed a voltage stability criterion based on change of sign of the Jacobian and the number of close solutions. This aspect was not investigated further until recently. In 1983, Palmer et. al. argued from a utilities point of view the importance of reactive power despatching for maintaining power system voltage security [11]. They also proposed a method for scheduling reactive equipment during normal and post contingency situations. Thus, we see that from the mid seventies to the eighties, an understanding of the voltage stability phenomena and the relation of the steady state load flow to voltage stability had

been developed. However, it was not until 1986, that a comprehensive index for evaluating the voltage stability of a system was proposed. This and the currently available methods will be discussed in the next section.

1.6 Currently Available Methods for Evaluating Voltage Stability

There are a number of methods available for evaluating voltage stability from a static (load flow) point of view. However, the most popular and widely used ones are :

1) Glavitch's Method

2) Minimum Singular Value Method

3) Energy function Method.

1.6.1 Glavitch's Method

In 1986, Kessel and Glavitch proposed the first voltage stability index [12]. This method provides a means to assess voltage stability without actually computing the operating point where the collapse takes place. Glavitch 's method is essentially based on a static or load flow mode. In this method, the load flow program is run several times and various parameters used to compute voltage stability are taken from this. This method is originally derived from a two bus network where one of the buses is the slack and the other is a PQ bus. A stability indicator L_i is derived which varies between zero and one and which characterises the existence of a voltage solution. The index essentially relates the complex power S_i, elements of bus admittance matrix Y_{ii} and voltage V_i in the relation

$$L_i = \frac{S_i}{Y_{ii} * V_i} \tag{1.6}$$

For a multibus system, the index has to be calculated for each bus. The maximum value (closest to one) is an indicator of the proximity to power flow divergence. The important condition for stability to be guaranteed is $L_i < 1$. The indicator L_i is a quantitative measure for the estimation of the distance of the actual state of the system to the stability limit. The local indicator L_j permits the determination of those nodes from which a collapse may take

place. The pattern of indicators is quite informative of the behaviour of the system, in that all nodes belonging to the same critical area show a similar development of the stability indicator. Experience has shown that a threshold of 0.2 can be applied to the critical indicator. If the indicator of the particular node exceeds this value, the area around this node is critical. When L_i of a single node or a group of nodes exceeds the value of 0.2, the situation becomes critical. Clustering of indicators means the formation of an area of similar behaviour. When the cluster separates from another cluster, the area has a strong tendency to separate from the stable area voltage wise.

Thus, the stability indicator L_i is able to characterise the load flow solution and the potential of the system to become unstable. This is bound to the load flow model and the assumption of a PQ node. The model does not reflect any dynamic behaviour. The indicator L_i is a very strong signal of the dangerous situation. The evaluation of L_i is also quite simple since all required parameters are available from the load flow solution.

1.6.2 Minimum Singular Value Method

As far back in 1975, Venikov et al. [6] had shown that it is the Jacobian of the load flow equation that characterises the steady state stability limits and therefore eigenvalues of the Jacobian may have a direct bearing on any bifurcation of the equilibrium state. Many subsequent researchers have noted the singularity of the Jacobian during a voltage collapse. In 1988, Tiranuchit et. al. proposed a global voltage stability index based on the minimum singular value of the Jacobian[13]. One of the most important aspects to be examined when deriving corrective control measures is the question "how close is the Jacobian to being singular?". Tiranuchit et al. showed that a measure of the nearness of a matrix A to singularity is its minimum singular value. Hence, the minimum singular value can give a measure of the nearness to instability or in other words, a 'distance' to collapse. If the minimum singular value is plotted against real power, it is seen that the minimum singular value is very sensitive to change in load near the steady state boundary. One disadvantage of this method, as pointed out by the authors themselves, is the large CPU time required for the computation of the minimum singular value for large systems. The more important use

of this index is the relation it provides for control. If var compensation either through shunt capacitors of excitation control is available, this index provides the answer to the problem of how to distribute the resources throughout the system for maximum benefit.

At about the same time, Lof, Arnborg and Anderson proposed a similar index, albeit with some modifications [14]. They contended that the minimum singular value of a sub matrix G_s of the Jacobian J can be used, where G_s describes the effect on the voltage magnitude of change in reactive power injection in the network. This matrix G_s is essentially a sub matrix of the Jacobian J with some modifications. They showed that the minimum singular value of G_s is a more reliable static voltage stability index. It is shown that the power flow Jacobian becomes singular when the matrix G_s becomes singular. When the minimum singular value of the Jacobian J and the sub matrix G_s are plotted against the active power, it is seen that it could become difficult to use the minimum singular value of the Jacobian J to determine how far the conditions of the system are deteriorated when the load is increased. The minimum singular value of J could be dependent on static angle stability problems at first and hence could be fairly constant before it suddenly starts to decrease much more rapidly when voltage problems become more dominant. Lof et. al. contend that the use of the matrix J is appropriate for the construction of a static stability index when the cause of instability could be either angle or voltage problems. The minimum singular value of matrix G_s is a better basis for a static voltage stability index for planning and system studies.

1.6.3 Energy Function Analysis Methods

Energy functions have long been used in power system angle stability and are now well established [15]. They are considered a reliable means of obtaining the critical clearing time in large power systems. As mentioned earlier, Tamura et. al. had shown the relationship between multiple load flow solutions and voltage instability. They showed that though a power flow may have a number of solutions, only one solution is an 'operable' solution or stable equilibrium point. The other solutions are unstable equilibrium points. These solutions are also called low voltage solutions. Tamura showed that as the load

increases, the number of low voltage solutions decrease until near the point of collapse a pair of close solutions are obtained. The Jacobian at this stage approaches singularity. De Marco and Overbye [16 - 18] defined an energy function (similar to the Lyapunov function), which relates the system bus voltage magnitudes and phase angles with the property that the operable solution defines a local minimum of this energy. The energy function shows the energy difference between the operable solution and the low voltage solution. As the system load increases and the system moves towards collapse, it is seen that the energy difference decreases and becomes zero at the point of collapse. The energy difference between the high voltage and low voltage solution can give an indication of the systems vulnerability to voltage collapse. An important aspect of the energy function method is that it shows how load variations can push the system into instability [16-18]. VAR limits on generators can also be incorporated in this function, since the energy function is essentially based on the load flow solution. The plot of energy measure against load is a valuable indicator of the proximity of the system to collapse. The only computation requirement is the determination of the low voltage solutions, which for large networks may be time consuming. This approach indeed shows promise of becoming a valuable index if certain other parameters like effect of transformer tap changer, voltage dependency of loads etc. are taken into account.

As incidents of voltage instability become more common and systems continue to be loaded closer to their stability limits, it becomes imperative that system operators be provided with tools that can identify potentially dangerous situations leading to voltage collapse. Voltage stability indices are valuable and powerful tools for system operators in evaluating the voltage stability of a power system. However, it should be noted that if a voltage stability index is to be really useful, it should be implemented on - line in an Energy Management System (EMS). This will allow system operators to continuously monitor the voltage stability index of a power system and swiftly react to any conditions that may trigger a voltage collapse. But, the on-line implementation of a voltage stability index presents many challenges, the principal among them being the computational burden imposed on the EMS. This is because most of the voltage stability indices are computation intensive and for

power systems of realistic size, the computational burden may use up much of the capability of the EMS.

1.7 Application of Artificial Neural Networks

As indicated earlier, perhaps the most important aspect of a practical voltage stability index is the computation effort and hence the speed of computation involved. This is because for the large, real life power systems with thousands of buses, computation speed becomes a critical factor when an on line calculation of the stability index is required. This on-line response is important so that the operators can take corrective steps if an abnormal situation is encountered and steer the system away from collapse. All the methods listed above are computationally intensive, when large systems are considered. It then becomes necessary to look at other alternative approaches to minimise computational burden and response time. Artificial neural networks have wide interest in the field of power engineering and applications have been reported from almost all fields of power engineering [21-23]. The artificial neural network is essentially a pattern recognition tool. It can be trained to recognise complex, non linear relationships between a number of different parameters. The response time of a trained ANN is extremely fast, since there are no complex computations involved. Thus, in situations where a swift response is required, as in the case of power system voltage stability index, an ANN based approach can prove an attractive alternative to the computationally intensive calculation of the index. The accuracy of the ANN's predictions while depending largely on the quality of training, has proved to be quite acceptable for other power system application like load forecasting, dynamic security analysis and transient stability .

1.8. Significance of Artificial Neural Networks in Modern Power System Control

The modern power system has become very complex and operates under a great deal of constraints. On the one hand, the general economic depression has forced many utilities to cut back on their expansion and modernisation plans, but on the other hand there is no noticeable decline in load growth. Also, the consumer demand for efficiency and

reliability has never been higher. Environmental and ecological factors have also contributed to making the expansion of power systems a time consuming process. Thus, through the nineties and beyond, the scenario for power system planners and designers is grim : they have to maintain very high standards of system reliability and efficiency with fewer resources to do it.

1.9 The Energy Management System

The complexity and size of the modern power system has given rise to a number of problems. These problems can significantly affect system security and efficiency, two of the most important aspects of modern power systems. One of the most important tools for the power system designer and operator in maintaining a high level of system security is the Energy Management System (EMS). The EMS is an upgraded version of the Supervisory Control and Data Acquisition (SCADA) systems which have been in service for quite a long time. In addition to performing routine control functions of SCADA, the EMS has enhanced capabilities for on-line monitoring of the power system and performing such tasks as unit commitment and generation scheduling, optimal power flow, contingency analysis, security assessment, energy exchange between utilities, state estimation, load forecasting etc. Thus, it can be seen that the EMS is a very important aspect of modern power system control and operation. The linking of protection, control and other devices through a local data communications network has enabled the control of entire substations from a central host computer. The EMS has made possible the analysis, control and operation of large power systems from a central location and dramatically improved the efficiency, reliability and co-ordinated operation of modern power systems.

1.10 Aim of the Thesis

One of the major stumbling blocks to on-line control of power systems through an EMS is the heavy computational burden imposed by most power system analysis software. Thus, computation speed, which in turn depends on the computer hardware specifications, is the deciding factor, which determines the on-line implementation of power system

functions. The initial investments required for sophisticated computing equipment are so high that in most cases, utilities are not able to afford them. This prompted researchers to look at alternatives to raw computing power. As described in the previous section, ANNs hold out considerable promise as a medium for on-line implementation of many EMS functions such as transient stability and voltage stability analysis. The response of a trained ANN to an input is extremely fast, and the memory requirement of an ANN based system is considerably lower than that of a conventional sequential program. Also, since power system conditions are a result of system loadings which form a pattern, the pattern recognition ability of ANNs would be a valuable tool in identifying the system loading conditions which can lead to abnormal system operation. An ANN based system would not require additional data acquisition equipment and therefore, the overall benefits both from a standpoint of computing speed, and economy would be considerable. An ANN based system in conjunction with an expert / fuzzy logic system, will result in the goal of an intelligent control centre, which can result in increased reliability, economy and efficiency of operation.

This work explores the application of ANNs for assessment of voltage stability of power systems. Simulations are performed on standard test power systems for two different voltage stability indices, and results are presented on the accuracy of the predictions of the ANN based system for both the indices. An attempt has also been made to map the network topology in terms of a neural network.

1.11 Thesis Organisation

This thesis consists of seven chapters. Chapter two presents an overview of artificial neural networks and their applications to power systems. Chapter three presents the energy function based voltage stability index and simulation results on two bus, five bus and twenty four bus power systems. Chapter four presents an artificial neural network based energy margin voltage stability indicator. Chapter five includes description of the load margin based voltage stability index and also simulation results on the New England 39 bus system and also the IEEE 24 bus system. Chapter six presents artificial neural network

based models for the 39 bus system and also the 24 bus system, one with line outages and the other without. The chapter also proposes an ANN model which takes into account the network topology. Chapter seven concludes the thesis with some suggestions for further research in this area.

Chapter 2

Application of Artificial Neural Networks to Power Systems

2.1 Introduction

Artificial Neural Networks have aroused wide interest in different branches of engineering. This is because artificial neural networks (ANNs) have several properties that make them attractive tools in engineering applications. The important properties are parallel distributed processing, high computation rates, fault tolerance, and adaptive capability. The areas in which ANNs are widely applied include control systems, robotics, and recently in power system engineering. This chapter presents the basic concepts of ANNs and their application to power system engineering.

2.2 Artificial Neural Networks

An artificial neural network can be defined as a highly connected array of elementary processors or neurons [19-20]. Neurons are linked with other neurons with interconnects analogous to the biological synapse. This highly connected array of elementary processors defines the system hardware.

Several neural network algorithms have been proposed, which have enabled researchers to apply neural networks to a wide range of engineering problems. The neural network derives its computing power through, first, its massively parallel distributed structure and, second, its ability to learn and therefore generalize. Generalization refers to the neural network producing reasonable outputs for inputs not encountered during training. The use of neural networks offers the following useful properties and capabilities:

1. Nonlinearity : A neuron is basically a nonlinear device. Consequently, a neural network, made up of a number of neurons is itself nonlinear. Nonlinearity is a highly useful property, particularly, if the system generating the input itself is nonlinear.

2. Input - Output Mapping : The neural network can be trained to recognize the hidden relationship between the input and output. The relationship between the input parameters and the output(s) may be nonlinear in nature.

3. Adaptivity : Neural Networks have a built-in capability to adapt their synaptic weights to changes in the sorrounding environment. In particular, a neural network trained to operate in a specific environment can be easily retrained to deal with minor changes in the operating environment conditions. Examples of adaptive neural networks are the ART1, and ART2 algorithms.

4. Fault Tolerance : A neural network, implemented in hardware form, has the potential to be inherently fault tolerant in the sense that its performance is degraded gracefully under adverse operating conditions. For example, if a neuron or its connecting links are damaged, recall of a stored pattern is impaired in quality. However, owing to the distributed nature of information in the network, the damage has to be extensive before the overall response of the system is degraded seriously.

5. VLSI Implementability : The massively parallel nature of the neural network makes it potentially fast for the computation of certain tasks. This same feature makes the neural network ideally suited for implementation using VLSI techniques. The particular virtue of VLSI is that it provides a means of capturing truly complex behaviour in a highly heirarchial fashion which makes it possible to use a neural network as a tool for real time applications involving pattern recognition, signal processing and control.

6. Uniformity of Analysis and Design : Basically, neural networks enjoy universality as information processors. This is because the same notation is used in all the domains involving the application of neural networks. This feature manifests itself in different ways:

a. Neurons, in one form or another, represent an ingredient common to all neural networks

b. This commonality makes it possible to share theories and learning algorithms in different applications of neural networks.

c. Modular networks can be built through a seamless integration of modules.

Though the advantages of neural network are many and varied, it does have some serious limitatations, when applied to real world situations. The most serious limitation of an artificial neural network structure seems to be the lack of tools or guidelines to arrive at an optimum neural architecture. The size and the number of layers vary with application and arriving at an optimum architecture is often based on the users experience and intuition. Another serious drawback with ANN solutions is the possibility of local minima solutions. Presently, there is no conclusive way of testing if the network has indeed settled down to a global minimum. This would be especially true for complex problems where there may exist complex hypersurfaces with the associated possibility of many local minima.

2.2.1 Models of a Neuron

A neuron is an information processing unit that is fundamental to the operation of a neural network. There are three basic elements of the neuron model, as described below:

1. A set of synapses or connecting links, each of which is characterized by a weight or strength of its own. Specifically, a signal x_j at the input of synapse j connected to neuron k is multiplied by the synaptic weight w_{kj}.
2. An adder for summing the input signals, weighted by the respective synapses of the neuron. The operations described here constitute a linear combiner.
3. An activation function for limiting the amplitude of the output of a neuron.

In mathematical terms, we may describe a neuron k by writing the following pairs of equations :

$$u_k = \sum_{j=1}^{p} w_{kj} x_j \qquad (2.1)$$

and

$$y_k = \varphi(u_k - \theta_k) \qquad (2.2)$$

where $x_1, x_2, \ldots\ldots x_p$ are the input signals; $w_{k1}, w_{k2}, \ldots\ldots w_{kp}$ are the synaptic weights of neuron k, u_k is the linear combiner output, θ_k is the threshold, φ is the activation function and y_k is the output signal of the neuron.

Figure 2.1 shows the model of a neuron. In the figure, x is the input, w is the connection weight, Σ is the summing junction, θ is the threshold, φ is the activation function and y, the output.

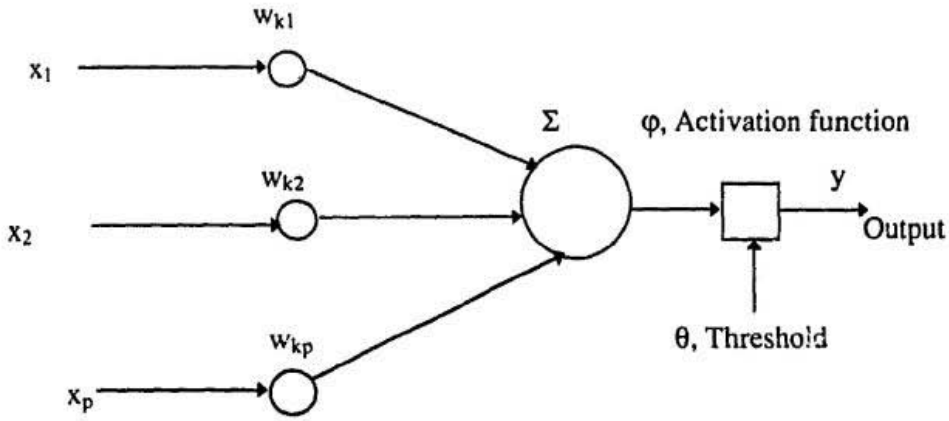

Fig. 2.1 Non linear model of a neuron.

2.2.2 Types of activation functions

The activation function, denoted by φ, defines the output of a neuron in terms of the activity level at its input. We can identify two basic types of activation functions :

1. Threshold functions : For this type of activation function, we have

$$\varphi(v) = \begin{cases} 1 & \text{if } v \geq 0 \\ 0 & \text{if } v \leq 0 \end{cases}$$

Correspondingly, the output of neuron k employing such a threshold function is expressed as :

$$y_k = \begin{cases} 1 & \text{if } v_k \geq 0 \\ 0 & \text{if } v_k < 0 \end{cases}$$

where v_k is the internal activity level of the neuron; that is,

$$v_k = \sum_{j=1}^{p} w_{kj} x_j - \theta_k \qquad (2.3)$$

Figure 2.2 illustrates the threshold function.

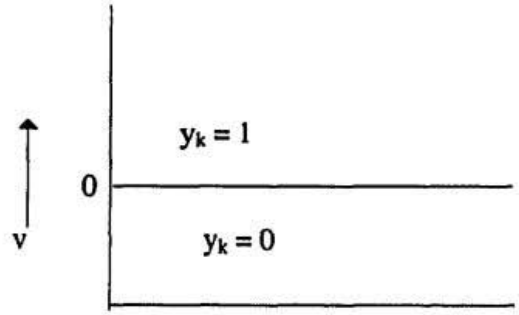

Fig. 2.2 Threshold function

2. Sigmoid Function : The sigmoid function is by far the most common form of activation function used in the construction of artificial neural networks. It is defined as a strictly increasing function that exhibits smoothness and asymptotic properties. An example of the sigmoid is the logistic function, defined by

$$\varphi_k = \frac{1}{1+\exp(-av)} \qquad (2.4)$$

where a is the slope parameter of the sigmoid function. By varying the parameter a, we obtain sigmoid functions of different slopes. In the limit, as the slope parameter approaches infinity, the sigmoid function becomes simply a threshold function. Whereas a threshold function assumes a value of 0 or 1, the sigmoid function assumes a continuous range of values from 0 to 1. Figure 2.3 shows the S shaped sigmoid function.

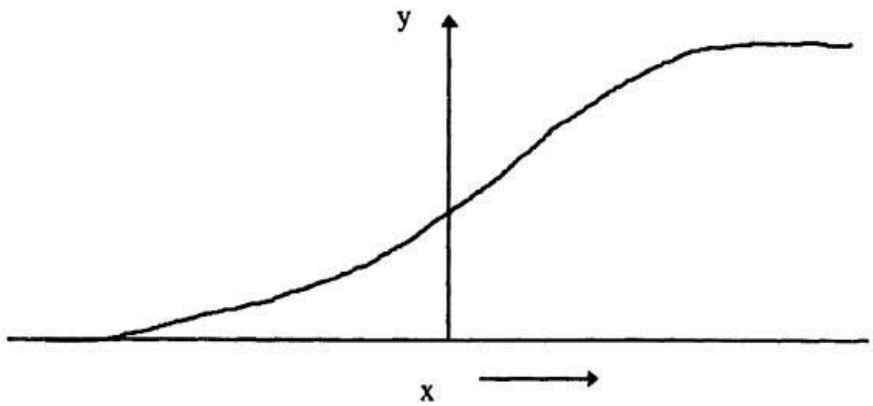

Fig. 2.3 Sigmoid Function

2.2.3 Network Architectures

The manner in which the neurons are structured is intimately linked with the learning algorithm used to train the network. In general, there are four types of network architectures [19]:

1. Single-Layer Feedforward Networks

A layered neural network is a network of neurons organized in the form of layers. In the simplest form of a layered network, we just have an input layer of source nodes that projects onto an output layer of neurons but not vice versa. In other words, this network is strictly of the feedforward type. Such a network is called a single layer network, referring to the output layer of computational nodes (neurons). In other words, we do not count the input layer of source nodes, because no computation is performed there.

Figure 2.4 illustrates the structure of a simple single layer network consisting of the input layer and the output layer.

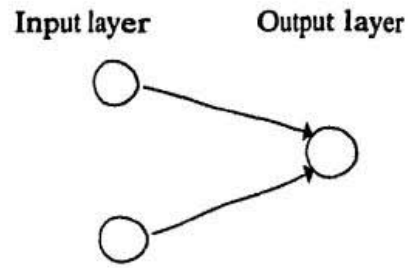

Fig. 2.4 Feedforward network with a single layer

2. Multilayer feedforward networks

The second class of feedforward neural network distinguishes itself by the presence of one or more hidden layers, whose computation nodes are correspondingly called hidden neurons or hidden units. The function of hidden neurons is to intervene between the external input and the network output. By adding one or more hidden layers, the network is able to extract higher order statistics, for the network acquires a global perspective despite its local connectivity by virtue of the extra set of synaptic connections and the extra dimension of neural interactions. The ability of hidden neurons to extract complex non linear patterns is particularly valuable when the size of the input layer is large. The source layers of the input layer of the network supply respective elements of the activation pattern (input vector) which constitute the input signals applied to the neurons in the second layer (i.e., the first hidden layer). The output of the second layer are used as inputs for the third layer, and so on for the rest of the network. The set of output signals of the neurons in the output (final) layer constitutes the overall response of the network to the activation pattern supplied by the input layer.

Figure 2.5 illustrates a simple multilayer network consisting of an input layer, a hidden layer and an output layer.

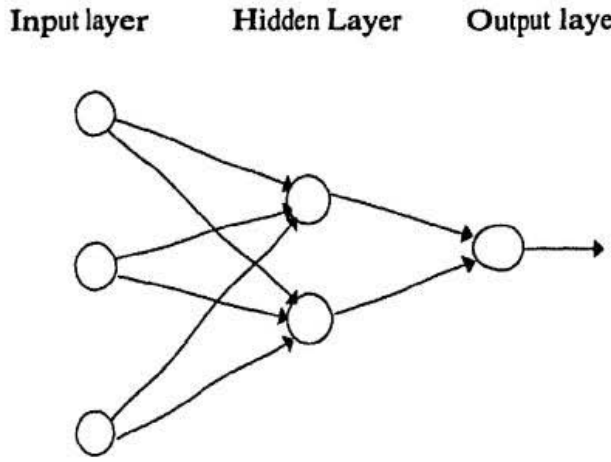

Fig.2.5. Simple multilayer network topology.

3. Recurrent Networks

A recurrent neural network distinguishes itself from a feedforward neural network in that it has at least one feedback loop. For example, a recurrent network may consist of a single layer of neurons with each neuron feeding its output signal back to the inputs of all the other neurons. A recurrent network may also be of the multilayered type, with feedback connections originating from both the hidden units and the output units. Figure 2.6 illustrates a simple recurrent network consisting of an input layer, an output layer and a feedback loop.

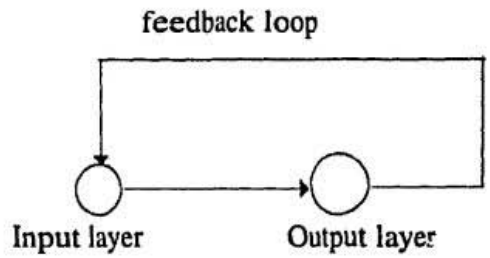

Fig.2.6 A simple recurrent network.

4. Lattice Structure

A lattice consists of a one dimensional, two dimensional or higher dimensional array of neurons with a corresponding set of source nodes that supply the input signals to the array; the dimension of the lattice refers to the number of the dimensions of the space in which the graph lies. A lattice neural network is really a feedforward network with the output neurons arranged in rows and columns.

2.2.4 Neural Network Algorithms

The most important property of a neural network is its ability to 'learn'. Learning may be defined as a process by which the free parameters of a neural network are adapted through a continuing process of stimulation by the environment in which the network is embedded. The two main types of learning algorithms are supervised learning and unsupervised learning. Supervised learning is performed under the supervision of an external 'teacher'. Unsupervised learning is performed in a self organised manner in that no external teacher is required to instruct synaptic changes in the network. A popular example of supervised learning is the error back propagation algorithm, while the Kohonen Network is a good example of the unsupervised learning. Table 2.1 below gives comparison of the features of different neural network algorithms [19].

In table 2.1 below, the following abbreviations are used :

BPN : Back Propagation Network

BAM : Bi - Directional Associative Memory

CPN : Counter Propagation Network

SOM : Self Organizing Map

STN : Spatio Temporal Network

ART : Adaptive Resonance Theory

Table 2.1 Comparative performance of different ANN algorithms

Type of ANN	Training time	Certainity to reach global minimum	Type of input pattern	Domain input pattern	Ability of report if mismatch occurs	Purpose
BPN	**Moderate**	**No**	**Analog**	**Spatial**	**No**	**General**
BAM	**Low**	**No**	**Digital**	**Spatial**	**No**	**General**
Hopfield	**Low**	**No**	**Digital**	**Spatial**	**No**	**General**
CPN	**Low**	**No**	**Digital**	**Spatial**	**No**	**General**
SOM	**Moderate**	**No**	**Analog**	**Spatial**	**No**	**General**
STN	**Moderate**	**No**	**Analog**	**Temporal**	**No**	**Speech**
ART	**Low**	**Possible**	**Analog**	**Spatial**	**Yes**	**General**
Boltzmann	**High**	**No**	**Digital**	**Spatial**	**No**	**General**

2.3 Back Propagation Algorithm

The development of the back propagation (BP) algorithm represents a landmark in neural networks in that it provides a computationally efficient method for the training of multilayer perceptrons. The basic idea of back propagation was first proposed by Werbos in 1974 [21] and subsequently popularised by Rumelhart et.al. [22].

Backpropagation is one of the most popular algorithms in use today. This is partly due to its simplicity, and applicability to a wide variety of engineering problems. Back propagation is ideal for complex pattern matching problems. The basic working of the algorithm can be summarized as follows. The network learns a predefined set of input-output example pairs by using a two phase propagate-adapt cycle. After an input pattern has been applied as a stimulus to the first layer of network units, it is propagated through each upper layer until an output is generated. This output is then compared to the desired output, and an error signal is computed for each output unit. The error signals are then

transmitted backward form the output layer to each node in the intermediate layer that contributed directly to the output. However, each unit in the intermediate layer receives only a portion of the total error signal, roughly based on the relative contribution the unit made to the original output. This process repeats, layer by layer, until each node in the network has received an error signal that describes its relative contribution to the total error. Based on the error signal received, connection weights are then updated by each unit to cause the network to converge toward a state that allows all the training patterns to be encoded.

The significance of the process is that, as the network trains, the nodes in the intermediate layers organize themselves such that different nodes learn to recognize different features of the total input space. After training, when presented with an arbitrary input pattern that is noisy or incomplete, the units in the hidden layers of the network will respond with an active output if the new input contains a pattern that resemble the feature the inidvidual units learned to recognize during training. Conversely, the hidden layer units have a tendency to inhibit their outputs if the input pattern does not contain the feature that they were trained to recognize.

As the signals propagate through the different layers of the network, the activity pattern present at each upper layer can be thought of as a pattern with features that can be recognized by units in the subsequent layer. The output patte · ·enerated can be thought of as a feature map that provides an indication of the presence or absence of many different feature combinations at the input. The total effect of this behaviour is that the BPN provides an effective means of allowing a computer system to examine data pattens that may be incomplete or noisy, and to recognize subtle patterns from the partial input

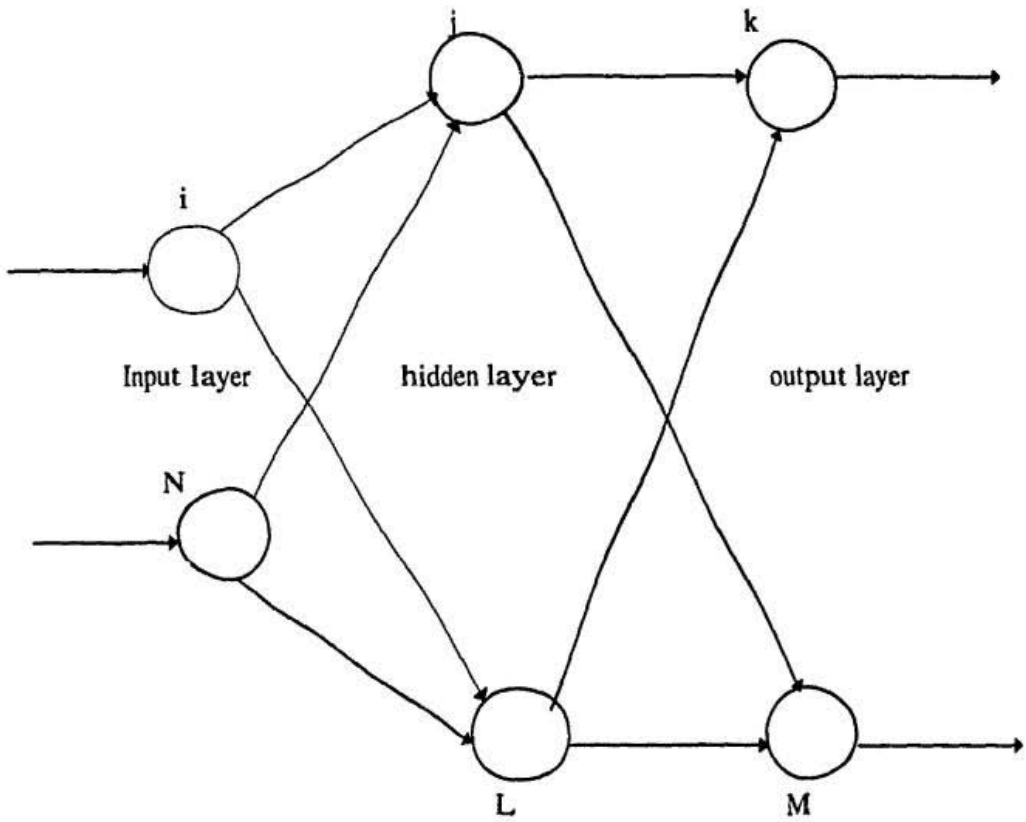

Fig. 2.7 Typical Architecture of a three layer backpropagation neural network

Figure 2.7 shows the typical architecture of a three layer BP network. The input layer has units from (1,.....i,.....N); the hidden layer has (1,.....j,.....L) units, the output layer has (1,.....k,.....M) units . The input units distribute the values to the hidden layer units. The net input to the j-th hidden unit is

$$net_{pj}^{h} = \sum_{i=1}^{N} w_{ji}^{h} x_{pi} + \theta_{j}^{h} \qquad (2.5)$$

where w_{ji}^{h} is the weight on the connection from the i-th input unit, and θ_{j}^{h} is a bias term. This term is a weight on a connection that has its input value always equal to 1. The use of the bias term is largely optional. The 'h' superscript refers to quantities on the hidden

layer. Assuming that the activation of this node is equal to the net input; then, the output of this node is

$$i_{pj} = f_j^h(net_{pj}^h) \tag{2.6}$$

where f represents the function adopted, eg. sigmoidal, gaussian, linear etc.

The equations for the output nodes are

$$net_{pk}^o = \sum_{j=1}^{L} w_{kj}^o i_{pj} + \theta_k^o \tag{2.7}$$

$$o_{pk} = f_k^o(net_{pk}^o) \tag{2.8}$$

where the superscript 'o' refers to quantities on the output layer.

The error at a single output unit is defined to be $\delta_{pk} = (y_{pk} - o_{pk})$, where the subscript 'p' refers to the p-th training vector, and 'k' refers to the k-th output unit. In this case, y_{pk} is the desired value, and o_{pk} is the actual output from the k-th unit.

The various steps involved in the backpropagation algorithm are summarized below.

1. Apply the input vector, $\mathbf{x}_p = (x_{p1}, x_{p2}, \ldots\ldots\ldots x_{pN})^t$ to the input units
2. Calculate the net-input values to the hidden layer units :

$$net_{pj}^h = \sum_{i=1}^{N} w_{ji}^h x_{pi} + \theta_j^h \tag{2.9}$$

3. Calculate the outputs from the hidden layer :

$$i_{pj} = f_j^h(net_{pj}^h) \tag{2.10}$$

4. Move to the output layer. Calculate the net-input values to each unit:

$$net_{pk}^o = \sum_{j=1}^{L} w_{kj}^o i_{pj} + \theta_k^o \tag{2.11}$$

5. Calculate the outputs :

$$o_{pk} = f_k^o(net_{pk}^o) \tag{2.12}$$

6. Calculate the error terms for the output units :

$$\delta_{pk}^{o} = (y_{pk} - o_{pk})\, f_k^{o'}(net_{pk}^{o}) \qquad (2.13)$$

7. Calculate the error terms for the hidden units :

$$\delta_{pj}^{h} = f_j^{h'}(net_{pj}^{h}) \sum_k \delta_{pk}^{o} w_{kj}^{o} \qquad (2.14)$$

It may be noted that the error terms on the hidden units are calculated before the connection weights to the output layer units have been updated.

8. Update the weights on the output layer :

$$w_{kj}^{o}(t+1) = w_{kj}^{o}(t) + \eta \delta_{pk}^{o} i_{pj} \qquad (2.15)$$

9. Update weights on the hidden layer :

$$w_{ji}^{h}(t+1) = w_{ji}^{h}(t) + \eta \delta_{pj}^{h} x_i \qquad (2.16)$$

The error term $E_p = \frac{1}{2} \sum_{k=1}^{M} \delta_{pk}^{2}$ gives an indication of how well the network is training. When this error is acceptably small for each of the training vector pairs, the training can be discontinued.

2.4. Important issues in applying back propagation algorithm

The important issues to be considered while applying the back propagation algorithm are listed below :

* Learning Rate
* Momentum
* Stopping Criteria
* Initialization
* Generalization
* Training set size

Each of these issues will be examined below.

2.4.1 Learning Rate.

The learning rate, η has a significant effect on network performance. Usually, η must be a small number of the order of 0.05 to 0.25, to ensure that the network will settle to a solution. A small value of η means that the network will have to make a large number of iterations. It is often possible to increase the value of η as training proceeds. Increasing η as the network error decreases will often help to speed convergence by increasing the step size as the error reaches a minimum, but the network may bounce around too far from the actual minimum value if the learning rate gets too large.

2.4.2 Momentum

Another way to increase the speed of convergence is to use a technique called momentum. When calculating the weight change value, $\Delta_p w$, we add a fraction of the previous change. This additional term tends to keep the weight changes going in the same direction and hence the term momentum. The weight change equations on the output layer then become

$$w^{o}_{kj}(t+1) = w^{o}_{kj}(t) + \eta \delta^{o}_{pk} i_{pj} + \alpha \Delta_p w^{o}_{kj}(t-1) \qquad (2.17)$$

In equation (2.17) above, α is the momentum parameter, and is usually set to a positive value less than one.

2.4.3 Stopping Criteria

The back propagation algorithm is considered to have converged when the absolute rate of change in the average squared error per epoch is sufficiently small. Typically, the rate of change in the average squared error is considered small enough if it lies in the range of 0.1 to 1 percent per epoch. However, it should be noted that there is always a possibility that the network may converge to a local minimum in weight space. Once a network settles on a minimum, whether local or global, learning stops. When a network reaches an acceptable solution, there is no guarantee that it has reached the global minimum, rather that a local one. If the solution is acceptable from the error

standpoint, it does not matter whether the minimum is global or local, or even if the training was halted at some point before a true minimum was reached.

2.4.4 Initialization

The first step in back propagation learning is to initialize the network. Weights should be initialized to small, random values, between $\pm$ 0.5. A good choice for the initial values of the free parameters of the network can be of tremendous help in a successful network design. The wrong choice of initialization values can lead to a phenomena called premature saturation. This refers to a situation where the instantaneous sum of squared errors remains almost constant for some period of time during the learning process.

2.4.5 Generalization

In back propagation learning, we typically start with a training set and use the back propagation algorithm to compute the synaptic weights of a multilayer perceptron by loading as many of the training examples as possible into the network. A neural network is said to generalize well when the input -output relationship computed by the network is correct for input/output patterns never used in creating or training the network. A neural network that is designed to generalize well will produce a correct input -output mapping even when the input is slightly different than the examples used to train the network. The Back Propagation network is quite good at generalization, and this coupled with its simplicity is the strongpoint of the algorithm.

2.4.6 Size of Training set

The ability of a network to generalize is influenced by three factors : the size and efficiency of the training set, the architecture of the network, and physical complexity of the problem at hand. The size of the training set will be dependent on the application intended and is largely an empirical value. Experience and experimentation are often the most important indicators of a correct or right training set size. Also, the number of input

and output parameters also influence the training set size. Generally, larger the number of input/output parameters, larger should be the training set.

2.5 Selected Applications to Power Systems

Artificial neural networks have been recently proposed as an alternative method for solving certain traditional problems in power systems where conventional techniques have not achieved the desired speed, accuracy, or efficiency [23-25]

Neural Network applications that have been proposed in the literature can be broadly classified into three main areas. Regression, Classification and Combinatorial Optimization. The applications involving regression includes Transient Stability [26], Load Forecasting [27], Synchronous Machine Modelling [28], and Contingency Screening [29]. Applications involving classification include Harmonic load identification, alarm processing, static security assessment and fault diagnosis [30-31]. In the area of combinatorial optimization, there is topological observability and capacitor control. This section provides an overview of the reported ANN applications to power systems.

2.5.1 Transient Stability

Stability of a power system deals with the electromechanical oscillations of synchronous generators, created by a disturbance in the power system. It is of prime importance to know if the disturbance will lead to loss of synchronism. When the disturbance is small and when the system oscillations following the disturbance is confined to a small region around an equilibrium point, concepts of linearized systems analysis can be applied to determine the stability of the power system. This is known as steady state stability assessment. However, when the disturbance is large and when the oscillatory transients are significant in magnitude, nonlinear system theory or explicit time domain simulations have to be used to analyse the system stability. The ensuing analysis is known as transient stability assessment.

Transient stability is determined by observing the variation of δ (rotor angle) as a function of time in the post fault period. The power system is said to be transiently stable for a given disturbance if the oscillations of all rotor angles damp out and eventually settled down to values within the safe operating constraints of the system. For any disturbance, the transient stability of a power system depends on three basic components : the magnitude of the disturbance, the duration of the disturbance, and the speed of the protective devices. There exists a critical clearing time (CCT), where if the fault is cleared before this time, the power system remains stable. However, if the fault is cleared after the CCT, the power system is likely to be unstable. The CCT is a complex function of pre-fault system conditions, disturbance structure, and the post fault conditions. There are two commonly used methods for calculating CCT, namely 1) Numerical Integration and 2) Lyapunov Energy Function method. The first method involves extensive time domain simulation of the power system while the scope of the second method is limited by its restrictive assumptions. Due to the many possible pre-fault operating conditions and types of faults, computational effort needed to assess the CCT for each of these scenarios is prohibitive.

2.5.2 The Neural Network Approach to evaluate CCT [26]

The estimation of CCT can be looked as a regression problem where pre-fault system parameters are used to predict the CCT for the corresponding fault. A multi-layered perceptron was proposed to be trained using back-propagation to learn a set of input attributes and the corresponding CCT's for a specified fault under varying operating conditions [26]. In the ANN approach, the inputs are the individual acceleration energy of the generators of the system accumulated during the fault, which in turn depends on rotor angle deviation, the centre of mass and the reduced electrical power output enerators during the fault. The output of the ANN is the CCT corresponding to the given contingency under the described inputs. During generation of training data, CCT for the corresponding input quantities is obtained by repetitive numerical integration of the post-disturbance system equations using different reclosing times. The CCT would correspond

to the maximum time for reclosure after the initial isolation of the line in order to maintain synchronous operation. Reference [26] reports results which compare the performance of the ANN based CCT predictor with the calculated values. The error in prediction was acceptable in most cases.

2.6 Load Forecasting

Forecasting electrical load in a power system with lead times varying from hours to days, has important economic advantages. The forecasted information can be used to aid optimal energy interchange between utilities thereby saving valuable fuel costs. Forecasts also significantly influence important decisions such as dispatch, unit commitment and maintenance scheduling. Most conventional methods used for load forecasting can be categorized under two approaches. One treats the load demand as a time series signal and predicts the load using the different time series analysis techniques. The second method recognizes the fact that the load demand is heavily dependent on weather variables. The general problem with the time series approach include the inaccuracy of prediction and numerical instability. The main reason for instability is not considering the weather information which is known to have a profound effect on load demand. The conventional regression type approaches use linear or piecewise representations for the forecasting function. The accuracy of this approach is dependent on the functional relationship between the weather variables and electric load which must be known . This approach cannot handle the non stationary temporal relationship between weather variables and load demand.

2.6.1 Neural Network Approach to Load Forecasting [27]

The ANN approach can combine both time series and regression approaches to predict the load demand. A functional relationship between weather variables and electric load is not needed. This is because an ANN can generate this functional relationship by learning the training data. In other words, the nonlinear mapping between the inputs and outputs is implicitly embedded in the ANN. The ANN approach proposed in [27] uses

previous load data combined with actual and forecasted weather variables as inputs, and the load demand as the output. Some of the weather parameters considered for training are temperature, wind speed, humidity/wind chill, rain, snow, rate of evaporation etc. The results show that ANNs can indeed be trained to predict the load demand at a much lower computation cost compared to conventional techniques.

2.7 Contingency Screening [29]

A contingency in a power system is an abnormal event (such as a fault), which could be potentially damaging to power system components. Contingency screening is a relatively fast and approximate method of identifying whether a contingency will result in a violation of any of the operating constraints of the power system. Contingency screening helps select a critical set of potentially damaging events for more accurate analysis.

Contingency selection in its simplest form, deals with forming a list of contingencies which may result in steady state voltage or thermal limit violations in the post contingency power flow condition. Usually, the Distribution Factor approach and the Performance Index approach are used for contingency screening. The proposed ANN approach for contingency screening is based on identifying the contingent branch overloads. A collection of ANNs are trained where each ANN is dedicated to a specific line outage. The inputs to the ANN are B_{ij} and $P_{net\,i}$ where B_{ij} is the susceptance between buses i and j, and P_{neti} is the net active power into bus i. The outputs are the line flows and a binary flag indicating secure/ insecure status.

2.8 Alarm Processing and Fault Diagnosis

The control centres of a power system are continually interpreting a large number of alarm signals to determine the status of the system components and to evaluate the power system operation. The process is very complex because of two key reasons :

1. Alarm patterns are not unique to a given power system problem. Same fault may manifest in different alarms based on the current topology and operating status of the power system.

2. Alarm patterns are likely to be contaminated with noise due to equipment problems, incorrect relay settings, interference etc.

Expert systems have been widely tested for analysing alarm signals. The formulation of rules however requires precise definitions of the power system and its operational strategies which may widely vary depending on the utility.

2.8.1 Neural Network Approach to Fault Diagnosis [30-31]

The ability of a power system operator to diagnose a system problem by analysing a set of multiple alarms is a form of pattern recognition. Accurate classification of noisy alarm patterns is also a key shortcoming in most of the conventional techniques. Therefore, ANNs with their ability to classify noisy patterns seems to be a logical choice for alarm processing. The ANN is also capable of associating different alarm patterns to the same system fault by training the ANN with a set of information rich data that represents different operating scenarios. The ANN training set is generated by first creating a credible set of contingencies and then deriving the possible alarm patterns under each fault. These patterns are generated by the relay protection schemes and power flow analysis. These patterns are then used to train a multi-layered perceptron using back propagation. This is one area in which the ANN appears to have great potential due to its intrinsic noise rejection and self learning capabilities.

Application of ANNs have been reported in the areas of contingency evaluation , dynamic security assessment [26], and control of DC Motors [32] . The above examples show that ANNs hold out great promise in providing a fast, reliable and accurate computation tool in power system applications.

Chapter 4 and Chapter 6 present the application of artificial neural networks for evaluation of voltage stability of two sample power systems for two different voltage stability indices. On-line voltage stability analysis is one area where ANNs can help

improve greatly the efficiency and capability of Energy Management Systems. This is due to the fact that voltage stability analysis is computationally intensive and imposes enormous burden on the EMS, if the computation has to be done on-line. ANNs, by virtue of their pattern recognition abilities, can eliminate the enormous computation costs associated with on-line calculation of voltage stability and hence improve considerably the efficiency, security and economy of operation of power systems.

Chapter 3

Energy Function Methods for Evaluation of Voltage Stability

3.1 Introduction

This chapter provides an overview of the energy function method and the various methods available to determine the multiple load flow solution. The energy function method is applied to the evaluation of voltage stability of three sample power systems, namely a 2 bus system, a 5 bus system and a 24 bus system. The simulations to determine the low voltage solutions and the energy margins for the three sample power systems are presented.

3.2 Overview of Energy Function Methods .

As explained in Chapter 1, the main thrust of research in the field of voltage stability has been to arrive at an index or more generally, developing a security measure to quantify how "close" a particular operating point is to voltage collapse. The crucial point in judging the effectiveness of the various methods is to see whether or not the "distance" of a given operating point to voltage collapse is physically reasonable and can provide planners and operators with an indication of when corrective action is necessary. The energy function method is a static voltage stability assessment tool which takes into account the operating condition of the power system, the power system parameters and the multiple load flow solutions. Before describing the application of energy methods for voltage stability, it would be useful to review their application to transient stability.

3.2.1 Application of energy method to transient stability [15]

Energy methods have been successfully applied to the transient stability problem, i.e., the equal area criterion. Consider a generator connected to an infinite power network. If the generator is represented by the classical model, the dynamic behavior of the generator rotor angle can be described by

$$M \frac{d^2\delta}{dt^2} = P_i - P_m \sin(\delta - \gamma) \qquad (3.1)$$

where M is the inertia constant

P_i , P_m, and γ are constants and δ is the machine angle.

Integrating equation (3.1) gives

$$\int M\,\omega \frac{d\omega}{dt} dt = \int [P_i - P_m \sin(\delta - \gamma)] \frac{d\delta}{dt} dt \qquad (3.2)$$

where ω is the speed of the generator.

Integrating again, we get

$$\frac{1}{2} M \omega^2 |_{\omega 1}^{\omega 2} = P_i\, \delta |_{\delta 1}^{\delta 2} + P_m \cos(\delta - \gamma) |_{\delta 1}^{\delta 2} \qquad (3.3)$$

If the limits are between the initial conditions ($\delta_1 = \delta_0$, $\omega_1 = 0$) and at clearing ($\delta_2 = \delta_c$, $\omega_2 = \omega_c$) then the left hand side of equation (3.3) gives the kinetic energy of the generator at fault clearing. This is represented by area A_1 in Fig. 3.1. Taking the limits between fault clearing ($\delta_1 = \delta_c$, $\omega_2 = \omega_c$) and at maximum angle swing ($\delta_2 = \delta_m$, $\omega_2 = 0$), then the left hand side of equation 3.3 is the negative of the kinetic energy at clearing. It is represented by the area A_2 in Fig. 3.1.

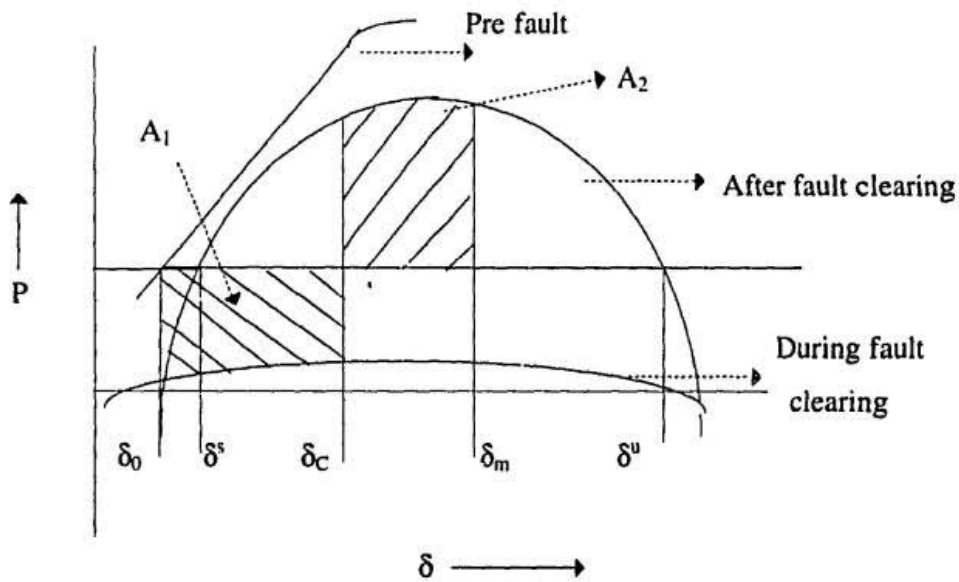

Fig. 3.1 Illustration of the Equal Area Criterion concept

We also note that at δ_m, since $\omega_m = 0$, all the kinetic energy which had been present at δ_c has now been converted to potential energy, and the areas in Fig. 3.1 are equal, and hence the name equal area criterion.

3.2.2 Application of Energy methods to voltage stability.

The energy margin method applies the Lyapunov direct method to determine the voltage stability at a given operating state. The application of the energy function to the voltage stability problem can be described as follows. Conceptually, the energy function defines an "energy well" in the voltage space (i.e. state space, with the voltage magnitudes and angles at all buses as the states). If the system were not subject to any disturbances, the current operating state of the system can be thought of as sitting at the bottom of this well at the stable equilibrium point (SEP). The SEP corresponds to the high voltage power flow solution. An actual system is always subject to some disturbances such as those due to customer load variations so that the system never sits precisely at the SEP. However, usually these disturbances can be considered small, so that the high voltage power flow solution provides a good approximation to the actual state of the system. The current operating point of the power system describes a local minimum of an energy well. However, due to random load variations, the true instantaneous point does not stay at the mathematically defined equilibrium point. These small random variations add a small amount of kinetic energy to the system. Under normal operating conditions, these variations are not of much consequence. However, when the system is operating under stressed conditions and is in the proximity to voltage collapse, the system state and hence the voltage magnitude is highly sensitive to load changes. Under such conditions, it may be possible that the random load variations may push the state out of the potential well that defined its stable operating point. A necessary condition for this to happen is that it receives energy greater than the potential value of the closest unstable equilibrium point (UEP). The UEP's correspond to those multiple load flow solutions which are practically " infeasible", i.e., it is physically impossible for the system to

operate at those points. These unstable equilibrium points correspond to the low voltage solutions of the power flow equations.

Thus, a low value of energy measure can alert the system operators of an impending voltage collapse. The energy function defines the height difference of the potential barrier between the operable solution and the low voltage solution. As the loading in the system increases, the system is pushed more and more toward the point of collapse and the height of the potential barrier decreases and the energy margin decreases. This is commonly known as the 'energy well concept', illustrated in Figure 3.2.

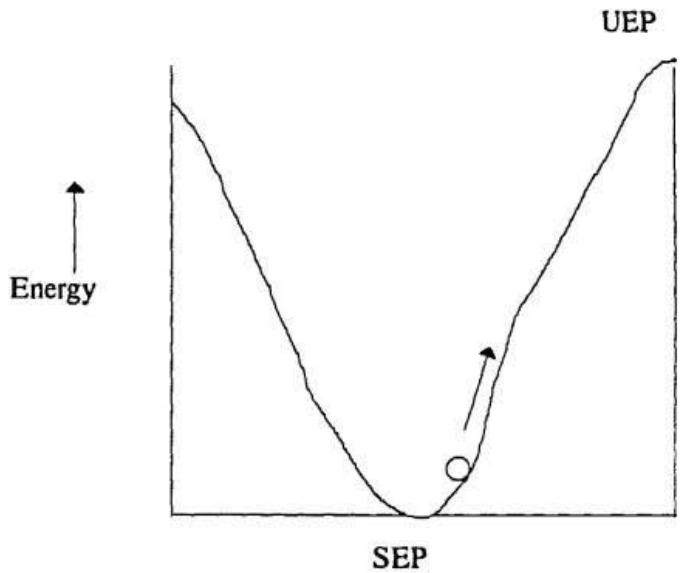

Fig. 3.2 Illustration of the energy well concept

In Figure 3.2, the system represented by the ball is initially at the stable equilibrium point (SEP) . A disturbance pushes the system up the energy well, and if the disturbance is strong enough, the system may roll up and reach the unstable equilibrium point (UEP). The difference in energy levels between the SEP and the UEP is called the energy margin. The calculation of energy margin is illustrated for a 2 bus, 5 bus and 24 bus system in Section 3.5. At the point of collapse, the low voltage and high voltage solutions merge and hence the potential barrier or energy margin is zero at that point. Thus, the height of

the potential barrier as measured by the energy difference between the steady state and the low voltage solution can provide an indicator of the system's vulnerability to voltage collapse. A low value of energy measure indicates that the potential barrier between the stable operating point and the unstable operating point is low, i.e., the system is near the point of collapse. The energy measure of a power system is a unique value and will vary from system to system depending on the system parameters, operating conditions and the low voltage solutions .

The energy measure as defined by Overbye and DeMarco[18] is :

Energy Measure

$$=$$

$$\frac{1}{2}\sum_{i=1}^{n}\sum_{j=1}^{n} B_{ij}\left|V_i^u\right|\left|V_j^u\right|\cos(\alpha_i^u-\alpha_j^u)+\frac{1}{2}\sum_{i=1}^{n}\sum_{j=1}^{n} B_{ij}\left|V_i^s\right|\left|V_j^s\right|\cos(\alpha_i^s-\alpha_j^s)+\sum_{i=1}^{n}\int_{V_i^s}^{V_i^u}\frac{Q_i(x)}{x}dx-P^T(\alpha^u-\alpha^s)$$

$$-\sum_{i=1}^{n}\sum_{j=1}^{n} G_{ij}\left|V_i^s\right|\left|V_j^s\right|\cos(\alpha_i^s-\alpha_j^s)(\alpha_i^u-\alpha_i^s)+\sum_{i=1}^{n}(V_i^s)^{-1}\sum_{j=1}^{n} G_{ij}\left|V_i^s\right|\left|V_j^s\right|\sin(\alpha_i^s-\alpha_j^s)(V_i^u-V_i^s)$$

(3.4)

In equation (3.4), n is the number of buses in the system, G_{ij} and B_{ij} are respectively the real and imaginary parts of the elements of the bus admittance matrix, V_i is the bus voltage magnitude, α_i is the bus voltage angle, P is the vector of the real power into each bus, and Q_i is the reactive power into bus i. The subscript s stands for the stable operating condition and the subscript u stands for the unstable operating conditions or the low voltage solutions of the power flow equations.

The energy function is thus a vector integration of the real and reactive power mismatch equations (with the reactive mismatch multiplied by the inverse voltage magnitude at each bus) between the high voltage power flow solution and a low voltage power flow solution.

The evaluation of the summation terms in equation (3.4) is straightforward. Since the equations are sparse, the computational cost for calculating these sums are not very high. For the non-generator buses, the integral term can be quite easily evaluated, provided the reactive load is modeled in the common form of either a polynomial or exponential

function of the bus voltage. For example, if the reactive load at bus i is modeled as a constant component plus a component linearly dependent upon the bus i voltage magnitude,

$Q_i = k_1 + k_2 V_i$

then the integral evaluates to

$$k_1 \ln\left(\frac{V_i^u}{V_i^s}\right) + k_2 (V_i^u - V_i^s)$$

At the generator buses in the system the voltage magnitude is generally specified, rather than the reactive power output. If the generator has reached the excitation limit, the integral term is approximated by

$$Q_{lim(max)} * \ln\left(\frac{V_i^u}{V_i^s}\right)$$

The procedure for calculating the voltage stability index using energy margin method is summarized below :

i) Run the base case load flow and obtain the solution

ii) For the same loading condition, obtain the low voltage solutions. Use the simplified search method [10], for obtaining the low voltage solutions. This procedure is described in detail in section 3.3

iii) Using both the steady state and low voltage solutions and the system parameters, calculate the energy margin.

In step ii of the procedure described, care should be taken to choose the low voltage solution which results in the lowest energy margin. The next section describes in detail the procedure for calculating the low voltage solutions.

The relationship between multiple load flow solutions and voltage stability has been investigated extensively by earlier researchers [8]. For an n bus power system, the maximum number of multiple load flow solutions possible is 2^{n-1}. It is seen that there is an inverse relation between the number of load flow solutions and the system loading. As the system loading increases, the number of load flow solutions is found to decrease and at the point of voltage collapse, the low voltage and high voltage solutions merge into

one. Section 3.3.1 illustrates the above fact with respect to a 5 bus power system. Thus, the number of low voltage solutions is an indicator of the voltage stability of a power system.

3.3 Low Voltage Power Flow Solutions

The determination of the appropriate low voltage solutions is of critical importance in applying the energy function approach. It is imperative that to apply the energy function approach, the low voltage solutions (UEP's) should be found with reasonable computational effort. In this section, the properties of, and, general solution algorithm for determining the low voltage load flow solutions of power systems will be examined. The general algorithm or the exhaustive search method is as given below :

1. Obtain the stable operating point power flow solution.
2. Using the quadratic algorithm proposed in [8] and derived below, calculate the low voltage solution for each load bus assuming that the voltages at all the other buses are fixed. The steps involved in this are the calculation of starting values of the bus voltages and substituting this value as the voltage guess in the next load flow run. This calculation is not performed on buses which are voltage controlled . Denote this voltage as V_i^u.

The Quadratic algorithm for calculation of starting values for the computation of low voltage solutions was first proposed in reference [8]. The algorithm proposes a simple means of arriving at starting values and is given below:

This algorithm gives a closed form expression for calculating the two solutions of the voltage at bus i when all other bus voltages are assumed fixed. Starting with the power flow equations at each bus in rectangular coordinates.

$$P_i = \sum_{j=1}^{n} e_i(e_j G_{ij} - f_j B_{ij}) + f_i(f_j G_{ij} + e_j B_{ij}) \qquad (3.5)$$

$$Q_i = \sum_{j=1}^{n} f_i(e_j G_{ij} - f_j B_{ij}) - e_i(f_j G_{ij} + e_j B_{ij}) \qquad (3.6)$$

where P_i is the real power at bus i, Q_i is the reactive power at bus i, e_i is the real part of the voltage at bus i, f_i is the imaginary part of the voltage at bus i, G_{ij} and B_{ij} are respectively the real and imaginary parts of the elements of the bus admittance matrix.

Rearranging the terms in equations (3.5) and (3.6),

$$P_i = G_{ii} (e_i^2 + f_i^2) + e_i C + f_i D \quad (3.7)$$

$$Q_i = - B_{ii} (e_i^2 + f_i^2) + f_i C - e_i D \quad (3.8)$$

where

$$C = \sum_{j=1, j\neq i}^{n} e_j G_{ij} - f_j B_{ij}) \quad (3.9)$$

$$D = \sum_{j=1, j\neq i}^{n} f_j G_{ij} - e_j B_{ij}) \quad (3.10)$$

Multiplying equations (3.7) by B_{ii} (3.8) by G_{ii}

$$P_i B_{ii} = B_{ii} G_{ii} (e_i^2 + f_i^2) + e_i B_{ii} C + f_i B_{ii} D \quad (3.11)$$

$$Q_i G_{ii} = - B_{ii} G_{ii} (e_i^2 + f_i^2) + f_i G_{ii} C - e_i G_{ii} D \quad (3.12)$$

Summing equations (3.11) and (3.12) and then solving for f_i , we get

$$P_i B_{ii} + Q_i G_{ii} = e_i B_{ii} C + f_i B_{ii} D + f_i G_{ii} C - e_i G_{ii} D \quad (3.13)$$

$$f_i = \alpha e_i + \beta \quad (3.14)$$

$$\alpha = \frac{G_{ii} D - B_{ii} C}{B_{ii} D + G_{ii} C} \quad (3.15)$$

$$\beta = \frac{P_i B_{ii} + Q_i G_{ii}}{B_{ii} D + G_{ii} C} \quad (3.16)$$

Substituting equation (3.13) into (3.7) to eliminate f_i, it can be rewritten as

$$P_i = G_{ii} \{(1 + \alpha^2) e_i^2 + 2\alpha\beta e_i + \beta^2\} + e_i C + (\alpha e_i + \beta) D \quad (3.17)$$

The two voltage solutions can then be determined by solving for e_i using the quadratic formula and then using (3.14) to solve for e_i,. One of the solutions will be the operable load flow solution voltage and the other root will give the starting value.

3. Select either V_i^s or V_i^u as initial voltage guesses for the rectangular Newton - Raphson algorithm. Form all of the possible $2^{n-m} - 1$ combinations of initial voltage guesses with at least one bus set to its V_i^u value (where n is the total number of buses, and m is the number of PV buses).

4. Compute the power flow solutions using the rectangular Newton - Raphson algorithm for each of the $2^{(n-m)} - 1$ initial voltage guess permutations.

The exhaustive search method presents a systematic method of creating a set of initial voltage guess vectors. However, in order to find a small set of actual solutions, this algorithm requires tests of $2^{(n-m)}$ - 1 initial voltage guesses. This would be computationally prohibitive in systems of realistic size.

As an alternative, a "Simplified Search" method is adopted, which reduces considerably the number of initial guesses required. The simplified search method is essentially the same as the exhaustive method, except that rather than forming all of the $2^{(n-m)}$ -1 initial voltage guess combinations, only the n-m combinations corresponding to the use of V_i^u at a single bus are calculated. This reduces considerably the computational complexity of the algorithm.

The application of the simplified search method to a sample 5 bus power system is illustrated in Section 3.3.1

3.3.1 Low Voltage solutions for sample 5 bus power system

A sample 5 bus power system is shown in Fig 3.3.

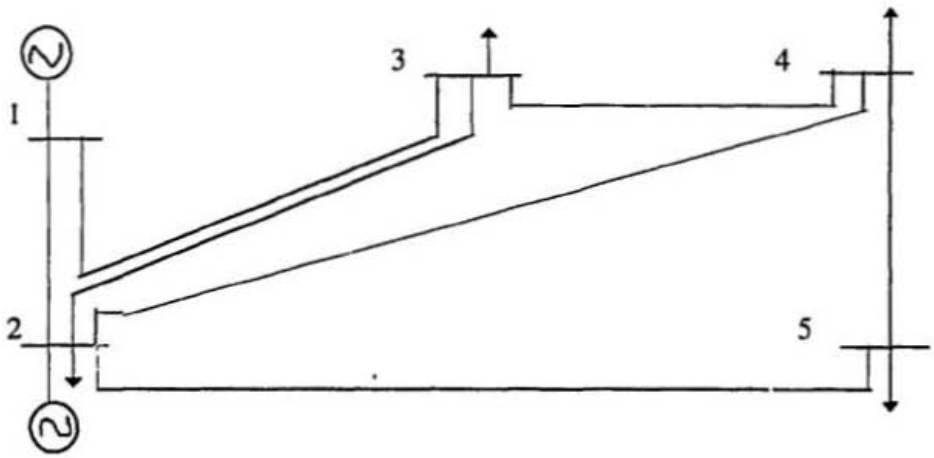

Fig. 3.3 Sample 5 bus power system

The five bus system shown in Fig. 3.3 has a slack bus, a voltage controlled bus and three load buses. The system has seven lines. The base case load flow results for this system are shown in Table 3.1.

Table 3.1 Load flow solution results for 5 bus system.

Bus No.	Voltage real part (e)	Voltage imaginary part (f)	Pgen in MW	Qgen in MVAR	Pload in MW	Qload in MVAR
1	**1.06**	**0.00**	**129.5**	**- 7.5**	**0.00**	**0.00**
2	**0.9994**	**-0.036**	**40.0**	**-41.5**	**20**	**10**
3	**0.9772**	**-0.0774**	**0.0**	**0.0**	**45**	**15**
4	**0.973**	**-0.0825**	**0.0**	**0.0**	**40**	**5.0**
5	**0.9614**	**-0.0958**	**0.0**	**0.0**	**60**	**10**

Using the Quadratic algorithm described earlier, the starting values for the voltages at all the four buses are determined. The starting values are as given below.

Table 3.2 Starting Values of voltages for 5 bus system

Bus Number	Starting Values for Voltage
2	**0.0152 + j 0.0102**
3	**0.0079 -j 0.0095**
4	**0.0051 -j 0.0090**
5	**0.0277 -j 0.0468**

The next step in the formation of all possible combinations of the solutions as given below:

The combination of solutions possible for the 5 bus system are

0 0 0 1

0 0 1 0

0 0 1 1

0 1 0 0

0 1 0 1

0 1 1 0

0 1 1 1

where 0 denotes the value of the steady state voltage and 1 denotes the starting value obtained by using the Quadratic formula and listed in Table 3.2. The load flow program is now run 7 times, once for each of the above combinations and the corresponding low voltage solutions are obtained.

The 7 possible roots of the 5 bus system for the base case loading are given below:

Table 3.3 Low voltage solution corresponding to 0 0 0 1

Bus Number	Voltage in p.u.
2	**0.9776 - j 0.2104**
3	**0.7740 - j 0.1741**
4	**0.7186 - j 0.1776**
5	**0.0184 - j 0.0550**

Table 3.4 Low voltage solution corresponding to 0 0 1 0

Bus Number	Voltage in p.u.
2	**0.9588 - j 0.2841**
3	**0.1772 - j 0.0866**
4	**0.0043 - j 0.0298**
5	**0.5679 - j 0.2503**

Table 3.5 Low voltage solution corresponding to 0 0 1 1

Bus Number	Voltage in p.u.
2	**0.9237 - j 0.3830**
3	**0.1693 - j 0.1004**
4	**0.0026 - j 0.3680**
5	**0.0149 - j 0.0800**

Table 3.6 Low voltage solution corresponding to 0 1 0 0

Bus Number	Voltage in p.u.
2	**0.9568 - j 0.2908**
3	**0.01722 - j 0.0319**
4	**0.1459 - j 0.1131**
5	**0.6278 - j 0.2788**

Table 3.7 Low voltage solution corresponding to 0 1 0 1

Bus Number	Voltage in p.u.
2	**0.9119 - j 0.4151**
3	**0.0165 - j 0.0470**
4	**0.0273 - j 0.0859**
5	**0.0103 - j 0.0786**

Table 3.8 Low voltage solution corresponding to 0 1 1 0

Bus Number	Voltage in p.u.
2	**0.9505 - j 0.3106**
3	**0.0272 - j 0.0493**
4	**0.0080 - j 0.0490**
5	**0.5713 - j 0.2718**

Table 3.9 Low voltage solution corresponding to 0 1 1 1

Bus Number	Voltage in p.u.
2	**0.9120 - j 0.4151**
3	**0.0165 - j 0.0470**
4	**0.0270 - j 0.0859**
5	**0.0103 - j 0.0786**

This procedure is repeated for different loading factors of K = 2, 3, 4, 4.5 (K is the multiple of base case loading) and the number of distinct solutions obtained for each loading factor. It is seen that the number of solutions decrease as the loading increases. The number of solutions obtained for each loading factor is tabulated in Table 3.10 below:

Table 3.10 Variation of number of roots with increase in load

Roots	K = 1	K = 2	K = 3	K = 4	K = 4.5
No. of distinct roots	**8**	**4**	**4**	**2**	**2**

The base case solution, starting values and the low voltage solutions corresponding to K= 4.5 are tabulated below :

Table 3.11 Load flow solution for 5 bus system for K = 4.5

Bus Number	Voltage in p.u.
1	**1.006 + j 0.000**
2	**0.9787 - j 0.2869**
3	**0.8394 - j 0.2869**
4	**0.8301 - j 0.3071**
5	**0.8001 - j 0.3577**

Table 3.12 Starting values for K= 4.5 for 5 bus system

Bus Number	Voltage in p.u.
2	**-0.1055 - j 0.0174**
3	**0.0119 - j 0.0543**
4	**0.0119 - j 0.0473**
5	**0.0166 - j 0.2486**

Table 3.13 Low voltage solution for 5 bus system for K = 4.5

Bus Number	Voltage in p.u.
1	**1.006 + j 0.0000**
2	**0.8810 - j 0.4732**
3	**0.4716 - j 0.4071**
4	**0.4239 - j 0.4269**
5	**0.0733 - j 0.2949**

3.4 Energy Margin Computation

This section presents the results of the computation of energy margin for the two bus, five bus and twenty four bus systems, based on equation (3.4). As seen in section 3.3, there are a number of combinations and therefore, a number of roots are possible for the 5 bus and 24 bus systems. If energy margins have to be calculated for each of the combinations for every loading condition, the computational complexity will make the method infeasible for practical implementation. Therefore, the following procedure is

adopted for simplification. For the base case loading, the energy margins are calculated for each of the possible combinations of the low voltage solutions. The combination resulting in the lowest energy margin is identified and this combination is used in the computation of energy margins for subsequent loading conditions also. This greatly reduces the effort required to calculate the energy margins for various system loading conditions.

Results of simulations carried out to determine the energy margins for a two bus, five bus and a 24 bus system are presented below :

The two bus system is as shown in Fig. 3.4 below. The power factor of the load is 0.0 and the voltage V_1 =1.0 p.u.

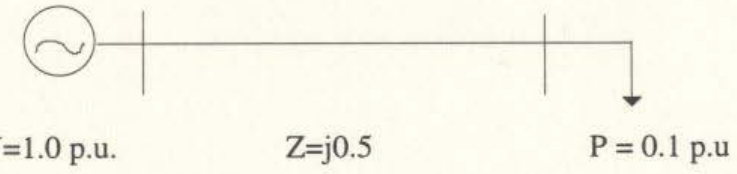

Fig. 3.4 Single line diagram of sample two bus system.

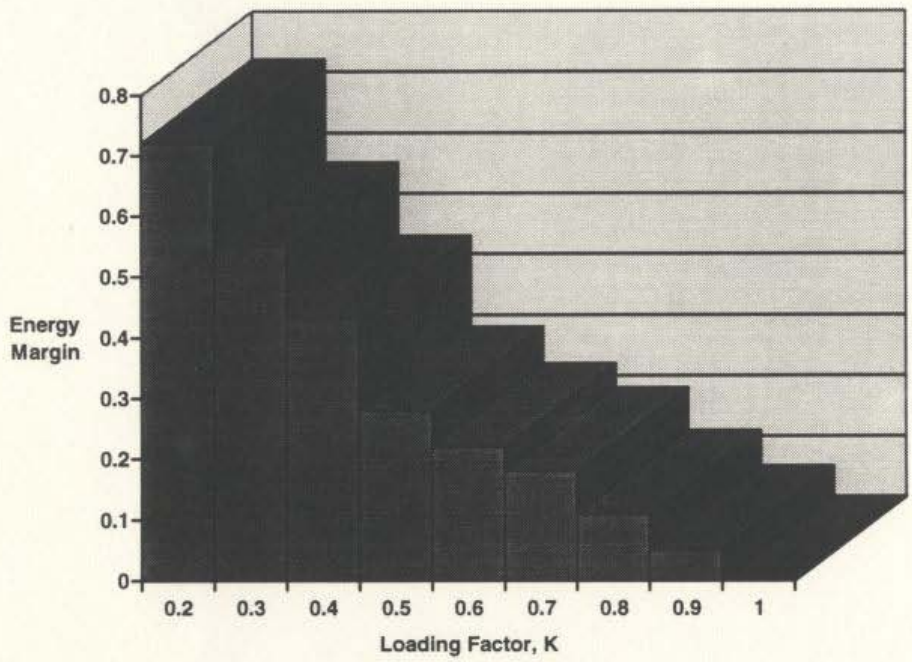

Fig. 3.5 Variation of energy Margin with loading for 2 bus system.

Figure 3.5 shows the variation of energy margin with loading for the two bus system. It can be seen that the energy margin steadily decreases with increase in load. Figure 3.6 shows the variation of energy margin with loading for the 5 bus system shown in Figure 3.3.

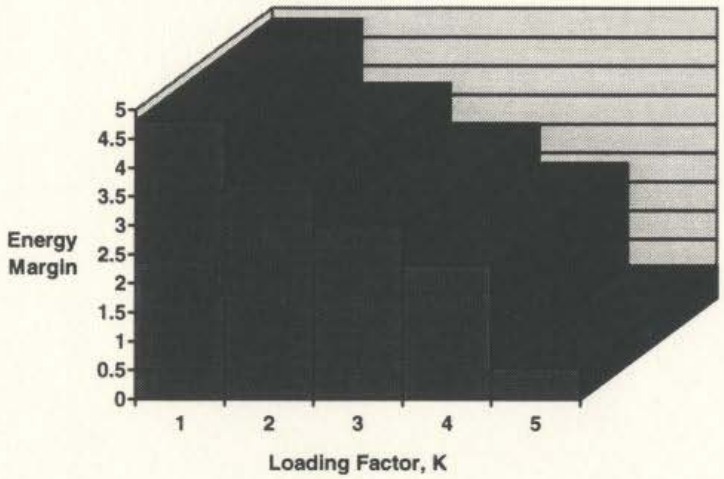

Fig. 3.6 Variation of energy Margin with loading for 5 bus system.

Figure 3.7 shows the 24 bus power system considered for study [34]. Table 3.14 shows the base case load flow results for the 24 bus system and Table 3.15 shows one low voltage solution for the base case loading.

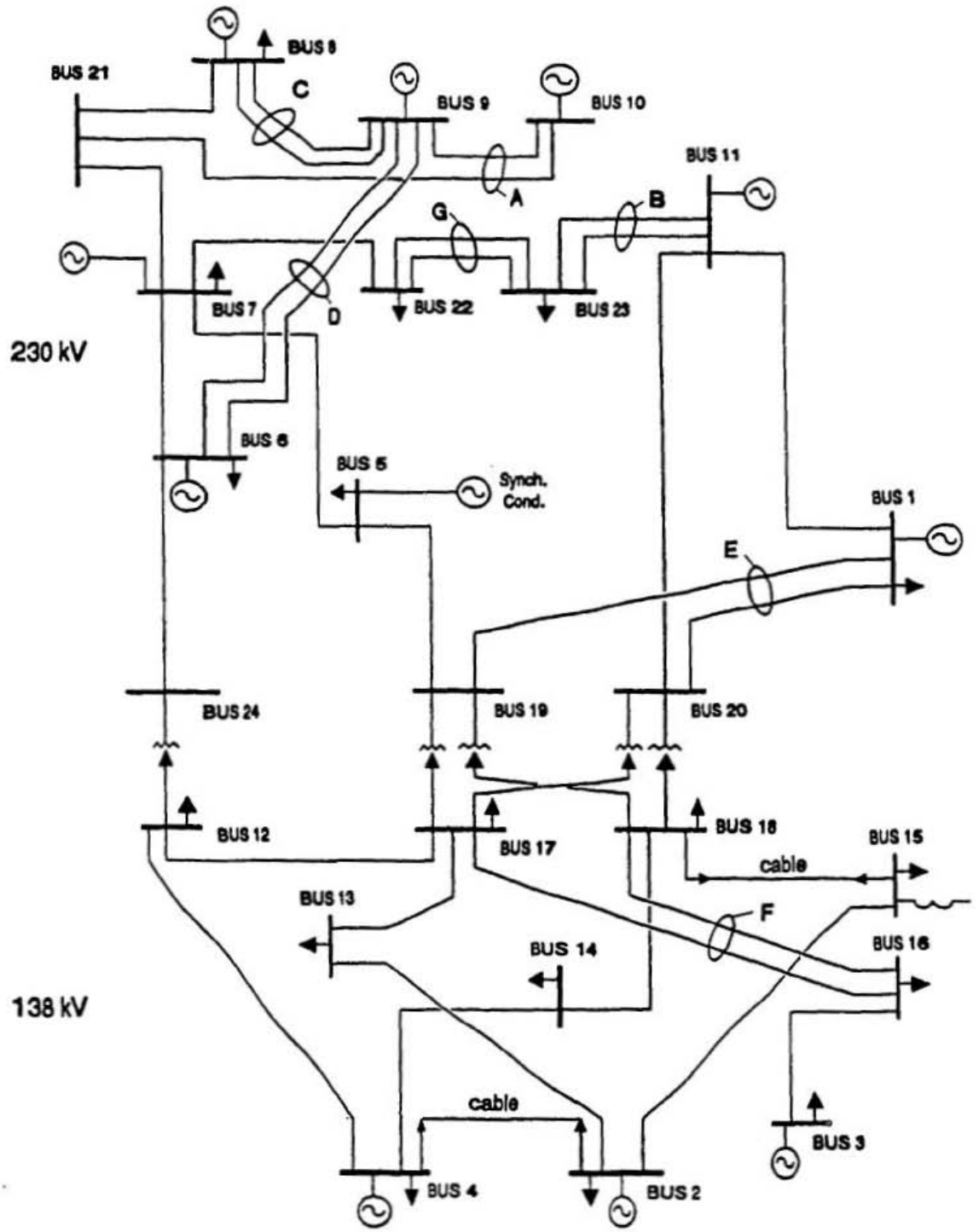

Fig. 3.7 24 Bus Power System considered for study

Table 3.14 Base Case Load Flow Results for 24 Bus system.

Bus No.	V. p.u.	Degrees	Load MW	Load MVAR	Generation MW	Generation MVAR
1	**1.0060**	**0.000**	**196.166**	**39.740**	**280.874**	**72.107**
2	**1.0027**	**-0.1320**	**71.804**	**14.805**	**62.400**	**30.496**
3	**0.9849**	**-0.1727**	**92.530**	**18.510**	**75.000**	**58.061**
4	**1.0024**	**-0.1307**	**79.949**	**16.286**	**62.400**	**24.970**
5	**0.9935**	**0.1670**	**143.609**	**28.870**	**0.0000**	**126.927**
6	**0.9400**	**0.3439**	**234.659**	**47.276**	**66.250**	**47.975**
7	**0.9500**	**0.3200**	**74.025**	**14.805**	**54.250**	**45.397**
8	**0.8910**	**0.4700**	**246.503**	**50.227**	**400.000**	**12.021**
9	**0.8892**	**0.4787**	**0.0000**	**0.0000**	**400.000**	**60.013**
10	**0.8448**	**0.5623**	**0.0000**	**0.0000**	**300.000**	**-6.605**
11	**0.9914**	**0.1305**	**0.0000**	**0.0000**	**458.500**	**-31.955**
12	**0.9909**	**0.0778**	**133.245**	**27.389**	**0.000**	**0.000**
13	**0.9623**	**-0.1280**	**54.7790**	**11.104**	**0.000**	**0.000**
14	**1.0091**	**-0.1340**	**52.5580**	**10.364**	**0.000**	**0.000**
15	**1.0825**	**-0.1440**	**100.674**	**20.727**	**0.000**	**0.000**
16	**0.9670**	**-0.1710**	**126.583**	**25.909**	**0.000**	**0.000**
17	**0.9769**	**-0.0480**	**129.543**	**26.649**	**0.000**	**0.000**
18	**1.0370**	**-0.1030**	**144.349**	**29.610**	**0.000**	**0.000**
19	**0.9930**	**0.0280**	**0.0000**	**0.0000**	**0.000**	**0.000**
20	**0.9750**	**-0.0144**	**0.0000**	**0.0000**	**0.000**	**0.000**
21	**0.9083**	**0.4260**	**0.0000**	**0.0000**	**0.000**	**0.000**
22	**0.9687**	**0.2285**	**133.985**	**27.389**	**0.000**	**0.000**
23	**0.9827**	**0.1619**	**94.7520**	**19.247**	**0.000**	**0.000**
24	**0.9549**	**0.2408**	**0.0000**	**0.0000**	**0.000**	**0.000**

Table 3.15 One low voltage solution for 24 bus system base case

Bus Number	Voltage Real Part (p.u.)	Voltage Imag. Part (p.u.)
1	**1.0060**	**0.0000**
2	**1.0603**	**-0.2128**
3	**0.97028**	**-0.2419**
4	**0.9978**	**-0.21193**
5	**1.0128**	**0.00666**
6	**0.9793**	**0.2118**
7	**0.9885**	**0.1808**
8	**0.9536**	**0.3476**
9	**0.9554**	**0.3557**
10	**0.9786**	**0.4455**
11	**0.9624**	**-0.2713**
12	**1.0054**	**-0.0228**
13	**0.9627**	**-0.2054**
14	**1.0084**	**-0.2137**
15	**1.0829**	**-0.228**
16	**0.9585**	**-0.2428**
17	**0.9848**	**-0.127**
18	**1.0405**	**-0.1826**
19	**1.0036**	**-0.0268**
20	**0.9913**	**-0.1084**
21	**0.9635**	**0.3033**
22	**0.00231**	**-0.00693**
23	**0.6210**	**-0.18247**
24	**0.9850**	**-0.12127**

The simulation results showing the variation of energy margin with loading for the 24 bus system are shown below :

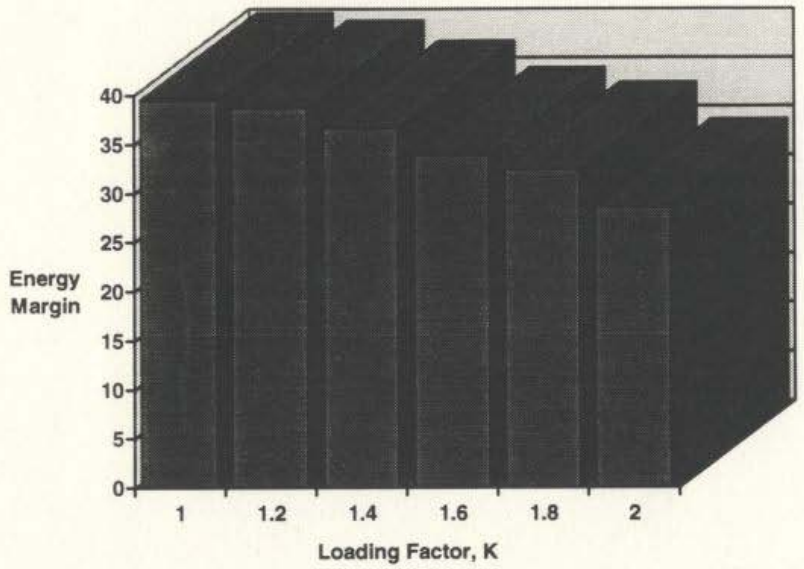

Fig. 3.8 Variation of Energy Margin with load for 24 bus system

The above three plots have presented the variation of energy margin with system loading for three different power systems. It may be realized that the magnitude of energy margin at a particular loading condition is unique to a system, i.e., a value considered large for one system may be small for another system. This is because the energy margin is intimately connected to the low voltage solutions, system parameters and loading patterns.

3.5 Effect of Contingencies on Energy Margin

The effect of contingencies on the energy margin of the 24 bus system was studied. Five of the most heavily loaded lines of the 24 bus system were identified and for each outage, the energy margin was computed. The lines considered for outage are 7 - 21, 6 - 9, 8 - 21, 6 - 24, 21 - 10. It was found that the energy margin of the system with a line outage was considerably lower than the one with no line outage. Figures showing the comparison of energy margins with and without line outages are shown below :

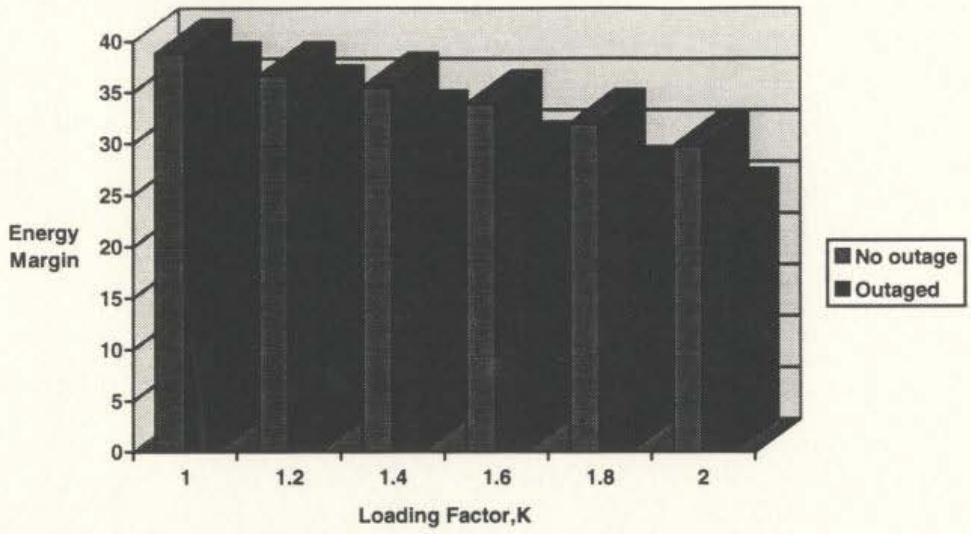

Fig. 3.9 Comparison of energy margin with line 7-21 out and with no outage

Figure 3.9 shows the comparison of energy margin with and without a line outage, for the different values of system loading. It can be seen that the energy margin for the case with a line outage is lower than that with no outage. Since the energy margin is a direct reflection of the voltage stability of a system, it can be said that a line outage has a detrimental effect on the voltage stability of a system. The energy margin is reduced due to a contingency, and thus the system is more prone to a voltage collapse.

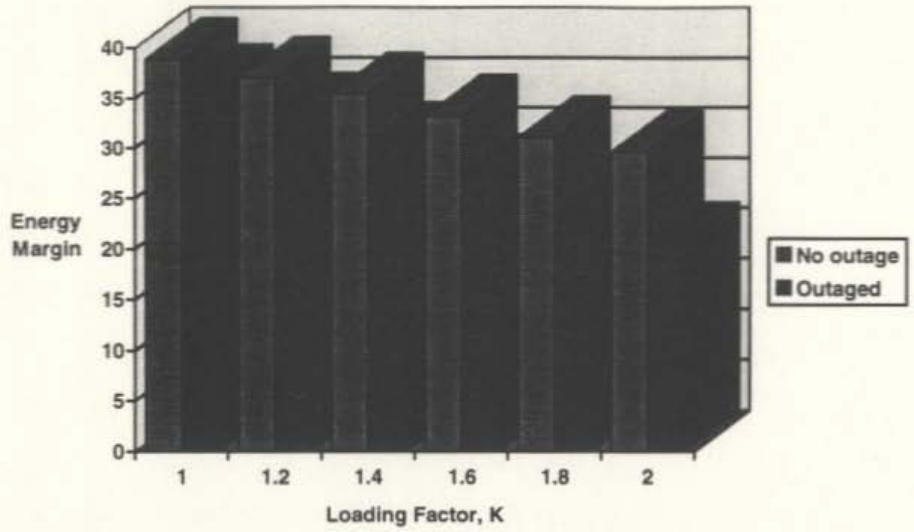

Fig. 3.10 Comparison of energy margin with line 6 - 9 out and with no outage.

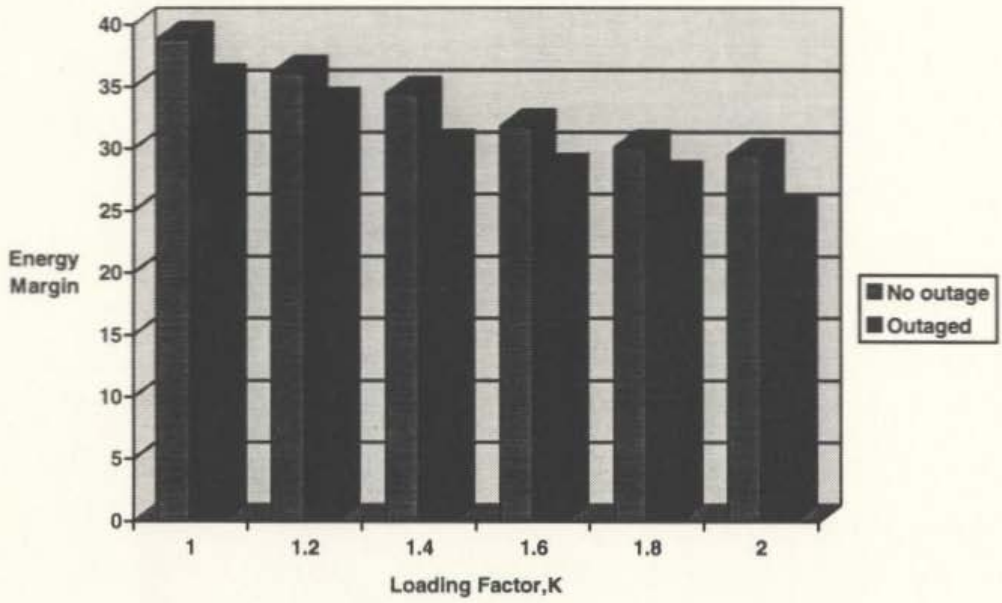

Fig. 3.11 Comparison of energy margin with line 8-21 out and with no outage

3.6 Summary

This chapter has presented the application of the energy function method as a voltage stability index and looked at the various steps involved in the computation of the index. The simplified search method to locate the low voltage solutions has been explained in detail with respect to a 5 bus system. Simulation results for computation of energy margin have been presented for a 2 bus system, 5 bus system and a 24 bus system. For the 24 bus system, simulations were repeated considering contingencies also. It was found that the energy margin is influenced significantly by contingencies and the value is considerably lower than that without any line outage.

The purpose of any voltage stability index is to serve as a tool for assessing the voltage stability of a power system. The energy margin based voltage stability index holds out considerable promise as an accurate index as it takes into account various factors that critically affect voltage stability of a power system, namely, the unstable equilibrium points, the random load disturbances, the system active and reactive loading and the system parameters. Also, the concept of energy margins is a well proven one, with successful application in transient stability studies. Thus, this index is an ideal candidate for implementation in an Energy Management System (EMS). The implementation of the energy margin based voltage stability index in an EMS environment does present some challenges, the principal one being the computational complexity. The energy margin method requires the location of the various low voltage solutions and for large scale power systems, even the simplified search method will prove to be computationally prohibitive. This is because for a n bus power system with m voltage controlled buses, even if the simplified search method is employed, 2^{n-m} power flows would have to be run to locate the low voltage solutions. This heavy computational requirement can be a burden on the capability of the EMS. Therefore, it is imperative that other approaches should be investigated, which would provide relief from the computational burden. Chapter 4 presents the application of artificial neural networks (ANNs) for evaluation of energy margins. ANNs offer an intelligent approach to evaluation of voltage stability index and can enhance the capabilities of the EMS.

Chapter 4

Artificial neural networks for voltage stability evaluation

4.1 Introduction

Voltage Instability has become an area of serious concern to system planners and operators. Even well developed systems have proved susceptible to voltage collapse, as detailed in Chapter 1. There is now a strong case for including voltage stability computation software in Energy Management Systems (EMS). In the modern day stressed power system, which is operating close to its voltage stability limits, such an on-line index would alert the system operator thus enabling corrective action to be taken to avoid a voltage collapse in the system. Other expected benefits of such an on-line index are improved security and economy of operation of the system. In fact, an on-line voltage stability index will give the system operator a very powerful tool with which to maintain a high level of system security. Due to the above cited reasons, it is expected that in the near future, Energy Management Systems will be equipped with on - line voltage stability indices.

The computation of the energy margin based voltage stability index was presented in Chapter 3. It may be seen that the method is computation intensive, since repeated load flows are required to find the low voltage solutions, even when using the simplified search method. In the context of a modern day power system, the on-line determination of the voltage stability index imposes significant computational burden on the EMS, and would require much of the capability of the Energy Management System. Thus, the implementation of the on-line voltage stability index would be at the cost of other important functions of the EMS. Hence, there is a need for investigating other approaches to implement an on-line voltage stability index.

Artificial Neural Networks (ANNs) appear to be excellent candidates as a medium for implementing an on-line voltage stability index. The main advantages of an ANN based on-line voltage stability index would be the enormous savings achieved in computation time

and effort. Also, the memory requirement of the ANN based scheme would be substantially lower than a conventional system. Recently, researchers have started showing interest in the application of ANNs for voltage stability evaluation [33, 36]. The application of an ANN will make an on-line voltage stability index feasible even for large systems. Artificial neural networks in combination with rule based expert systems can greatly enhance the overall capability of the EMS by providing "intelligent" solutions to power system problems. Of course, it is important that the problem at hand lends itself to ANN application by allowing interpolation and extrapolation to work. This chapter describes the application of a back propagation (BP) neural network to the evaluation of the energy margin based voltage stability index.

4.2 Selection of the ANN algorithm

The main criteria for the selection of the ANN algorithm are simplicity and ease of implementation, accuracy of predictions, and ease of testing. The back propagation algorithm (BP) is by far the most popular of the ANN algorithms, especially for power system applications. The back propagation algorithm does not involve complex formulae or equations and hence lends itself to implementation by any standard software. Another important factor in favor of the BP based ANN is its ability to generalize. By generalization, it is meant that once the network has been trained on a set of samples, it has the ability of recognize a new pattern. This ability is especially useful in power system applications, since the system may undergo changes from time to time, and it would be very difficult to train the network for all possible system conditions. This ability of the BP algorithm to generalize also enables easy testing of the algorithm. Once the ANN is trained, a new input can be presented to the network and the output compared to the expected value. Also, a number of high quality BP based ANN software packages are available commercially and this enables easy application of the BP based ANN to a problem. Considering all the above aspects, it was decided to implement the ANN based voltage stability index using the BP algorithm. A three layer ANN comprising of an input layer, a hidden layer and an output layer was selected for the implementation.

4.3 Selection of Input Parameters

Perhaps, the most important aspect of the implementation of an ANN based system is the selection of the input parameters. The input parameters should be such that they contain the underlying relationship, albeit, nonlinear, to the output. In other words, the input parameters should each strongly influence the output. Another important consideration, especially if it is desired to implement the ANN based system in an EMS environment is that, all the input parameters should be available in the EMS. The main consideration being that the system operator should get an idea of the voltage stability of the system from the data readily available in the EMS. Additional data acquisition equipment should not be called for, since this will increase the overall cost of the system. In chapter 3, it has been shown that the energy margin is influenced by a variety of factors like active and reactive power of the load, high and low voltage magnitudes, system parameters etc. Taking into account all the above factors, the following structure was decided upon.

The input layer of the ANN receives the input vector :

$u = [u_P, u_Q, u_{PV}]$ with

$u_P = [P_1, P_2, \ldots\ldots\ldots\ldots P_n]$

$u_Q = [Q_1, Q_2, \ldots\ldots\ldots\ldots Q_n]$

$u_{PV} = [V_{PV1}, V_{PV2}, \ldots\ldots\ldots\ldots V_{PVj}]$

where P_n , Q_n are the real power and reactive power at the n-th load bus, and V_{PVj} is the voltage magnitude at the j-th PV (Generator) bus. For the 24 bus power system, shown in Figure 3.7, the input layer received 64 inputs (the voltages at all PV buses, the active power generations at all PV buses, the active and reactive power loads at all buses). The output layer of the ANN consisted of one node, i.e., the energy margin. Thus, the neural network is designed in such a way that it can predict the energy margin for any given system operating condition, since all the above input parameters are readily available from the Energy Management System.

4.4 Training of the Neural Network

This is another important stage in the implementation of the neural network. A crucial aspect of the training of a neural network is the number of training sets used. The number of training sets should be large enough for the network to form meaningful patterns. Also, it is important to include conditions like different loading conditions, different generations, different values for slack bus and PV buses etc. in the training set. This will help enhance the generalization ability of the network. For the 24 bus power system, a number of training sets were generated considering a variety of operating conditions such as varying load power factor, different voltage magnitudes of the PV buses, different system loads etc. For each such condition, the loading factor, K , (K is the multiple of the load with respect to the base case load) was varied from 1 to the point of divergence of the load flow solution, in discreet steps. Thus, a wide range of operating conditions were selected as the training input. A total of 175 training sets covering all the above mentioned system conditions were used for training the network.

Another important aspect of the training of a BP based neural network are the training parameters, namely, the learning rate and the training tolerance. These factors greatly affect the efficiency of training and also the performance of the network. A low value of learning rate will result in enormously large training times, while a very high learning rate may result in instability. Usually, it is advisable to use a learning rate of 1.0 at the start of training. After the network has learnt about 80 % of the training facts, the learning rate can be slightly reduced. It is found that this results in overall reduction of the total training time. The training tolerance defines the error permitted in the output during the training stage. A high value of training tolerance will result in an inaccurate network, but also will reduce the training time considerably. A low value of training tolerance, while improving the accuracy, will correspondingly increase the training times. In fact, training tolerances below a 'threshold' value will result in the network not training at all. Thus, the learning rate and training tolerance should be selected judiciously taking into account the need for accuracy as well as reasonable training times.

The software package used was Brainmaker [37], marketed by California Scientific Software Inc. Brainmaker uses the Backpropagation algorithm and has many features that make it user friendly and permits easy handling and editing of input data. The salient features of Brainmaker are :

1) The Netmaker Toolbox, which permits editing of the input data, and converts it into a form compatible with the Brainmaker package. Netmaker permits data to be presented in analog form, which is a big advantage as compared to other software packages. Also, normalization of data is automatically performed by Netmaker. Additionally, Netmaker has facilities for specifying data as input, output or irrelevant.

2) Once Netmaker has organized the data into a form acceptable to Brainmaker, the file is transferred to Brainmaker. Brainmaker has facilities for specifying the training parameters such as learning rate, training tolerance and transfer function. Brainmaker permits changing of learning rate and training tolerance while training is going on. Various transfer functions like sigmoid, linear threshold, step function, linear and gaussian are available in Brainmaker. The number of hidden layers can also be adjusted to meet system requirements. For example, if the number of inputs are large, it may be useful to increase the number of hidden layers. Thus, this feature enables the user to alter the system architecture based on experience. Brainmaker also creates a test file by taking a specified percentage of data from the input data file and also periodically tests the network.

In the case of the 24 bus system, the initial learning rate was chosen as 1.0. After about 80 % of the facts were learnt, the learning rate was changed to 0.9. The above step was performed for training tolerances of 0.1 and 0.075. The transfer function selected was sigmoid (Figure 2.2) , which is the most popular one for BP applications. For an ANN package running on a PC- 486 machine, the training time for a tolerance of 0.1 was 45 minutes, while that for a tolerance of 0.075 was about 70 minutes. Table 4.1 shows one set of input training data. In Table 4.1, V stands for voltage, P_L for active power, Q_L for reactive power, and P_G for active power generation. The subscripted numerals indicate the bus number. The energy margin corresponding to the data in Table 4.1 is 36.081.

Table 4.1 Table showing the input parameters for one set of input training data.

V_2	V_3	V_4	V_5	V_6	V_7	V_8	V_9	V_{10}	V_{11}
1.023	1.01	1.022	1.015	1.002	1.005	1.015	1.02	1.03	1.00
P_{L2}	P_{L3}	P_{L4}	P_{L5}	P_{L6}	P_{L7}	P_{L8}	P_{L9}	P_{L10}	P_{L11}
0.718	0.925	0.799	1.345	2.346	0.740	2.469	0.800	0.140	0.712
P_{L12}	P_{L13}	P_{L14}	P_{L15}	P_{L16}	P_{L17}	P_{L18}	P_{L19}	P_{L20}	P_{L21}
1.332	0.548	0.525	1.006	1.265	1.295	1.443	0.891	0.726	0.918
P_{L22}	P_{L23}	Q_{L2}	Q_{L3}	Q_{L4}	Q_{L5}	Q_{L6}	Q_{L7}	Q_{L8}	Q_{L9}
1.339	0.947	0.387	0.499	0.499	0.775	1.26	0.399	1.33	0.92
Q_{L10}	Q_{L11}	Q_{L12}	Q_{L13}	Q_{L14}	Q_{L15}	Q_{L16}	Q_{L17}	Q_{L18}	Q_{L19}
0.718	0.629	0.718	0.295	0.543	0.682	0.689	0.778	0.498	0.124
Q_{L20}	Q_{L21}	Q_{L22}	Q_{L23}	P_{G2}	P_{G3}	P_{G4}	P_{G5}	P_{G6}	P_{G7}
0.421	0.821	0.735	0.519	0.624	0.75	0.62?	0.542	0.50	0.542
P_{G8}	P_{G9}	P_{G10}	P_{G11}						
4.00	4.5	3	4.584						

4.5 Test Results

After the training of the network, the network was tested on data it had not seen before. This included system loading at different power factors, different values of loading factor and PV bus voltage. The tests were conducted on networks trained on tolerances of 0.1 and 0.075. The test results for both cases are presented below .

Figure 4.1 illustrates the performance of the trained ANN for prediction of energy margins. Input patterns for which the network had not been trained were presented to the network, trained with tolerances of 0.1 and 0.075. The predictions of the ANN for both tolerances are plotted along with the expected or calculated value of the energy margin. It may be seen that the predicted value closely matches the expected value. Though the

network was tested with over 20 test inputs, Figure 4.1 shows only seven sample cases and the results.

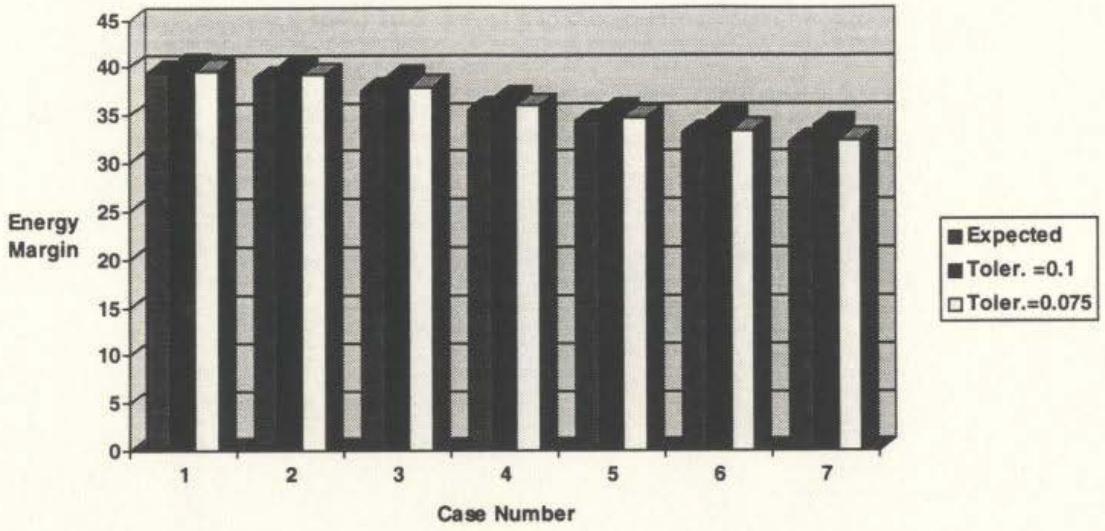

Figure 4.1 Neural Network Performance Evaluation

It may be seen that the predicted value of energy margin closely matches the expected value for both training tolerances, though the tolerance of 0.075 gives more accurate results. Table 4.2 shows some of the important design parameters of the neural network.

Table 4.2 : Design parameters for the Neural Network.

Power System Considered	24 Bus system
Number of layers	Three
Number of input parameters	**64**
Number of output(s)	**One**
Number of training sets	**175**
Learning Rate	**1.0**
Transfer Function	**Sigmoid**
Training Tolerance	**0.075 and 0.1**

As can be seen from Table 4.1, the ANN consisted of an input layer, a hidden layer and an output layer. The input and hidden layers have identical structures in that the number of nodes is equal to the number of inputs. Choosing the number of hidden layers is largely a matter of experience and experimentation. If, after training, the output results indicate that the ANN is not able to map the relationships accurately, it might be worthwhile to change the number of hidden layers. For the work reported in this thesis, it was seen that one hidden layer was adequate to obtain accurate results. The output layer had only one node, i.e., the energy margin. To fully appreciate the effect of training tolerance on the prediction accuracy of a neural network, it is necessary to compare the percentage error in prediction of the two tolerances. Figure 4.2 compares the percentage errors in prediction of the network for tolerances of 0.1 and 0.075. It is seen that the prediction accuracy of the network trained with a tolerance of 0.075 is much higher than that trained with a tolerance of 0.1. Though, this comes at the expense of longer training times, the greatly increased accuracy in the predictions should compensate for this.

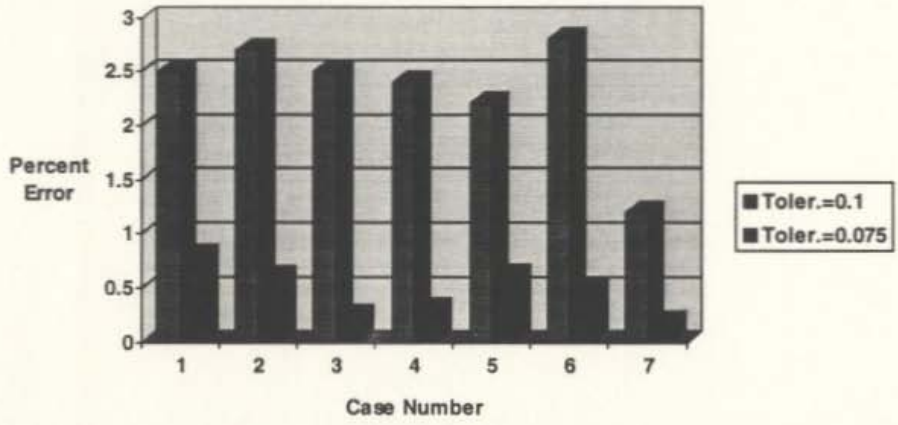

Fig. 4.2 Comparison of percentage prediction error for two tolerances

4.6 ANN models considering system contingencies

Chapter 3 described the effect of contingencies on the energy margin of the system . An attempt has been made to construct an ANN model for evaluating the effect of contingencies on the energy margin. A separate ANN is used to represent each contingency. The training set for this ANN was generated as follows. A contingency was simulated and the energy margins corresponding to this contingency condition were calculated for a variety of system operating conditions such as different power factors, different system loading, different values of PV bus voltages and PV bus generations. The input parameters were selected to be the active and reactive powers of PV and PQ buses, the voltages at the PV buses and the generations at the PV buses. Sixty training sets were generated for each contingency. Five such ANN models were constructed to represent five line outages. The lines considered for outage are 7 -21, 6 -9, 8 - 21, 21 - 10, 6 - 24. The performance results for the ANN models are shown in Figures 4.3 to 4.6

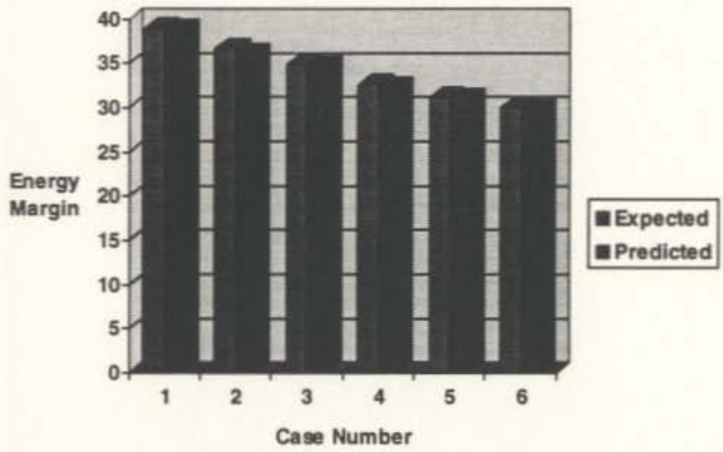

Fig. 4.3 Neural Network Performance considering outage of line 7 - 21

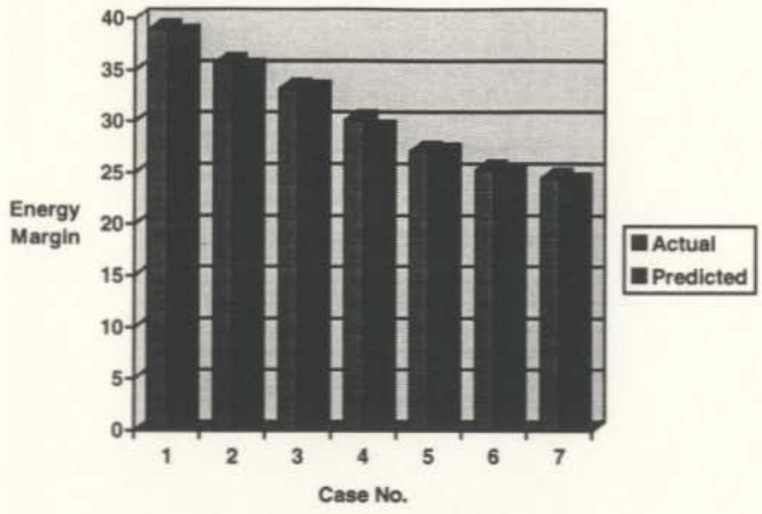

Fig. 4.4 Neural Network considering outage of line 6 - 9.

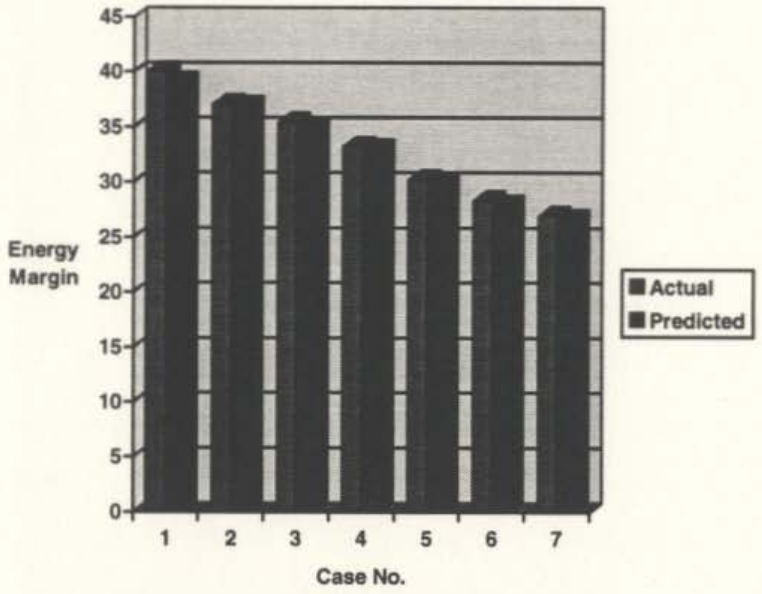

Fig. 4.5 Neural Network Performance with line 8-21 out

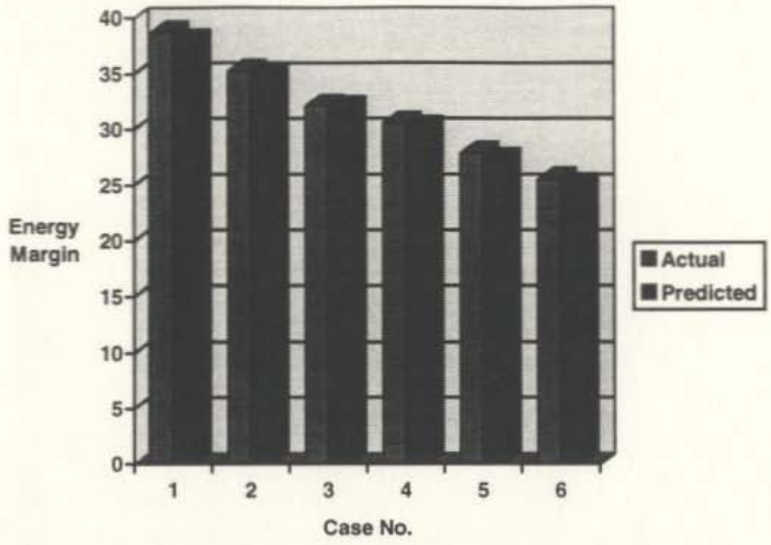

Fig. 4.6 Neural network performance with line 21 - 10 out.

The above ANNs were designed with a training tolerance of 0.075. It can be seen that the prediction accuracy of the ANNs are indeed very high, with the predicted value closely matching the expected value. As observed in Chapter 3, the energy margin is lower for the system with contingencies, as compared to a system with no outage.

4.7 Application in an EMS Environment

As mentioned in Chapter 2, an on-line voltage stability index would be a very useful tool to the system operator in avoiding incidents of voltage collapse. An on-line voltage stability index implemented as part of an Energy Management System (EMS), can complement other functions of the EMS like optimal power flow, unit commitment, network control, and make use of the system parameters already monitored. However, the main challenge for the implementation of an on-line voltage stability index has been the computational complexity involved in the context of the modern day power system. This is where ANNs can play an important role in making possible an on-line voltage stability index, without the associated computational burden. The ANN based stability index uses input parameters already monitored by the EMS, and thus does not require additional data acquisition equipment. More importantly, ANNs can bring in a different perspective to the

operation of an EMS in that they can upgrade the " intelligence" of the EMS by virtue of their inherent properties. By judicious selection of training sets, ANNs can be trained to recognize virtually any system condition without adding to the computational burden.

Figure 4.7 shows the block diagram of the proposed scheme integrating the ANN based voltage stability evaluation system into the EMS. The Remote Terminal Units (RTUs) collect the various data from various locations in the power system and relay them to the Supervisory Control and Data Acquisition system (SCADA). The SCADA takes various control actions like switching on and off of circuit breakers, transformer taps, capacitor banks etc. The SCADA is connected to the Man Machine Interface (MMI), which allows the operator to interact with the EMS. The ANN based voltage stability evaluator gets its inputs from the SCADA. The inputs required for the ANN, like active and reactive power at load points, the power generation, and voltage at the PV buses are readily available from the SCADA system. The ANN based system, after performing the voltage stability evaluation, alerts the system operator to any potentially dangerous situation, so that corrective action can be taken.

Figure 4.7 indicates the possible architecture of an ANN based Energy management system.

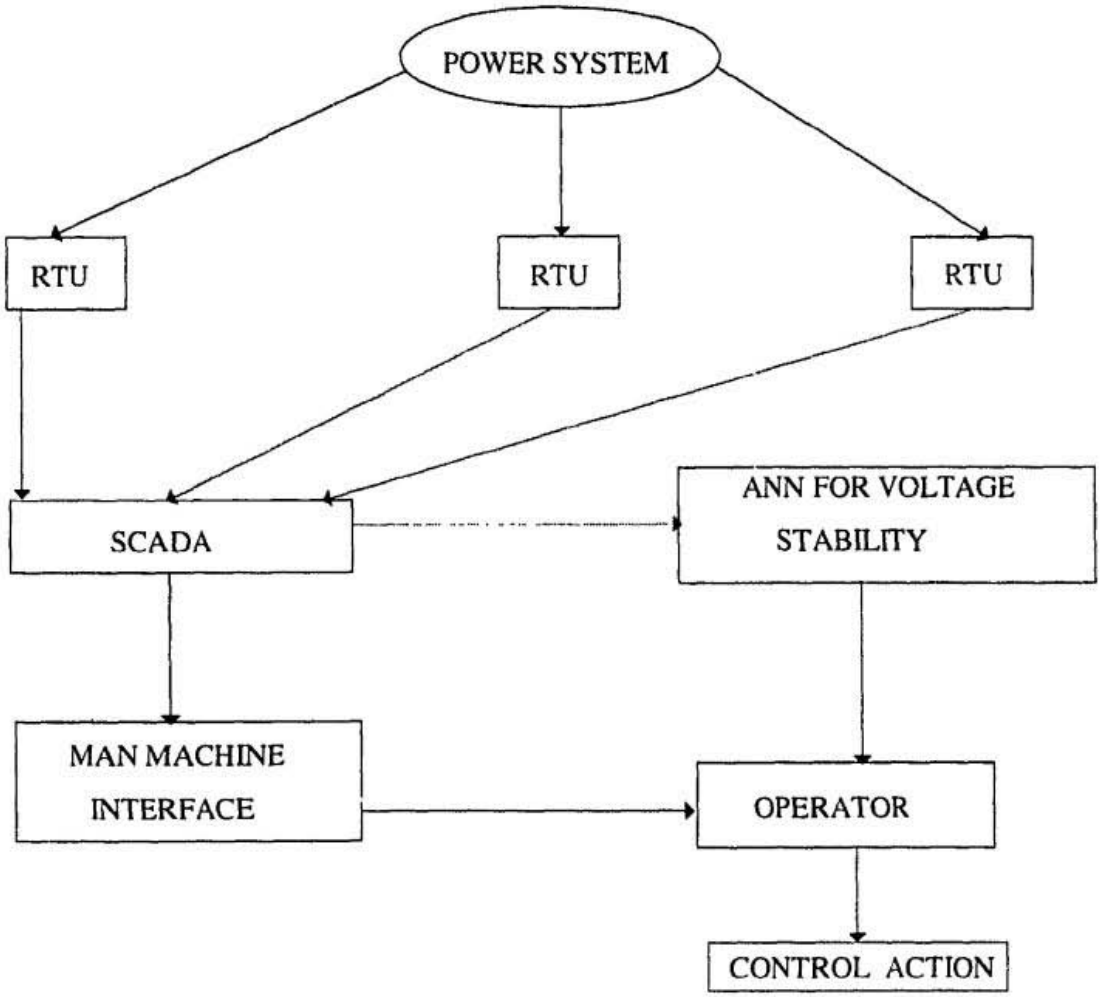

Figure 4.7 Block Diagram for integrating ANN based voltage stability monitor into EMS.

4.8 Summary

This chapter has presented results on the ANN implementation of a system to evaluate the voltage stability of a power system. The prediction accuracy of the ANN is quite high and closely matched the calculated value. The highest percentage error encountered was only 7 %, and it is believed that this error can be further reduced by training the network with a larger training set. Also, it is seen that the training tolerance

influences the prediction accuracy to a considerable extent. A lower training tolerance leads to more accurate results, but comes at the expense of a higher training time.

The input parameters presented to the network are readily available from the EMS, thus lending this model to easy application in an EMS environment. The effect of training parameters like learning rate and training tolerance on the network performance was studied, and optimum parameters were selected. ANN models were also implemented for contingencies, with a separate ANN being used for a contingency. Here too, the ANN model gave good results in predicting energy margins from system parameters.

Chapter 5

Application of Load Margin Method for Evaluating Voltage Instability

5.1 Introduction

The voltage stability of a power system is intimately connected to the system loading, and has indeed been called load stability. The power system moves closer towards instability as the loading increases and at a particular loading point, it loses stability. The Jacobian of the load flow equation at this point is singular. Conventional voltage stability indices have been developed to provide an indicator of the voltage stability of the system, based on the system conditions. They typically provide a numerical value of the index, which in most cases in unique to a system. For example, the index based on the minimum singular value [13], provides a value based on the singular value decomposition of the Jacobian at that operating point. The energy margin method provides a value, which is unique to the system. In both the above cases, it is essential that the operator is aware of the significance of the numerical value of the index obtained from the EMS. In other words, it would be helpful if the operator has a reasonable amount of expertise in the analysis of voltage instability. This would help the operator in appreciating the situation better. However, this may not always be possible and hence there is a need for an index which can provide a Mega Watt (MW) margin to instability. This would be an extremely useful tool in an EMS environment, as it would give the system operator the load margin the system has before it moves irrevocably into collapse. This aspect is important from the point of view of the current trend to keep the user interface of the EMS as simple and direct as possible.

Most currently available voltage stability indices compute the voltage stability by uniformly increasing the load until the singularity of the Jacobian is reached. Thus, in most cases, the point of collapse, as given by these indices, will correspond to the point of maximum system loading possible. However, the MW margin obtained from this point may not be a true indicator. This is because of the fact that the system load need not always increase uniformly. The direction or pattern of increase is of great importance in

$$f(x, \rho) = g \begin{bmatrix} V \\ \theta \end{bmatrix} - \begin{bmatrix} P \\ Q \end{bmatrix} = 0 \qquad (5.1)$$

where

$$x = \begin{bmatrix} V \\ \theta \end{bmatrix} \qquad \rho = \begin{bmatrix} P \\ Q \end{bmatrix}$$

Here x is the system state vector, and ρ is the parameter vector whose elements are active and reactive load power, and active generator power. Let J_x and J_ρ be the Jacobian matrices of the vector function f with respect to x and ρ respectively. For a given parameter vector ρ_i, a system state vector x_i can be obtained by solving equation (5.1). Each parameter vector ρ_i represents a specific system condition in terms of active and reactive loads, and active generation. The system reaches its voltage stability critical point if the parameter vector ρ^* and the corresponding system state vector x^* are such that the power flow Jacobian matrix J_x is singular. Let S denote the hypersurface in the N dimensional parameter space such that $J_x(x^*, \rho^*)$ is singular if ρ^* is a point on S.

Given an initial system operating point (x_0, ρ_0) , we have to find the parameter vector ρ^* on S such that the distance between ρ_0 and ρ^* , $k = |\rho \cdot - \rho_0|$, is a local minimum for the distance between ρ_0 and S.

Assuming that S is a smooth hypersurface near ρ^*, a normal vector to this hypersurface at (x^*, ρ^*) is given by

$$\eta^* = w_x J_\rho \qquad (5.2)$$

where w^* is the left eigenvector of $J_x (x^*, \rho^*)$ corresponding to the zero eigenvalue. And η^* is normalized such that $|\eta \cdot| = 1$. Starting from the initial system operating point (x_0,ρ_0) , the system is stressed by incrementally increasing ρ along a particular direction. Each time ρ is increased, equation (5.1) is solved to obtain the system state vector x. And ρ is continuously increased along the same direction until, at the voltage stability critical point (x^*, ρ^*) the power-flow Jacobian matrix J_x becomes singular; that is

$$\rho^* = \rho_0 + k\eta \tag{5.3}$$

where k is the distance between the initial system operating point (x_0, ρ_0) and the voltage stability critical point (x^*, ρ^*) as $k = |\rho^* - \rho_0|$.

For a given initial system operating point (x_0, ρ_0), ρ can be increased along different directions. Obviously, the value of k depends on the direction along which ρ is increased. The objective is to find the direction of the parameter vector ρ such that k is the local minimum.

The following procedure determines the vector η^* along which the distance between the initial equilibrium point (x_0, ρ_0) and the singular point (x^*, ρ^*) is the shortest :

1. Let η_0 be an initial guess for the direction η^*, $\eta_0 = 1$.
2. Stress the system by incrementally increasing ρ along the direction of η, until J_x becomes singular; that is, determine k_i , ρ_i and x_i so that $\rho_i = \rho_0 + k_i \eta_i$ is on the surface S.
3. Set $\eta_{i+1} = w_i J_\rho$, and $|\eta_{i+1}| = 1$.
4. Iterate steps 1, 2 and 3 until η_i converges to a value η^*. Then, $\rho^* = \rho_0 + k^* \eta^*$ is the corresponding equilibrium condition.

The above described procedure is illustrated on a simple 2 bus power system shown in Fig. 5.1.

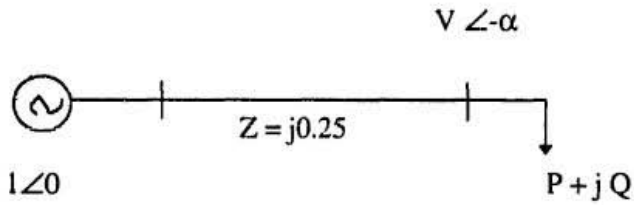

Fig. 5.1 A simple radial system

Corresponding to equation 5.1 , we have

$$f(x,\rho) = \begin{bmatrix} 4V\sin\alpha - P \\ 4V\cos\alpha - 4V^2 - Q \end{bmatrix} = \begin{bmatrix} 0 \\ 0 \end{bmatrix} \tag{5.4}$$

with

$$x = \begin{bmatrix} V \\ \alpha \end{bmatrix} \quad \text{and} \quad \rho = \begin{bmatrix} P \\ Q \end{bmatrix} \tag{5.5}$$

The Jacobian matrices are

$$J_x = \begin{bmatrix} 4V\cos\alpha & 4\sin\alpha \\ -4V\sin\alpha & 4\cos\alpha - 8V \end{bmatrix} \tag{5.6}$$

and

$$J_\rho = \begin{bmatrix} -1 & 0 \\ 0 & -1 \end{bmatrix} \tag{5.7}$$

The determinant of J_x is

$$\det(J_x) = 16\,V - 32\,V^2 \cos\alpha \tag{5.8}$$

On the singular surface S , $\det(J_x) = 0$, that is,

$$16\,V - 32\,V^2 \cos\alpha = 0$$

or $$V = \frac{1}{2\cos\alpha} \tag{5.9}$$

Equation (5.8) describes the relationship between V and α when J_x is singular. From equations (5.4) and (5.8) , we have the following expression describing the singular surface S in the parameter space :

$$P^2 + 4Q - 4 = 0 \tag{5.10}$$

Assume that the system has the initial condition given below :

$P_0 = 0.8$ $\quad Q_0 = 0.4$ $\quad V_0 = 0.8554$ $\quad \alpha_0 = 13.52^0$

Table 5.1 shows the iterative process of finding the point of voltage instability which is closest to the initial operating condition .

Table 5.1 Calculation of shortest distance to instability for system in Fig 5.1 [40]

Iteration	Left eigen vector η_i	The distance to Instability (k_i)	P_i , Q_i
1	**0.9725 - 0.2331**	**1.0725**	**1.8430, 0.1500**
2	**0.6776 - 0.7354**	**0.4173**	**1.0828, 0.7069**
3	**0.4869 - 0.8735**	**0.4061**	**0.9977, 0.7541**
4	**0.4443 - 0.8959**	**0.4024**	**0.9788, 0.7605**
5	**0.4405 - 0.8977**	**0.4016**	**0.9769, 0.7605**
6	**0.4378 - 0.8991**	**0.4015**	**0.9758, 0.7610**

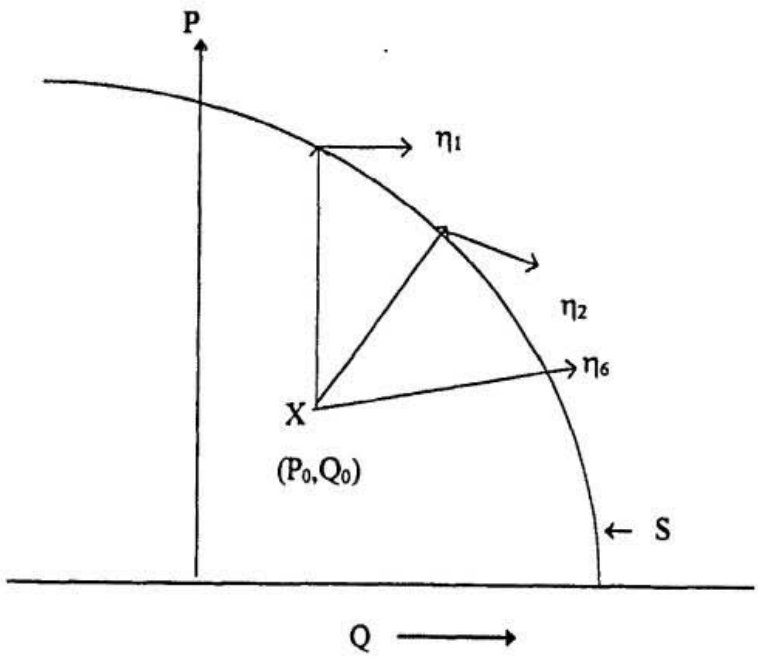

Fig. 5.2 Singular surface S in the P-Q plane

the initial operating condition. The surface S represents the locus of all combinations of P and Q which result in singularity of the Jacobian. All points below S represent voltage stable conditions and all points above S represent unstable conditions. The figure shows three different directions of load increase. If the load was increasing in the direction shown by the vector η_1, the load margin (MW at the singular point - MW at the current operating point) is quite high. However, if the load direction is given by either η_2 and η_6, it can be seen that the singular surface is quite close and hence the load margin is considerably lesser than that for η_6. Thus, the direction of load increase is an important factor in determining the minimum distance to collapse.

Knowing the direction of the nearest instability point is of great use to system operators, since they can identify dangerous loading trends which may push the system faster towards collapse. If the system loading is in a direction that will bring on the collapse quicker than that for a uniform load increase, then the system operators can take immediate remedial action before the situation becomes critical.

5.4 General Description of the procedure

For any system, the general procedure for finding the minimum distance from an initial load level P_0, Q_0 to the singular surface S is as follows :

1. Increase load from P_0, Q_0 in some direction until an eigenvalue of the Jacobian is practically zero. The load level P_1, Q_1 corresponding to this point is the stability limit. This point lies on or is extremely close to S.
2. For the conditions at P_1, Q_1, perform modal analysis and determine the left eigenvector of the full Jacobian matrix. The left eigenvector contains elements which provide the increments of MW and MVAR load for each bus. The eigenvector points in the shortest direction to singularity, which is therefore normal to S.
3. Go back to the base case load level P_0, Q_0 and load the system again, but this time in the direction given by the left eigenvector found in (2). When S is reached, a new left eigenvector is computed.

4. Again, we return to the base case P_0,Q_0 and load the system in the direction of the new eigenvector given in (3) above. This process is repeated until the computed eigenvector does not change with each new iteration. This process will then have converged.

When it has converged, the solution gives the minimum vector (P and Q) distance to S from P_0 and Q_0. This process can be applied to large systems also, however, S is no longer a simple locus, but a hypersurface in a parameter of dimension 2N, where N is the number of buses. The shape of the hypersurface is not known, hence this process may find only a local minimum.

5.5 Application to the 39 bus New England System

The above algorithm is implemented in VSTAB, a commercial voltage stability software package marketed by PowerTech Labs. The work reported in this thesis made use of the INS option of VSTAB [41] to determine the nearest instability points for the 39 bus New England System [41], which is a very popular system for testing voltage stability techniques.

The New England 39 bus system is as shown in Figure 5.3. The procedure for computation of the nearest instability point using the INS option of VSTAB is described later in this section. The procedure involves repeated solutions of the load flows as the program attempts to find a local or global minimum of the distance to instability. Thus, in most cases, a number of iterations are required.

This section also presents simulation results on the effect of variation of load on the load margin of the 39 Bus New England Power System.

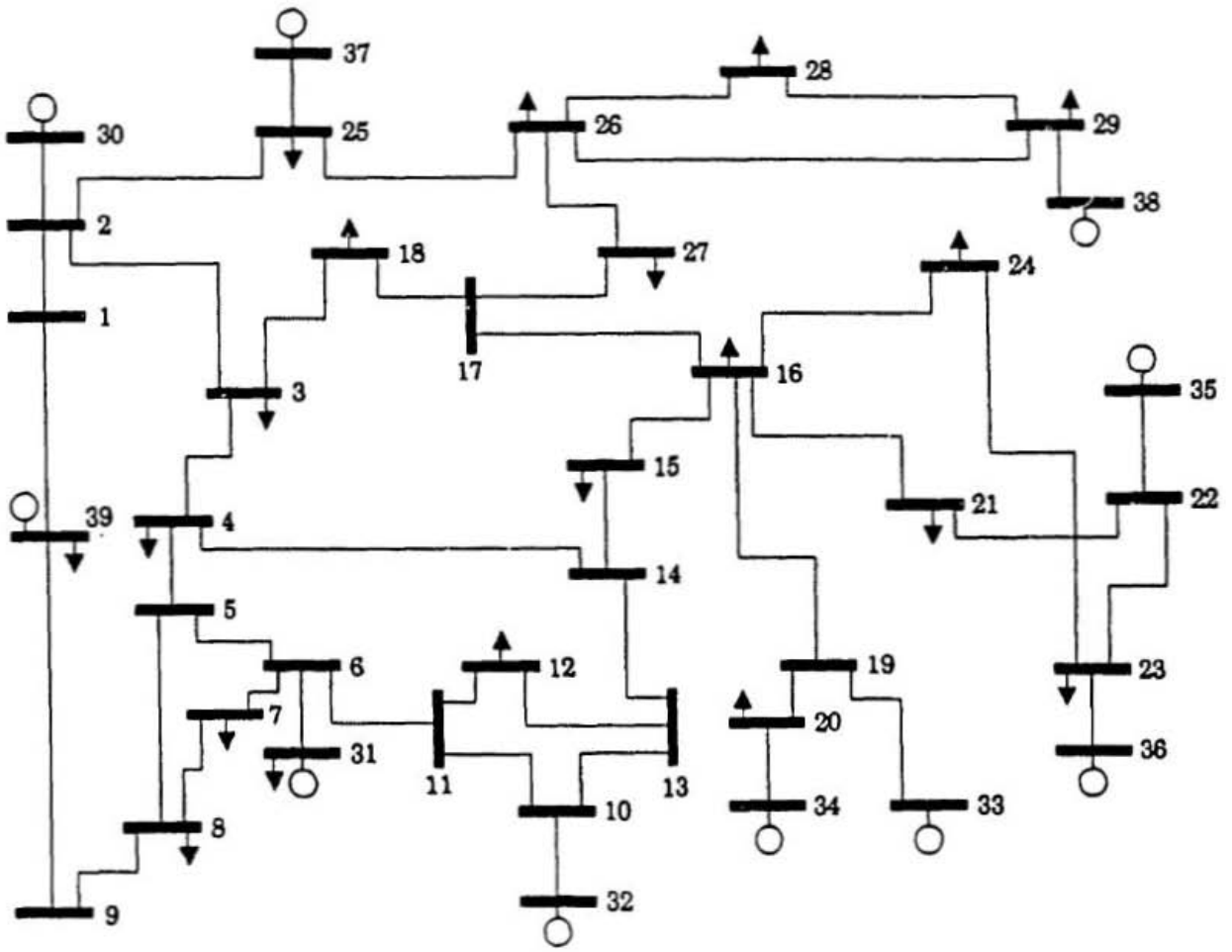

Fig. 5.3 39 Bus New England Power System [41]

The procedure for finding the nearest instability point using VSTAB is given below :

1. VSTAB requires a solved load flow as an input before proceeding with the calculations. Therefore, a solved base case load flow result of the 39 bus system was generated.

2. VSTAB requires a file with a *.prm extension, which specifies the options required. The other files required are with *.chc , *.gds, *.ins, and *.mrv which specify the loading pattern, generation, nearest instability point calculation, and parameters for modal analysis respectively.

3. The information about the load margins is contained in the *.out or *.pvt files. These files contain the load flow results and the PV curve respectively, for all the iterations.

4. VSTAB, with the nearest instability option, was run for various values of K, the loading factor.

The program requires a number of iterations to arrive at the nearest instability point for a particular operating point. This is due to the fact that repeated load flows are required for each load direction. Before arriving at the load direction leading to the nearest instability point, the program tries out various directions of load increase. Figure 5.4 shows the load margin in MW plotted against the loading factor, K.

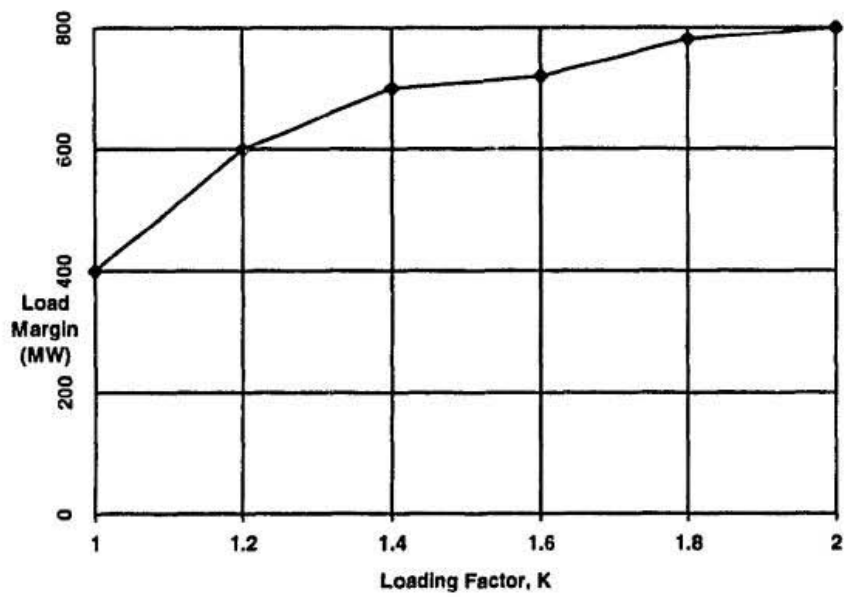

Fig. 5.4 Plot of Load Margin in M.W. against Loading Factor, K

As mentioned earlier, there is no guarantee that the program will converge to the global minimum. The results obtained may represent a local minimum in the hypersurface, as each time the program attempts to find the minimum distance to collapse. Also, the shape of the hypersurface also influences the value of the load margin. For the two bus system shown in Figure 5.1, the shape is almost a straight line. But, for a multi bus system like the 39 bus system, the shape can be quite complex and the program attempts to find the local minimums in this complex hypersurface, for each loading condition. It may be observed that there is an apparent contradiction in the figure in that the load margin is more at larger loads. This is because of the fact that the program is getting trapped in a local minimum and the shape of the hypersurface may be such that the local minimums at higher loadings are larger than that at lower loadings.

5.6 Effect of Contingencies on Load Margin of IEEE 24 bus system

The IEEE 24 bus system is shown in Fig. 5.5 [35]. The system has 10 generators and 38 lines. For different loading conditions, the load margin was determined. After that, five of the most heavily loaded lines were identified to study the effect of contingencies on the load margin . The difference between the systems shown in Figures 5.5 and 3.5 is in the bus numbering and the base case loading. The system topology remains the same.

To study the effect of contingencies on the load margin, the following procedure was adopted.

1. The input data was modified to take into account the contingency.
2. The new data file was used as input to a load flow program and the new load flow results obtained.
3. This new load flow result was used as input to the VSTAB software and the load margin determined.

This procedure was repeated for all the five contingencies and the corresponding load margins determined.

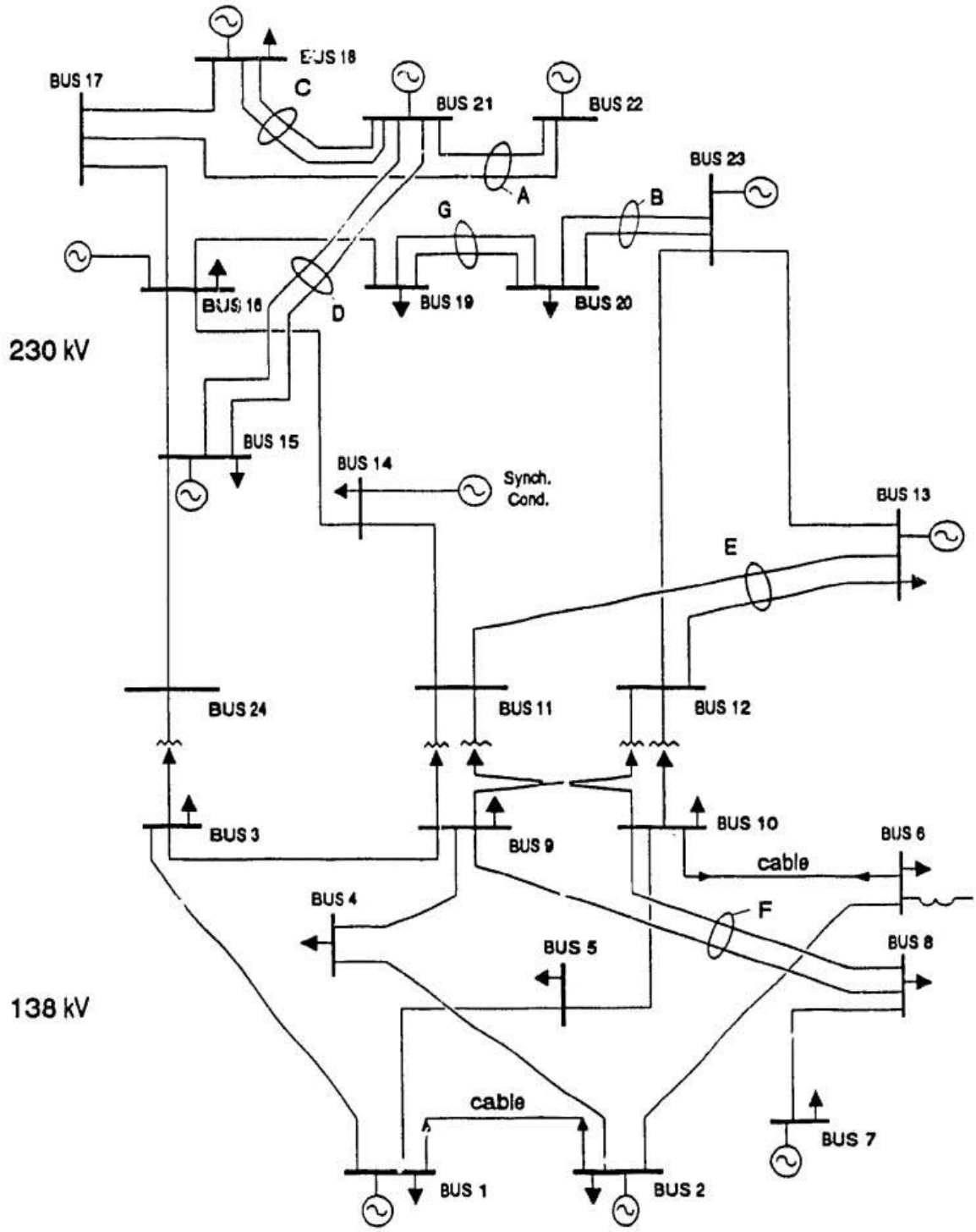

Fig. 5.5 IEEE 24 Bus Reliability Test System

Table 5.2 shows the load flow results for the IEEE 24 Bus Reliability Test System.

Table 5.2 Load flow results for IEEE 24 Bus System.

Bus No.	Voltage p.u.	Voltage Degrees	Load MW	Load MAR	Generation MW	Generation MVAR
1	1.006	0	108	22	192	78.53
2	1.023	-14.559	37.0	20.0	192.4	29.04
3	1.000	-19.51	13.0	37.0	0.000	0.000
4	1.022	-14.445	74.0	15.0	0.000	0.000
5	1.015	0.433	21.0	14.0	0.000	0.000
6	1.002	8.166	136.0	128.0	0.000	0.000
7	1.005	7.625	125.0	25.0	200.0	34.27
8	1.015	14.48	131.0	35.0	0.000	0.000
9	1.020	14.89	135.0	36.0	0.000	0.000
10	1.030	20.81	165.0	40.0	0.000	0.000
11	1.000	8.43	0.000	0.000	0.000	0.000
12	0.9672	-9.174	0.000	0.000	0.000	0.000
13	0.9870	-13.77	165.0	54.0	394.0	0.000
14	1.0122	-14.3	104.0	39.0	0.000	150.0
15	1.0140	-15.18	217.0	64.0	155.0	0.000
16	0.9782	-18.14	100.0	20.0	155.0	0.000
17	0.9832	-9.877	0.000	0.000	0.000	0.000
18	1.0217	-11.95	233.0	68.0	400.0	0.000
19	1.006	-3.619	151.0	37.0	0.000	0.000
20	0.9917	-3.18	128.0	26.0	0.000	0.000
21	1.0199	12.76	0.000	0.000	400.0	0.000
22	0.9988	7.913	0.000	0.000	0.000	0.000
23	1.0004	6.976	0.000	0.000	660.0	0.000
24	0.963	-0.138	0.000	0.000	0.000	0.000

Table 5.3 shows the loadings of the lines selected for outage for base case loading.

Table 5.3 Loadings of lines selected for outage in IEEE 24 bus system.

Line	Line Loading (MW + j MVAR)
1 - 5	**58.85 + j 5.85**
1 - 3	**45.68 + j 6.43**
2 - 6	**67.03 + j 5.57**
2 - 4	**67.75 + j 11.52**
7 - 8	**75.06 + j 29.49**

Table 5.4 shows the load margin for outage of each line. Load Margin without contingency for base case load was 387 MW.

Table 5.4 Variation of load margin with line outage for base case load.

Line Outaged	Load Margin
1 - 5	**316 MW**
1 - 3	**360 MW**
2 - 4	**313 MW**
2 - 6	**163 MW**
7 - 8	**234 MW**

Thus, it is seen that the load margin is affected to a considerable degree by line outage. This means, that in the event of a line outage, the load margin available to the system is reduced and the system may reach the collapse point more quickly. Similar tests were conducted on the 24 bus system, but with different system loading conditions. In all cases, the load margin after an outage was found to be considerably lower than that without an outage.

5.7 Summary

This chapter has presented the detection of the nearest instability point or the load margin for the 39 bus New England System and the IEEE 24 bus power system. It can be seen that the load margin is a useful tool for the system operator in identifying potentially dangerous system conditions. The nearest instability point determined need not always correspond to the global minimum. This is because of the fact that for large systems, the hypersurface of the singularity locus is quite complex and may be uneven. Simulations were carried out on the IEEE 24 bus system to study the effect of contingencies on the load margin. The load margins are considerably reduced in the event of line outage. This has important implications from the point of view of a system operator, in that the operator has to resort to corrective measures to prevent the system from moving closer to collapse in the event of a contingency. The next chapter will describe the application of artificial neural networks for evaluating load margins.

The implications of knowing minimum load power margins are significant. These margins represent the true worst case load increases for system loadability with respect to voltage collapse. In other words, these margins give the operator the maximum load in MW the system can take, before sliding into instability. This is as opposed to other voltage instability indices, which give only a numerical value of the index and do not provide any information on the power margin available. Thus, determining the minimum load margins can help the operator in taking corrective control actions as soon as the margin reaches a critical value. This critical value can be based on the MW and MVAR reserves available in the system.

Chapter 6

Artificial Neural Networks for Evaluation of Load Margins

6.1 Introduction

As mentioned in Chapter 5, most of the currently available methods for voltage stability evaluation compute the voltage stability index by uniformly increasing the load until the singularity of the Jacobian is reached. Effectively, this means that the point of collapse given by these indices will correspond to the point of maximum system loading possible assuming that the loads increase uniformly. However, in practice, the system load does not increase uniformly. The utility has very little control on the direction of load increase. It would be very helpful if the system operators can know the worst case load increases for system loadability with respect to voltage collapse. The load margin index presented in Chapter 5 is thus a very useful tool for the system operator since it gives in MegaWatt terms the maximum load the system can take before sliding into instability. Other voltage stability indices give only a numerical value of the index and do not provide any information on the power margin available. The information on minimum load margins available can help the operator in taking corrective control actions as soon as the load reaches a critical value. This critical value depends on the MW and MVAR reserves available in the system.

The computation of load margins was presented in Chapter 5. It can be seen that the method is computation intensive since numerous load flows and iterations are required before the program converges to a local or global minimum. Thus the implementation of an on-line load margin index in an Energy Management System (EMS) environment presents a considerable challenge.

Artificial Neural Networks (ANNs) present the possibility of implementing an on-line voltage stability index. Chapter 2 presented the application of ANNs to different power system problems like transient stability evaluation, load forecasting, fault diagnosis etc. An ANN based on-line voltage stability index in an EMS environment would result in

considerable savings in computation time and effort. An ANN based approach can make an on-line load margin index feasible even for large power systems. This is due to the fact that a trained ANN requires very little computation time or memory. This chapter describes two neural network models designed to evaluate the load margins.

6.2 Selection of the ANN algorithm

The different aspects of the selection of a suitable ANN algorithm have been detailed in Chapter 4. Based on those considerations, it was decided to use the back propagation algorithm for evaluating load margins.

6.3 Selection of Input Parameters

The selection of the input parameters is a crucial aspect in the implementation of an ANN based system. The input parameters should be such that they should strongly influence the output and have an underlying relationship to the output. Since the ANN based load margin index is to be implemented in an EMS environment, it is important that all the input parameters should be available in the EMS without the use of additional data acquisition equipment. In chapter 5 it was seen that the load margin was influenced by the direction and magnitude of the load increase and also the reactive power generation. Taking into account the above factors, the following structure was decided .

The input layer of the ANN receives the input vector :

$u = [\, u_P,\ u_Q,\ u_{PV} \,]$ with

$u_P = [\, P_1, P_2, \ldots\ldots\ldots P_n \,]$

$u_Q = [\, Q_1, Q_2, \ldots\ldots\ldots Q_n \,]$

$u_{PV} = [V_{PV1}, V_{PV2}, \ldots\ldots\ V_{PVj}\,]$

where P_n , Q_n are the real power load and reactive power load at the n-th bus, and V_{PVj} is the voltage magnitude at the j-th PV bus. For the 39 bus New England System, the input layer received 60 inputs (the voltages at all PV buses, the active power generations at all PV buses, the MW and MVAR loads at all buses). For the IEEE 24 Bus Reliability System, the output in both cases is the corresponding load margin.

6.4 Training of the Neural Network

The strategy for training a neural network has already been outlined in Chapter 4. For the 39 bus power system, a number of training sets were generated considering a variety of operating conditions, such as varying load power factor, different voltage magnitudes of the PV buses, different system loads etc. For each such condition, the loading factor, K, (loading factor is the multiple of the base case loading) is calculated. A wide range of operating conditions were selected as the training input. A total of 170 training samples were used as the training set. For the 39 bus system, the initial learning rate was chosen as 1.0. After about 80 % of the facts were learned, the learning rate was reduced to 0.9.

The Brainmaker Package, marketed by California Scientific Software and described in Chapter 4, was used to implement the ANN model. For the 39 bus system, the sigmoid transfer function was used and the number of hidden layers was specified as one.

6.5 Test Results for the 39 Bus New England Power System

After the training of the network, the network should be tested on data it had not seen before. This included system loading at different power factors, different values of loading factor, and PV bus voltage. Table 6.1 shows one such training set, for the New England 39 Bus system, which consists of 60 inputs.

In Table 6.1, V represents the voltage at the PV (voltage controlled) buses, P_L represents the active power in p.u., Q_L represents the reactive power and P_G represents the active power generation in p.u. The output, i.e., the load margin is also specified in p.u. For the specific set of input training data, the output was 3.98 p.u. 170 such input and output data pairs representing a wide spectrum of system operation were used for training the input.

Table 6.1 One set of input training data.

V_{29}	V_{30}	V_{32}	V_{33}	V_{34}	V_{35}	V_{36}	V_{37}	V_{38}	V_{39}
1.0475	0.982	0.9831	0.9972	1.0123	1.0493	1.0635	1.0278	1.0265	1.03
P_{L3}	P_{L4}	P_{L7}	P_{L8}	P_{L12}	P_{L15}	P_{L16}	P_{L18}	P_{L20}	P_{L21}
3.22	5.00	2.338	5.220	0.085	3.200	3.294	1.580	6.80	2.74
P_{L23}	P_{L24}	P_{L25}	P_{L26}	P_{L27}	P_{L28}	P_{L29}	P_{L31}	P_{L39}	Q_{L3}
2.475	3.086	2.24	1.39	2.81	2.06	2.835	0.092	11.02	0.024
Q_{L4}	Q_{L7}	Q_{L8}	Q_{L12}	Q_{L15}	Q_{L16}	Q_{L18}	Q_{L20}	Q_{L21}	Q_{L23}
1.84	0.84	1.76	0.880	1.530	0.323	0.300	1.030	1.150	0.784
Q_{L24}	Q_{L25}	Q_{L26}	Q_{L27}	Q_{L28}	Q_{L29}	Q_{L31}	Q_{L39}	P_{G29}	P_{G30}
-0.922	0.472	0.170	0.755	0.276	1.269	0.046	2.50	2.50	5.729
P_{G32}	P_{G33}	P_{G34}	P_{G35}	P_{G36}	P_{G37}	P_{G38}	P_{G39}		
6.50	6.320	5.08	6.50	0.0	5.40	8.30	10.0		

Table 6.2 illustrates the structure and important design parameters of the ANN, for the 39 Bus System.

Table 6.2 Important design parameters for the Neural Network

Power system Considered	39 Bus New England System.
Number of layers	Three
Number of input parameters	58
Number of output(s)	1
Number of training sets	170
Learning Rate	1.0
Transfer Function	Sigmoid.
Training Tolerance	0.1

Figure 6.1 shows the testing results of the trained ANN. The expected values of the load margin were obtained by repeated simulations using VSTAB software. Testing of the network was done with 17 test cases or 10 % of the training sample, for the sake of clarity, results are shown for only 7 sample cases.

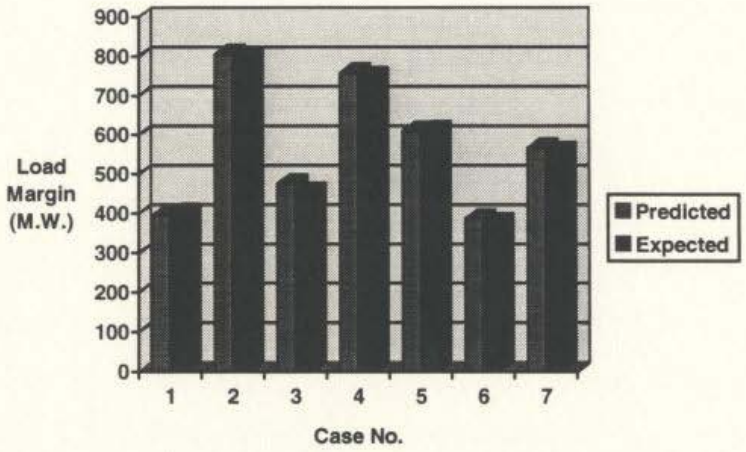

Fig. 6.1 Performance evaluation of neural network.

Figure 6.1 illustrates the comparison of the predicted value of load margin with the expected value. As can be seen , the predicted value closely matches the expected value. Figure 6.2 illustrates the percentage error in predicted value of load margin. It is seen that the maximum percentage error in the predictions is only 3.5 %, whereas a minimum percentage error of 0.5 % is achieved. Thus, Figures 6.1 and 6.2 indicate that given the appropriate system parameters, the ANN based system can predict the load margin of a power system with a high degree of accuracy.

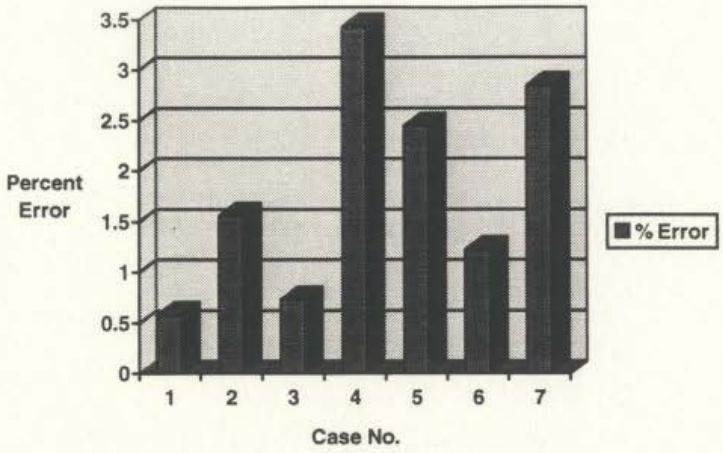

Fig. 6.2 Neural Network Performance evaluation.

6.6 ANN models to evaluate effect of contingencies on load margin .

The IEEE 24 Bus system, shown in Figure 5.5 was selected to implement this model. Chapter 5 presented the effect of contingencies on load margin of the IEEE 24 Bus system. It was found that contingencies have a considerable effect on the load margin. It is essential that an on-line voltage stability index be able to evaluate the load margin in the event of a contingency in the shortest possible time. For large scale power systems, this would rule out standard computation methods, since the computation costs in terms of speed and economy would be quite high. Artificial neural networks offer an 'intelligent' solution to this dilemma.

The approach outlined in Section 4.6 of Chapter 4, proposed a separate ANN model for each contingency, since it did not take the network topology into account. The new approach proposed in this section for the ANN based model for contingency evaluation is to include information regarding the network topology in the training set. The detailed procedure for design of the network is given as follows. Five of the most heavily loaded lines were selected, as detailed in chapter 5. Each of the five lines was outaged and training sets created for each of the above outaged cases, and for one case with all lines in service. The training sets were created by change of load, change in PV bus values, power factors etc. The network topology information, in the form of line power flows for each of the five

lines, was obtained for each such case. This line power flow information consisting of active and reactive powers, was included as additional inputs in the training set. For example, for the line 1- 5, the real and reactive power flow from bus 1 to bus 5 was considered. Table 6.3 shows one such training set, for the case in which line 1 - 5 of the IEEE 24 Bus System is outaged.

In table 6.3 shown below, V stands for voltage of the PV (voltage controlled) buses, P_L stands for the active power load, Q_L for the reactive power load , P_{LINE} and Q_{LINE} stand for the line power flows, all values being in per unit. The outaged lines are denoted as follows.

Line 1 corresponds to line 1 - 5

Line 2 corresponds to line 1 - 3

Line 3 corresponds to line 2 - 6

Line 4 corresponds to line 2 - 4

Line 5 corresponds to line 7 - 8

For the above input training data set, the output, i.e., the load margin was 2.59 p.u.

Table 6.3 One set of input training data for line 1 - 5 outaged

V_2	V_7	V_{13}	V_{15}	V_{16}	V_{18}	V_{21}	V_{23}	P_{L1}	P_{L2}
1.005	0.917	1.014	0.9782	1.0217	1.0119	1.004	1.023	1.08	0.97
P_{L3}	P_{L4}	P_{L5}	P_{L6}	P_{L7}	P_{L8}	P_{L9}	P_{L10}	P_{L13}	P_{L14}
1.8	0.74	0.71	1.36	**1.25**	**1.71**	**1.75**	**1.95**	**2.65**	**1.94**
P_{L15}	P_{L16}	P_{L18}	P_{L19}	P_{L20}	Q_{L1}	Q_{L2}	Q_{L3}	Q_{L4}	Q_{L5}
3.17	1.0	3.33	1.81	**1.28**	**0.22**	**0.2**	**0.37**	**0.15**	**0.14**
Q_{L6}	Q_{L7}	Q_{L8}	Q_{L9}	Q_{L10}	Q_{L13}	Q_{L14}	Q_{L15}	Q_{L16}	Q_{L18}
1.28	**0.25**	**0.35**	**0.36**	**0.40**	**0.54**	**0.39**	**0.64**	**0.20**	**0.68**
Q_{L19}	Q_{L20}	P_{G2}	P_{G7}	P_{G13}	P_{G15}	P_{G16}	P_{G18}	P_{G21}	P_{G23}
0.37	**0.26**	**2.0**	**3.94**	**1.55**	**1.55**	**4.0**	**4.0**	**6.6**	**1.924**
$P_{LINE\,1}$	Q_{LINE1}	P_{LINE2}	Q_{LINE2}	P_{LINE3}	Q_{LINE3}	P_{LINE4}	Q_{LINE4}	P_{LINE5}	Q_{LINE5}
0.0	**0.0**	**0.3007**	**0.153**	**0.822**	**0.022**	**0.6703**	**0.1724**	**0.7499**	**0.4974**

Table 6.4 Design parameters for the Neural Network.

Power System Considered	IEEE 24 Bus System.
Number of layers	Three
Number of input parameters	60
Number of output(s)	1
Number of training sets	220
Learning Rate	0.1
Transfer Function	Sigmoid
Training Tolerance	0.075

Table 6.4 shows the important design parameters of the neural network. After training the ANN was tested with various cases and the test results are given below. It may be noted that the test data was not included as part of the training data.

The philosophy behind design of this ANN model was that a single ANN should be capable of evaluating the load margins of a power system under normal operating conditions as well as under with line outages. The ANN model introduced in Chapter 4 uses separate ANN for each contingency. The model proposed in this section eliminates the need for having several parallel ANNs and hence can give savings in terms of training time, cost and complexity. This has been made possible by including the network topology information along with the training data. Though the proposed model has been trained with input data for 5 line outages, it can easily be extended for larger systems.

Figures 6.3 to 6.8 illustrate the performance of the ANN based model in evaluating the load margins in presence of contingencies.

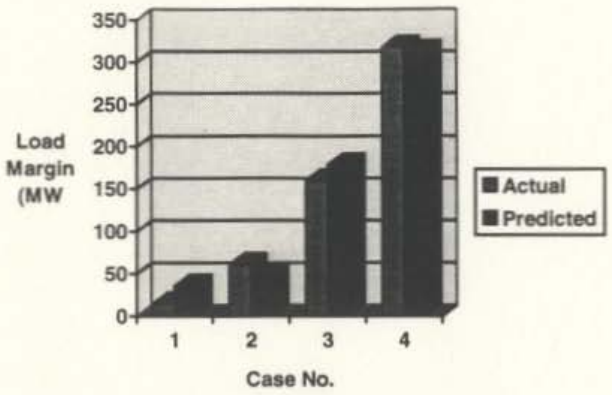

Fig. 6.3 Neural Network Performance Evaluation for line 1- 5 outage.

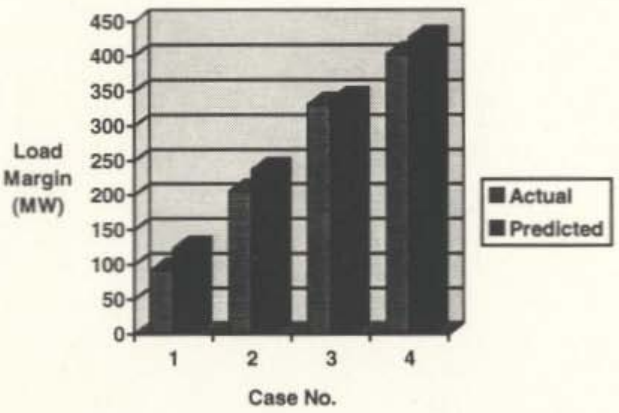

Fig.6.4 Neural Network Performance Evaluation for line 1-3 outage

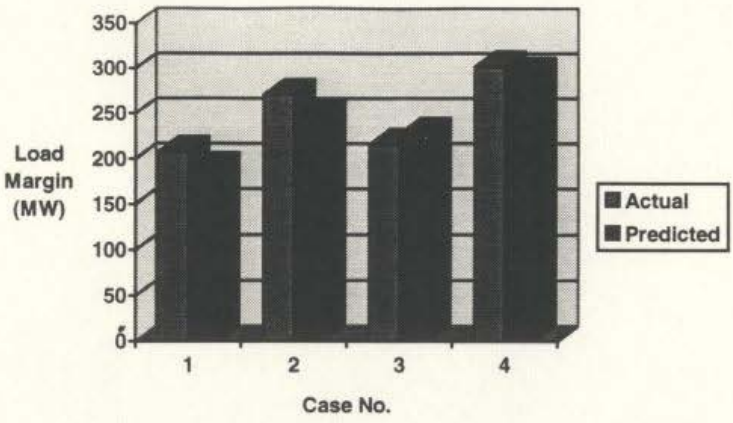

Fig. 6.5 Neural Network Performance Evaluation for line 2-6 outage.

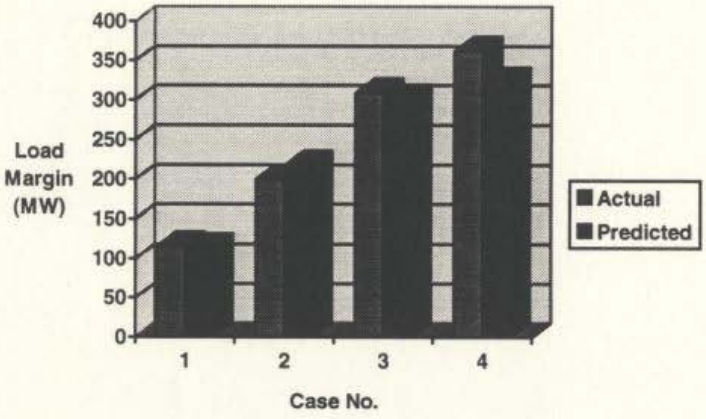

Fig. 6.6 Neural Network Performance Evaluation for line 2-4 outage.

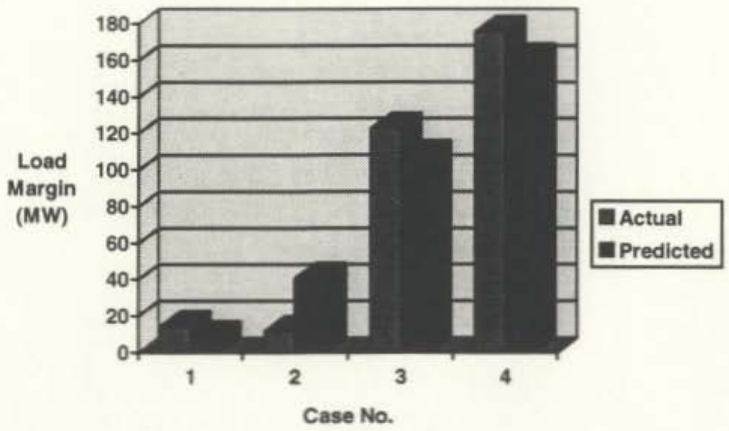

Fig. 6.7 Neural Network Performance for line 7-8 outage.

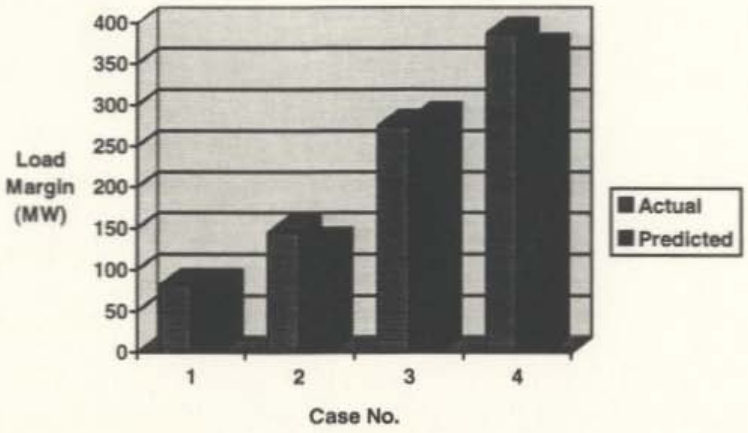

Fig. 6.8 Neural Network Performance evaluation for no line outage.

It can be seen that the predicted value of load margin closely matches the actual value for all cases, i.e., with contingencies and with all lines in service. This shows that a single ANN model trained with network topology information, can predict load margins for all system conditions.

6.7 Summary

As described in Chapter 5, load margins are a significant pointer to the MW reserves of a power system and on line monitoring of the load margins can be very useful. Load margins represent the minimum load the system can take before sliding into instability. Knowing the MW and MVAR reserves available, the system operator can take corrective action like shedding non essential load, allocating more MW or MVAR reserves etc. before the system moves irrevocably into voltage instability. However, calculation of the load margins is a computationally intensive procedure and involves repeated solutions of power flows until the program converges to a local or global minimum. In the context of on-line implementation of load margin in an EMS environment, this can impose a considerable computation burden. An ANN based system, on the other hand, will impose a much lesser computational burden and is also much quicker, since repeated iterations are not required. This chapter has presented two ANN models. The first, implemented on the 39 Bus New England System, predicts the load margin for the system under normal operating conditions, i.e, with all lines in service. The second ANN model, implemented on the IEEE 24 Bus Reliability Test System, can evaluate the effect of contingencies on load margin and a single model with suitable inputs can be used to predict the load margin of large systems under normal operating conditions as well as under contingencies. This single ANN model which takes into account the network topology, can result in significant savings in computation costs and eliminate the need for separate neural network models for each contingency. It may be noted that all the inputs to the ANN are parameters readily available from the SCADA, without any need for additional data acquisition equipment. The trained ANN model, used in conjunction with SCADA and other EMS functions, as outlined in the block diagram of Figure 4.7, can be a valuable tool to the system operator in maintaining power

system voltage stability, by offering a fast, economical and intelligent solution. However, it may be noted that the accuracy of the predictions of the ANN will depend largely on the effectiveness of the power system software used in generating the training set data. There is no guarantee that the load margin obtained is a global minimum, since there exists a possibility of getting trapped in the several local minima existing in a complex hypersurface. Ideally, the training set should contain data based on the global minimum obtained. But, at present there is no way of finding if VSTAB has located a global or local minimum. This problem should be addressed further in future research into better mathematical methods to arrive at a global minimum everytime.

Chapter 7

Conclusions

7.1 Contributions of this research

Human civilization, as we know it today owes a lot to electrical power. In fact, most of the conveniences and lifestyle we take for granted have been made possible due to the reliable and efficient operation of the modern power system network. However, the rapid industrialization and modernization of the society has placed a lot of stress on the power system network. The load levels are rising, and the consumers are demanding efficiency and reliable supply of power as never before. But, utilities have fewer resources to meet these demands. This in turn has given rise to a host of new problems hitherto unknown, the most prominent of which is voltage instability. The interesting aspect of the voltage stability problem is that even well developed, strong , and interconnected systems are experiencing this problem. Unless utilities are able to commit huge resources into building new transmission and generation facilities, this problem will continue to stay and even worsen and major system collapses may be a possibility.

In this scenario, power system operators have a vital role to play in ensuring system security and efficient operation. The primary role of a power system operator is to ensure that the system is operating in a healthy condition and take corrective action in the event of any abnormality. In performing this task, the system operator has the help of powerful tools like the Energy Management System (EMS) . The EMS is a very versatile system which has capabilities for control, monitoring and analysis of power system conditions. It is expected that in the near future, EMS will be equipped with capabilities for on-line voltage stability analysis software functions, so as to enable the system operator to take immediate corrective action .

A number of voltage stability indices have been developed by various researchers for the purpose of quantifying the voltage instability of a power system. This thesis has studied two popular voltage stability indices and presented simulations on test power systems. These indices are computation intensive and require repeated power flow solutions. For large power systems, this can

be quite time consuming and heavy investments in terms of computer hardware are required if real-time response is desired. This has been the motivation in investigatigating other 'intelligent ' solutions to this problem. Artificial Neural Networks (ANNs) have aroused considerable interest as pattern recognition tools in solving various power system problems.

The voltage stability indices investigated in this research are the energy margin approach and the load margin approach. The energy margin method, takes into account the system operating conditions, the load disturbances, and the multiple solutions of the power flow equations , in assessing the voltage stability of a power system. Simulations are carried out on the effect of loadings and contingencies on the energy margin of a 24 Bus Power System. It was found that contingencies have a detrimental effect on the energy margin and the energy margin was considerably lower as compared to normal operating conditions. The load margin index give in Mega Watt terms the maximum load the system can take before sliding into instability. Thus, determining the load margins can help the system operator in taking corrective control actions as soon as the margin reaches a critical value. This critical value will depend on the MW and MVAR reserves available in the system. Simulations were carried out on the effect of loadings and contingencies on the load margins of the 39 Bus New England System and the 24 Bus IEEE Reliability Test System. It was found that contingencies have a significant effect on the load margins and tend to reduce them.

Three ANN models were developed in the course of this research. All three ANN models were implemented on the back propagation algorithm. The effect of parameters like training tolerance and learning rate on the accuracy of prediction and the training time were investigated. One of the main considerations in developing the training sets for all the three ANN models was that all training parameters should be readily available from the EMS. For the 24 Bus Power system used for investigating the energy margin based index, an ANN model was developed which could predict the energy margin from the system operating conditions. The inputs to the ANN were the active and reactive power, the voltage at the voltage controlled buses, and the active power generation. Separate ANN models were used for each contingency . The ANN model for the 39 Bus New England Power System used the system parameters like active and reactive power at load, voltage at voltage controlled buses, and the active power generation to predict the load margin. The ANN model for the IEEE 24 Bus Reliability Test System considers contingencies also, and makes

use of the network topology information in the form of line power flows, to predict the load margin for contingencies as well as normal operating conditions. Thus this model eliminates the need to have separate ANN models for each contingency

Test results on the three ANNs have shown that Artificial Neural Networks can predict with reasonable accuracy, the voltage stability index of a power system. The inputs required by the ANN are system parameters, which are in any case, available from the SCADA system. Thus, there is no need for additional data acquisition equipment. Also, a single ANN model, trained with network topology parameters, can predict the voltage stability index of a power system, under normal operating conditions as well as under contingencies. This will result in reduced overall costs and complexity of implementation. This approach, in principle, can be extended to larger systems too. Thus artificial neural networks can become a viable tool in the EMS and be of invaluable help to the system operator in fast, accurate and intelligent assessment of voltage stability of power systems. This will enable electric power utilities to operate the system in the most efficient way with the available resources.

7.2 Suggestions for future work

The work reported in this thesis can be extended in the following areas :

1. The voltage stability indices considered in this thesis assume a constant power load model, which is not always the case with a practical power system. Suitable load models can be incorporated in the voltage stability indices and this would indicate the influence of the types of loads on power system voltage stability.

2. Due to the limitations of the neural network software, the present study has used sample test power systems only. This work can be extended to larger power systems if suitable data can be obtained from Electric power utilities in North America.

3. Different Artificial Neural Network algorithms like Self Organizing Maps, and Learning Vector Quantization can be studied for suitability of application to the voltage stability problem. These algorithms are self-learning and have the potential to be competitive with conventional back propagation algorithm.

References:

[1] IEEE Committee Report, " Voltage Stability of Power Systems, Concepts, Analytical Tools and Industry Experience " , *IEEE Publication 90 TH0358-2PWR, 1990.*

[2] C.W.Taylor , " *Power System Voltage Stability* " , EPRI Power Engineering Series, 1994.

[3] IEEE Tutorial Course " Reactive Power : Basics , Problems and Solutions", *Course Text 78EH00262-6-PWR, 1978.*

[4] A.R.Bergen , " *Power Systems Analysis*", Prentice Hall Series in Electrical and Computer Engineering , 1986.

[5] R.K.Gupta, Z.A.Alaywan, R.B.Stuart and T.A. Reece , " Steady State Voltage Instability operations perspective ", *IEEE Transactions on Power Systems , Vol.5, pp.1345-1354, November 1990.*

[6] V.A.Venikov, V.I Stroev, V.I.Idelchuk and V.I.Tarasov, "Estimation of Electric Power System Steady State Stability in load flow calculations", *IEEE Transactions on Power Apparatus and Systems, Vol.94, No.3, pp.1034-1038 , May - June 1975.*

[7] W.R.Lachs , " Voltage Collapse in EHV Power Systems " , Paper No. A78 057-22, *IEEE - PES Winter Meeting , January 1978.*

[8] Y.Tamura, H.Mori and S.Iwamoto, " Relationship between voltage stability and multiple load flow solutions in electric power systems", *IEEE Transactions on Power Apparatus and Systems, Vol.102, No.5, pp.1115-1125, May 1983.*

[9] S.Abe, Y.Fukunago, A.Isano and B.Kondo, " Power system voltage stability ", *IEEE Transactions on PAS, Vol.101, No.10, pp. 3830-3841 , Oct. 1982.*

[10] Y.Tamura and S.Iwamoto ," A Load flow calculation for ill conditioned power systems " , *IEEE Transactions on Power Apparatus and Systems, Vol.100, No.4, pp.1736-1744, April 1981.*

[11] R.E.Palmer, R.C.Burchett and H.I.Happ ," Reactive Power Despatching for Power System Voltage Security", *IEEE Transactions on Power Apparatus and Systems, Vol.102, No.6 pp.3905-3909, December 1983.*

[12] P.Kessel and H.Glavitch , " Estimating the voltage stability of a power system " , *IEEE Transactions on Power Delivery , Vol.1, No.3, pp. 346-354, July 1986.*

[13] A.Tiranuchit , R.J.Thomas , R.A. Duryea and F.T. Luk , " A Posturing Strategy against voltage instabilities in Electric Power Systems " , *IEEE Transactions on Power Systems, Vol.3, No.1, pp. 87-93, Feb. 1988.*

[14] P.A.Lof, D.J.Hill, S.Arnborg and G.Andersson , " On the Analysis of long term voltage stability" *International Journal of Electrical Power and energy systems, Vol.15, No.4, pp.229-236,1993.*

[15] M.A.Pai " *Power System Stability* ", North Holland Systems and Control Series , Vol.3, 1986.

[16] C.L.Demarco and T.J.Overbye , " An Energy based security measure for assessing vulnerability to voltage collapse ", *IEEE Transactions on Power Systems , Vol. 5, No.2, pp. 582-591, May1990.*

[17] T.J.Overbye and C.L.Demarco , " Voltage security enhancement using energy based sensitivities " *IEEE Transactions on Power Systems , Vol.6, No. 4, pp. 1196-1202, August 1991.*

[18] T.J.Overbye , " Use of Energy Methods for online assessment of power system voltage stability " , *IEEE Transactions on Power Systems , Vol. 8, No.2, 1993, pp. 452-458, May 1993.*

[19] S.Haykin " *Neural Networks, A Comprehensive Foundation* " IEEE Press, 1994

[20] J.A.Freeman and D.M.Skapura, " *Neural Networks, Algorithms, Applications and Programming Techniques* " Addison- Wesley, 1993.

[21] P.Werbos, " *Beyond Regression: New Tools for Prediction and Analysis in the Behavioral Sciences* ". PhD Thesis, Harvard, Cambridge, MA, August 1974.

[22] J.McClelland and D.Rumelhart, " *Parallel Distributed Processing* ", Volumes 1 and 2. MIT Press, Cambridge, MA , 1986.

[23] Proceedings of *First International Forum on Application of Neural Networks to Power Systems*, Seattle, WA, July 1991.

[24] Proceedings of *Second International Forum on Application of Neural Networks to Power Systems*, Yokohoma, Japan, September 1993.

[25] Proceedings of *Intelligent Systems Application to Power Systems*, Montpellier, France, September 1994.

[26] D.J.Sobajic and Y.H.Pao, " Artificial Neural Network based Dynamic Security Assessment for Electric Power Systems," *IEEE Transactions on Power Systems, Vol.4, pp.220-229., February 1989.*

[27] T.M.Peng, N.F.Hubele, and G.G.Karady, " Conceptual approach to the application of neural network for short term load forecasting ," *Proceedings of the 1990 ISCAS Vol. 3, pp.2942-2945., New Orleans, May 1990.*

[28] M.Chow and R.J.Thomas," Neural Networks synchronous machine modelling", *Proceedings of the 1989 ISCAS Vol. 1, Portland, , pp.494-498, May 1989.*

[29] R.Fischl, M.Kam, J.C.Chow, and R.Riccardi, " Screening Power System Contingencies using a back propogation trained multiperceptron", *Proceedings of the 1989 ISCAS Vol. 1, Portland, pp. 486-489, May 1989.*

[30] P.A. Joniken, " Neural Network models for fault detection and diagnosis", *Proceedings of IJCCN, pp.239-244, , Seattle, WA, May 1991.*

[31] H.Tanaka, S.Matsuda, H.Ogi,Y.Izui, H.Taoka, and T.Sakaguchi, " Design and evaluation of neural networks for fault diagnosis", *Second Symposium on Expert System Applications to Power Systems, Seattle, WA, pp.345-356, July 1989.*

[32] S.Weerasurya and M.A.El-Sharkawi," Identification and control of a DC Motor using a back propagation neural network ", *Paper No. 91 WM 288-1 EC, IEEE-PES Winter Meeting, New York, February 1991.*

[33] H.Mori and Y.Tamura," An Artificial Neural Network approach to monitoring power system Voltage instability," *Proceedings of Bulk Power System Voltage Phenomena : Voltage Stability and security, Deep Creek Lake, MD, August 1991.*

[34] A.Mohamed and G.B.Jasmon, " Real Time Power System Security Algorithm", *IEE Proceedings, Vol. 135, Pt. C, No.2, pp.98-105, March 1988.*

[35] Reliability Test System Task Force, " IEEE Reliability Test System", *IEEE Transactions on PAS, Vol. PAS - 98, No. 6, pp. 2047-2054, Nov/Dec 1979.*

[36] B.Jeyasurya, " Application of artificial neural networks for voltage stability assessment", *Electric Power Systems Research*, 29 (1994), pp. 85-90.

[37] California Scientific Software Inc. " *Brainmaker - Users Guide and Reference Manual*", 1990

[38] F.Alvarado, I.Dobson, and Y.Hu, " Computation of closest bifurcations in power systems", *IEEE Transactions on Power Systems, Vol. 9, No.2, pp. 918-924, May 1994.*

[39] J.Lu, C.Liu , and J.S.Thorp, " New Methods for computing a saddle node bifurcation point for voltage stability analysis", *94 SM 514-0 PWRS, 1994 IEEE PES Summer Meeting, San Francisco, CA, July 1994.*

[40] P.Kundur, " *Power System Stability and Control*", McGraw Hill, 1993.

[41] Power Tech Labs Inc. " *VSTAB Users Manual*", January 1995.